2023

Investigating the Effect of Antibody-Mediated Feedback on Ongoing Germinal Center Responses

Alexandru Barbulescu

INVESTIGATING THE EFFECT OF ANTIBODY-MEDIATED FEEDBACK ON ONGOING GERMINAL CENTER RESPONSES

A Thesis Presented to the Faculty of
The Rockefeller University
in Partial Fulfillment of the Requirements for
the degree of Doctor of Philosophy

by
Alexandru Barbulescu
November 2023

INVESTIGATING THE EFFECT OF ANTIBODY-MEDIATED FEEDBACK ON ONGOING GERMINAL CENTER RESPONSES

Alexandru Barbulescu, Ph.D.
The Rockefeller University 2023

Antibodies play a crucial role in protection against a wide range of pathogens. As such, the goal of most vaccinations is to induce immune memory in the form of long-lasting, high-affinity serum antibody titers, which requires the participation of B cells in the germinal center (GC) response. It is well-established that pre-existing antibodies can influence the outcome of future humoral responses; however, whether antibody from an ongoing response can feedback onto contemporaneous GCs to influence B cell clonal selection and affinity maturation in real-time remains poorly understood.

Here we present a genetic mouse tool to interrogate the effect of antibody-mediated feedback on ongoing GC responses. We have designed an oligoclonal B cell transfer mouse model with B cell receptor specificities to non-overlapping epitopes on the same antigen, allowing us to distinguish between epitope-specific and epitope-non-specific effects of secreted antibody. In addition, we have genetically engineered a Blimp-1-DTR mouse that allows for temporally controlled ablation of plasma cells and, therefore, depletion of antibody titers. Combining these two models has revealed that high levels of antibody produced during B cell responses can modulate *inter*clonal selection in the GC by suppressing GC B cells that bind the same epitopes. However, a “traveling wave” of antibody is not required to guide *intra*clonal selection and, therefore, is not a

driver of affinity maturation. We propose antibody-mediated suppression via epitope masking may be an important mechanism in guiding the development of primary GCs towards epitopes that are poorly represented in the serum antibody compartment, thereby maintaining diversity within humoral responses.

To my mom, who has shown me the definition of perseverance.

ACKNOWLEDGEMENTS

I am grateful to have received my scientific training at The Rockefeller University, which has such a rich and influential history. It is an absolute privilege to be surrounded by such passionate and brilliant minds – a privilege that I try not to take for granted.

I'd like to thank all my previous mentors, without whom I would not have had the opportunity to study here. Their belief in my potential and investment in my success have left a significant imprint on me, and in the future I can only hope to affect the lives of students as much as my mentors have influenced mine.

It has been an absolute pleasure to work under Dr. Victora, who has been an excellent mentor throughout my PhD. Throughout my time in lab, I always felt I was working with him rather than for him. While I will always have a deep admiration for his scientific mind, what I will remember most are his displays of humanity during tough times. Of all his achievements, one of the most important is the wonderful lab environment he has fostered over the years. I am thankful for every lab member I have had the pleasure of interacting with over the past 5 years. In particular, I would like to thank Dr. Jonatan Ersching, who was my first mentor in lab and a good friend. We tragically lost Jonatan in October of 2020, and he is dearly missed.

I would like to thank Tom Langelaar, who has been working with me on this project for the past year. The two of us made a great team and together we were very productive at the bench. More importantly, we've established a friendship that will last a lifetime.

I would like to thank my family, who has been incredibly supportive throughout my training. Finally, I would like to thank my wife for keeping me balanced throughout my PhD. Regardless of how difficult my day in lab was, as a surgeon, her day was even harder. Coming home and spending time with her always provided me with perspective and brightened up my day.

TABLE OF CONTENTS

LIST OF FIGURES

CHAPTER 1: Introduction

Antibodies confer protection against a variety of pathogens, both during active infection and upon repeat encounters (Pollard & Bijker et al., 2021). It follows that the main goal of most vaccination strategies is to produce long-lived, high affinity antibodies, and vaccine efficacy is predominantly determined by the magnitude of neutralizing serum titers achieved (Nabel, 2013). As such, great efforts have been made into understanding the protective mechanisms of antibodies and devising approaches to elicit their sustained production.

Far less is known about the role antibodies play in regulating humoral responses. It is now appreciated that pre-existing antibodies can modulate recall responses and influence the specificity of responding B cells, although both inhibitory and activating effects have been observed (Heyman, 2000; Tas et al., 2022). Nevertheless, it is clear the repertoire of pre-existing serum antibody is a parameter that helps dictate B cell clonal selection into secondary responses (NcNamara et al., 2020; Tas et al., 2022) . However, whether antibodies can feedback onto contemporaneous primary humoral responses and modulate their outcome in real-time, is a topic of ongoing debate. Further deciphering this potential mode of self-regulation will allow for a better understanding of the output of primary B cell responses and will therefore help inform vaccine design.

Structure of the antibody molecule

Antibodies are Y-shaped molecules composed of two identical heavy and light chains linked together by disulfide bonds. Each antibody has two antigen binding regions that are formed by a combination of the heavy and light variable (V_H and V_L) domains at the N-terminus of each chain (Figure 1). Antibodies contact their antigen via six complementarity-determining region (CDR) loops, three emanating from V_H and the other three from V_L. Tremendous diversity exists in the amino acid sequences of CDR loops, allowing for antibodies to recognize virtually any antigen. Most of the variability among antibodies lies within the sequence, length, and structure of HCDR3s, which frequently dominate antigen interactions (Stanfield and Wilson, 2019). HCDR3 loops can vary in length from 1 to 21 amino acids in mice and 1 to 35 amino acids in humans and long HCDR3s have been shown to access recessed portions of viral antigens (Zemlin, 2003). For example, C05, a broadly neutralizing antibody against influenza, uses its 24-amino acid-long HCDR3 to penetrate the sialic acid binding site of hemagglutinin in a way that competes with glycan binding (Ekiert, 2012). The wide range of possible HCDR3s is attributed to their encoding nucleotide sequences being formed *de novo* from the junction of V, D and J gene segments during the process of V(D)J recombination. Along with the combinatorial diversity generated from the quasi-stochastic union of various gene segments, additional steps of nucleotide resection and addition of non-templated nucleotides at the VDJ junction results in nearly limitless possibilities for HCDR3 sequences (Jung & Alt, 2004). CDR1s and CDR2s, on the other

hand, are encoded within V gene segments of heavy and light chains, and as such, are far less diverse.

The antigen binding sites of the antibody are located within the Fab (fragment antigen binding) regions, which are comprised of V_H and V_L along with the constant region of the light chain (C_L) and the first constant region of the heavy chain (C_{H1}). In most antibody classes, the Fab is connected to the rest of the protein by a flexible hinge region that allows the antibody to stretch and adopt multiple conformations for binding antigen in various configurations. The immunoglobulin arm opposite the two Fabs is the Fc (fragment crystallizable) region, which consists of C_{H2} and C_{H3} in a typical IgG1 antibody. Fc regions dictate the effector functions of antibodies by interacting with Fc receptors (FcRs) present on various cells of the immune system to modulate downstream processes. Although the Fc is termed the constant region, in actuality it adopts a variety of functionally important conformations depending on its specific isotype and glycosylation pattern.

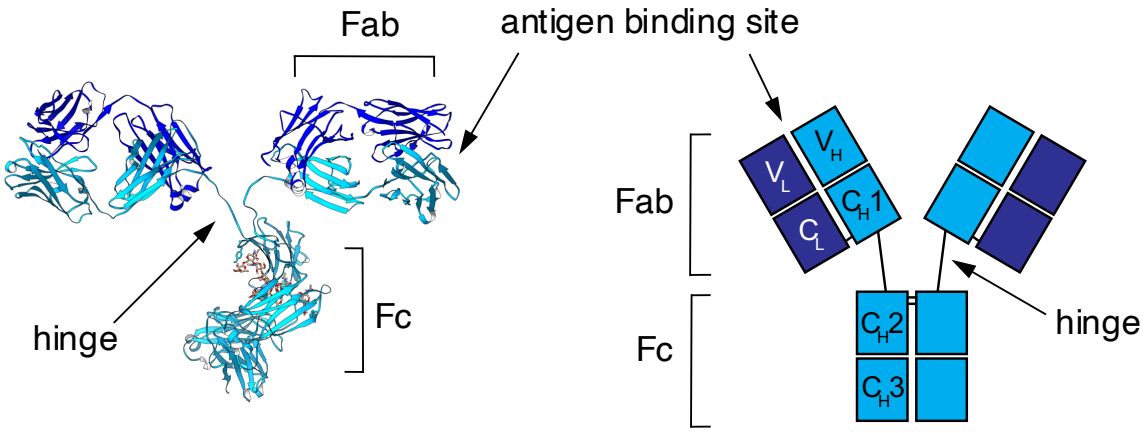

Figure 1: Structure of the antibody molecule
(Left) 2.80 Å crystal structure of a mouse IgG2a antibody (PDB ID: 1IGT)
(Right) Cartoon representation of an antibody used throughout the remainder of this text.

Antibody isotypes

Circulating antibodies are found as four main isotypes: IgM, IgG, IgA, and IgE. The isotype is determined by the sequence of the constant regions, and therefore, each isotype has a different Fc portion that orchestrates its specific downstream functions. IgM is typically the first isotype to be secreted during a primary B cell response, and it serves as a first line of humoral defense against invading pathogens. Due to its early formation, IgM is relatively low affinity. In compensation for its weak binding, IgM is secreted as a pentamer consisting of five antibodies held together by disulfide bonds and a protein called the J-chain. Pentamerization increases the avidity of the interaction, creating ten binding sites all tethered to one unit to allow for multi-site binding (Lu et al., 2018). Once bound to antigen, the unique structure of IgM enables it to readily activate

the complement system, a proteolytic cascade that results in opsonization of antigen and formation of membrane pores in bacterial cells (Kemper et al., 2023). The half-life of serum IgM is relatively short, ranging from 2 days in mice to 5-8 days in humans (Vieira at al., 1988). IgG is the most abundant serum antibody, with normal a normal range of 6 – 16 g/L in humans. It is divided into four different subclasses, IgG1-4 in humans and IgG1, IgG2a/b/c, and IgG3 in mice, numbered in order of their relative quantities in serum (Lu et al., 2018). Along with serving as potent neutralizers due to their higher affinity, IgG antibodies in immune complexes can also engage FcγR receptors on a multitude of cell types to recruit various downstream effector functions. IgG is longer-lived than IgM, with a half-life of approximately 1 week in mice and 3 weeks in humans (Booth, 2018).

Although its serum levels are relatively low, IgA is the most abundant antibody, as it is predominantly present in the intestine and other mucous membranes such as the respiratory epithelium. At these mucosal sites IgA serves to neutralize respiratory and gastrointestinal pathogens, while in the gut it is thought to help establish and maintain homeostasis between the host and commensal bacteria (Ng et al., 2022). IgE is found in very small amounts and plays an important role in defending against parasites but is also involved in the development of allergic responses (Anvari et al., 2019).

Fcγ receptors

Fcγ receptors form the link between antibodies and their effector functions. They are present on nearly all leukocytes and bind the Fc portion of IgG antibodies to transduce various signals throughout an immune response. Type I FcγRs are members of the immunoglobulin superfamily and bind the hinge proximal region of the C_{H2} domain of IgG molecules in a 1:1 stoichiometric ratio. Signals transmitted by type I FcγRs can be either activating or inhibitory depending on the intracellular signaling domain they possess. In mice, FcγRI, FcγRIII, and FcγRIV are activating due to the presence of an associated immunoreceptor tyrosine activation domain (ITAM), whereas FcγRIIb is inhibitory resulting from its immunoreceptor tyrosine inhibitory domain (ITIM). Type II FcγRs DC-SIGN (SIGN-RI in mice) and CD23 are C-type lectins that are primarily anti-inflammatory and/or immunomodulatory (Figure 2A). They function by increasing the threshold for myeloid cell activation and play a role in B cell selection and affinity maturation (Bournazos and Ravetch, 2017; Wang and Ravetch, 2019).

Apart from FcγRI, all FcγRs display low affinity for IgG. Consequently, most FcγRs are engaged only when IgG is bound to antigen to form multimeric immune complexes, which increases the avidity of the interaction. This is an essential form of regulation, as it prevents inappropriate and excessive FcγR signaling by ensuring antibody effector function is limited only to the time antigen is present. The downstream effects of FcγR ligation primarily depend on two main factors – the specific FcγRs that are bound and the responding cell type. Most leukoctyes express more than one type of FcγR. In

addition, the expression of FcγRs is dynamic and can change throughout an immune response, particularly during leukocyte differentiation and in response to various cytokines at inflammatory sites. IgG subclasses also demonstrate different propensities for binding to activating versus inhibitory FcγRs (A/I ratio), with human IgG1 and IgG3 and mouse IgG2a/c having the highest A/I ratios. Increasing A/I ratios by switching the isotype of IgG enchances tumor killing in a melanoma mouse model, and methods to improve A/I ratios in antibodies via Fc mutations or slight modifications in glycosylation show promise in the efficacy of monoclonal anti-tumor antibodies (Clynes et al., 1998; Clynes et al., 2000; Nimmerjahn & Ravetch, 2005).

Fc glycoforms and their role in FcγR binding

All IgG1 antibodies are glycosylated at asparagine 297 in the C_{H2} domain with a core, biantennary glycan composed of four *N*-acetylglucosamine and three mannose saccharide units (Figure 2B). Glycosylation is a crucial component of antibody function, as disruption of the core glycan results in reduced binding affinity to FcγRs and abrogates *in vivo* FcγR-mediated effector functions. Although interaction with FcγRs occurs mostly through amino acid residues of the antibody, glycans stabilize the Fc in structural conformations that allow for FcγR binding (Subedi & Barb, 2015). The core glycan can be extensively modified via the actions of several glycosyltransferases, and these modifications dictate the FcγR binding profile of the antibody. Two important glycan modifications are fucosylation and terminal sialylation, and the relative proportions of these modifications can influence the balance between inflammatory and

immunoregulatory processes of the immune system. Antibodies with afucosylated glycans display increased affinity to the activating FcγRIII, which promotes inflammatory effects, and modifications to increase FcγRIII activation have been utilized in anti-CD20 therapy to improve outcomes in patients with follicular lymphomas (Robert et al., 2017). Reduced fucosylation of IgG also predicts development of severe disease in secondary dengue infections (Bournazos et al., 2021). When an antibody glycan is sialylated, the Fc adopts a “closed” structural conformation that shifts its binding away from activating type I FcγRs to immunoregulatory and anti-inflammatory type II FcγRs (Ahmed et al., 2014). This is most evident with intravenously administered immunoglobulin (IVIg) therapy, in which the sialylated fraction of IgG is responsible for its anti-inflammatory effect in patients suffering from acute inflammatory diseases (Kaneko et al., 2006).

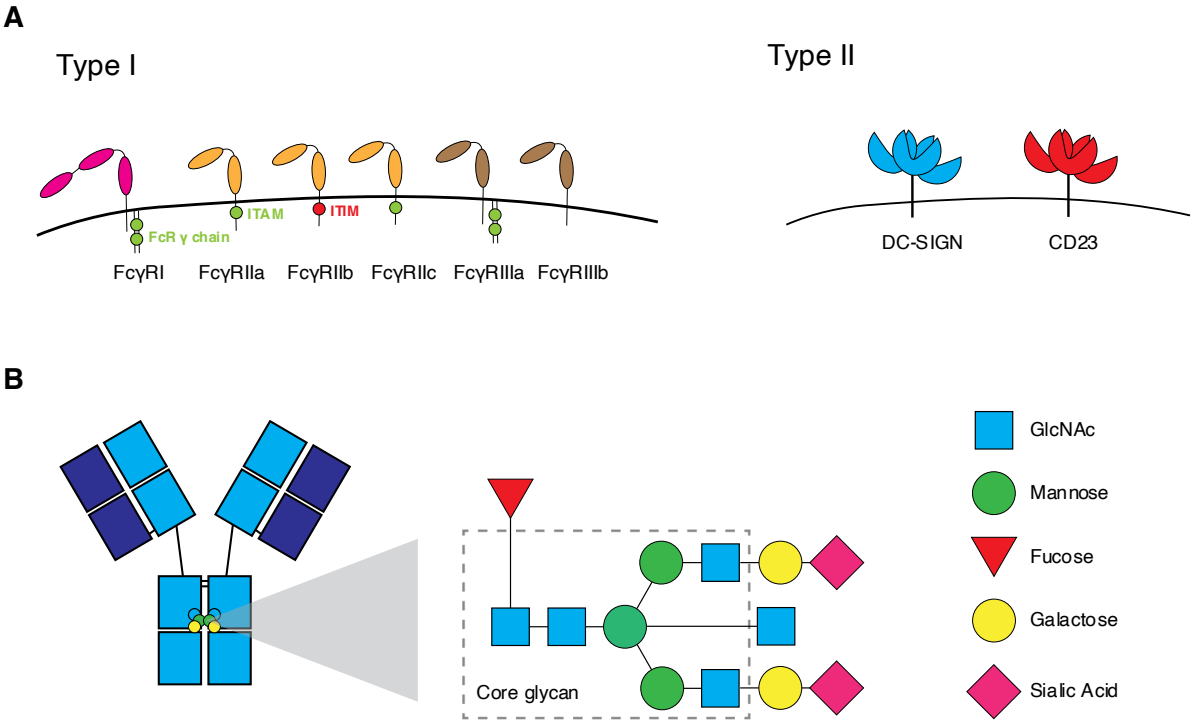

Figure 2: Fcγ Receptors and Antibody Glycosylation
A) Cartoon depictions of type I (left) and type II (right) Fcγ receptors. Type I FcγRs are either activating or inhibitory depending on the presence of downstream signaling motifs. Type II FcγRs predominantly mediate immunomodulatory effects when engaged.
B) IgG1 antibodies are glycosylated with a core glycan at N297 in their C_{H2} domains. Additional modifications to the core glycan modulate the FcγR binding profile of the antibody.
Figures are inspired by Bournazos et al., *Annu. Rev. Immunology*, 2017.

Neutralization and effector functions of antibodies

In the context of infection, the two mechanisms of antibody function are neutralization and Fc mediated protection. Neutralization, the simpler of the two, occurs when antibodies bind pathogens or toxins in such a way that their entry into host cells is impaired. Most commonly, this occurs when responses are directed towards epitopes close in proximity or directly within the receptor binding sites (RBS) of viral surface proteins, which directly blocks viral attachment. This is evident with responses against the hemagglutinin (HA) protein of influenza, as antibodies targeted closest to the RBS demonstrate the highest neutralization capabilities (Sicca et al., 2020). Neutralization can also occur when antibodies inhibit a viral process necessary for cell entry. Again, using influenza as an example, antibodies against the membrane proximal stem of HA inhibit viral entry by preventing the conformational change necessary for viral fusion with endocytic membranes, without blocking viral attachment *per se* (Sui et al., 2009). Finally, neutralization can occur with antibodies targeted to proteins outside those required for entry. Influenza neuraminidase (NA) is required for the release of emergent viral particles from host cells by cleaving sialic acid residues that mediate binding to HA, and antibodies against NA can impair its catalytic function and prevent propagation of viral infection. Interestingly, these antibodies act in a manner similar to oseltamivir, a competitive inhibitor of influenza NA used to treat infection in patients at high risk of complications (Madsen et al., 2020).

Fc mediated effector functions occur predominantly via interactions of IgG molecules with Fcγ receptors expressed by various leukocytes and include antibody-dependent cellular cytotoxicity (ADCC), cellular activation, phagocytosis, and release of cytokines, to name a few. Granulocytes release pre-formed cytotoxic compounds such as proteases and antibacterial peptides when activating FcγRs are cross-linked by immune complex, and macrophages phagocytose antigen coated with IgG. Activation of FcγRIIIa on natural killer cells triggers cell activation and degranulation, resulting in membrane pore formation and activation of apoptotic pathways in target cells. Antigen presenting cells such as dendritic cells undergo maturation in response to FcγR ligation, upregulating MHCII expression along with various co-stimulatory molecules (Bournazos, 2017). Thus, antibody not only mediates recognition of opsonized antigens by cells of the innate immune system, but also modulates adaptive immune responses via influencing antigen presenting cell maturation and T cell priming.

Antibodies are produced by B cell responses

The ultimate protective function of a B cell is to produce antibodies. This can happen in two ways – B cells can either directly differentiate into antibody secreting plasma cells, or they can become memory cells that are poised to differentiate into plasma cells upon future encounters with similar antigens. Two important features of effective antibody responses are their ability to increase in affinity overtime while maintaining sufficient diversity. The affinity of an antibody determines its efficiency of binding; an antibody with 10-fold higher affinity will equally bind its target at a concentration 10-fold less than

its lower-affinity variant. Therefore, from the standpoint of protective immunity, it is advantageous to achieve the highest possible affinity antibody titers following infection or immunization. In parallel, it is important to maintain diversity in the specificities of antibody responses, especially in the context of viruses that readily mutate their genomes to escape immune pressures. Antibody responses that are disproportionally focused on one or a few epitopes readily select for viral escape mutants (Lee et al., 2019). A way to prevent escape is to ensure sufficient diversity in the antibodies targeting an antigen, as the likelihood a pathogen can simultaneously produce multiple evasive mutations is low. This same concept is utilized in anti-retroviral therapy against HIV, as drug combinations that target various pathways of the viral life cycle are utilized to minimize the risk of viral resistance (Atta et al., 2019). Thus, the primary goal of most vaccination strategies is to elicit high affinity neutralizing antibody titers while also maintaining sufficient diversity to protect against pathogenic variants. How this is achieved is discussed in the following sections.

Generation of B cell diversity in the naïve repertoire through V(D)J recombination

Humans and mice have 10^{12} and 10^{8} circulating naïve (antigen-inexperienced) B cells at any given time, respectively, and every naïve B cell has a unique binding specificity encoded by its B cell receptor (Briney et al., 2019; Schroeder, 2006). As the genome is estimated to contain ~20,000 protein coding genes, it is impossible for this vast BCR diversity to be encoded in the germline (Nurk et al., 2022). Instead, during their

development in the bone marrow, B cells undergo semi-random genetic recombination events to produce unique coding sequences that are translated into the BCR.

The immunoglobulin heavy chain locus spans a massive 1250 kilobases (Kenter et al., 2023). It is organized into a multitude of gene segments separated by intervening DNA – when recombined together, these gene segments form the coding sequence for the BCR (Figure 3). The first set of gene segments at the 5' end of the locus are the V genes, of which there are ~129 in humans. The V gene codes for the N-terminus of the antibody and includes the sequences for CDR1 and CDR2. Downstream of the V genes are a set of 27 D gene segments and a set of 9 J gene segments (Rodriguez et al., 2023). During a process called V(D)J recombination, one V gene is selected and paired in a semi-random fashion with one D and one J gene segment. This combination of individual gene segments already creates a multitude of options for the sequence of the variable region. Furthermore, at the junction between V, D, and J segments, both resection and addition of non-templated nucleotides can occur, and this junctional nucleotide sequence becomes the highly diverse CDR3 of the variable region. Once the V, D, and J segments are recombined, they form the coding sequence for the V_H region of the antibody. A similar process occurs at the light chain loci, as V gene segments are recombined with J gene segments to form the variable regions of kappa or lambda light chains. In mature B cells, the heavy and light chain loci are transcribed, and the V_H and V_L regions are spliced together with exons encoding the constant regions to form the coding sequence of the entire BCR (Willerford et al., 1996).

V(D)J recombination occurs in manner that is entirely independent of antigen. In addition to the combinatorial diversity from selection of individual V, D, and J elements and the removal and addition of nucleotides at the V-D-J junction, the pairing of heavy and light chains creates even further possibilities for the structure of the BCR. Thus, the process of V(D)J recombination is responsible for ability of the naïve B cell repertoire to recognize and respond to virtually any foreign antigen.

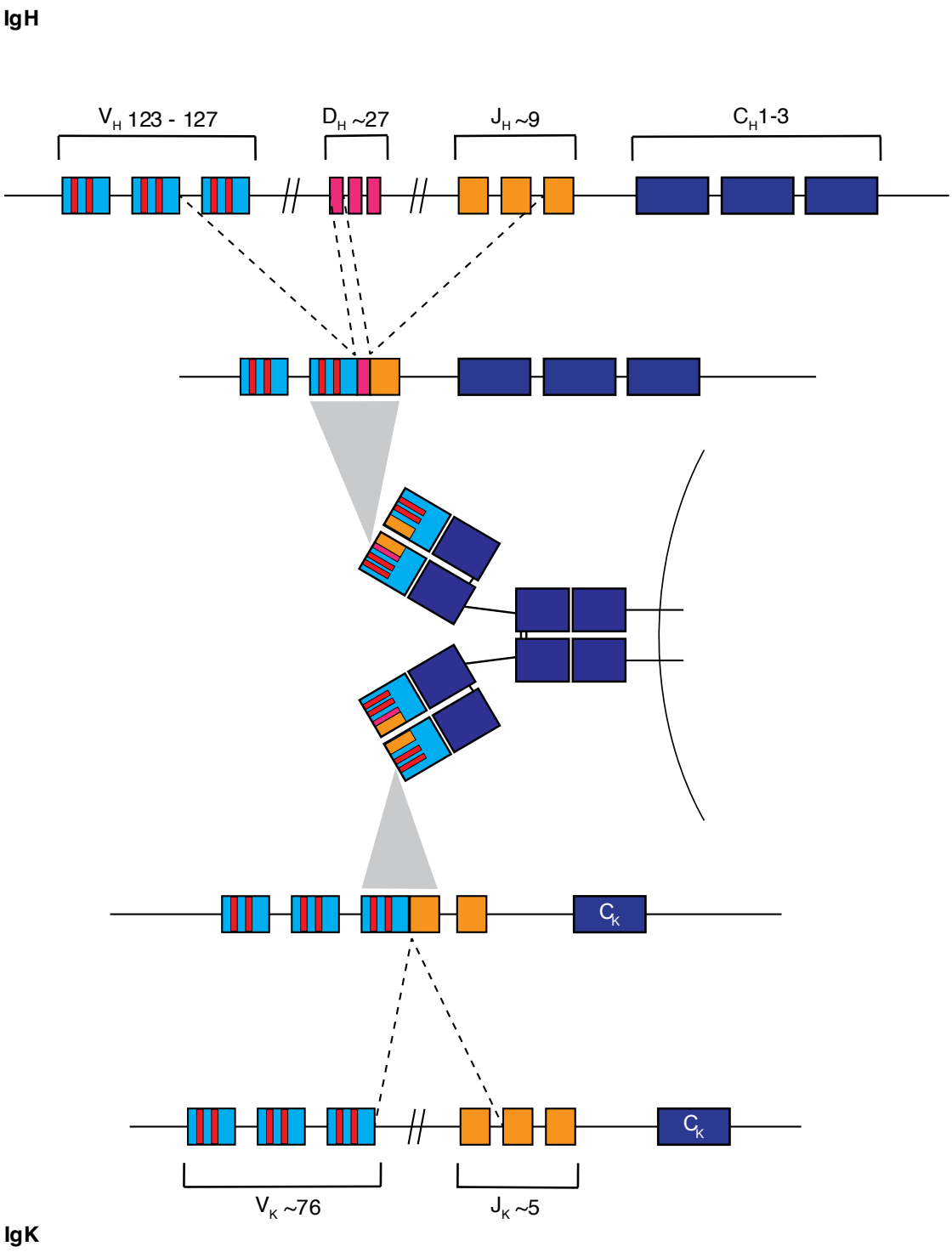

Figure 3: V(D)J Recombination generates diversity in the naïve B cell repertoire
Cartoon depiction of recombination of heavy chain (top) and kappa light chain (bottom) loci during B cell development.

T cell interactions at the T-B border determine entry into the germinal center response

During immunization or infection, the subset of naïve B cells that bind the offending antigens via their BCRs become activated and begin to proliferate to form B cell clones. A B cell clone is defined as a population of B cells derived from the same naïve ancestor, and they are usually identified by the sharing of their V, D, and J segments and identical nucleotide lengths of their CDR3s. B cell responses can be T cell-independent or T cell-dependent, and the balance between the two is decided by the nature of the antigen. With antigens that induce strong signaling through co-receptors (such as TLRs), B cells can differentiate directly into short-lived plasmablasts that secrete low-affinity antibody. Also, when antigen is highly multivalent, engagement of multiple BCRs on the same B cell circumvents the requirement of T cell help for differentiation into plasmablasts (Elsner and Shlomchik, 2020).

Canonical B cell responses require T cell help. In the absence of T cells, affinity maturation of antibody responses does not occur, and soluble antigens with low valency fail to elicit a response. In addition to signaling through the BCR upon binding, B cells internalize their antigen, which is then shuttled to degradative endosomal compartments for the ultimate production of peptides that are presented on MHCII molecules. The antigen-presenting feature of B cells allows for their interaction with cognate $CD4^+$ T cells present in secondary lymphoid organs. This process is relatively rapid, as B cell blasts can be observed interacting with T cells at the T-B border within 2 days of immunization (Garside et al., 1998; Okada et al., 2005; Schwickert et al., 2011). Signals

at the T-B border instruct the fate-decision of the B cell. From here, B cells can differentiate into extrafollicular plasmablasts or migrate to the center of the follicle and become germinal center (GC) B cells (Paus et al., 2006).

The T-B border represents the first bottleneck in B cell clonal selection. T cells discriminate among B cells based on their BCR affinity, which is conveyed via peptide-MHC-II density on the surface of the B cell. B cells with higher germline affinities can internalize more antigen and therefore present more peptide to cognate T cells. This creates a competitive dynamic for activation, proliferation and GC entry that is governed by T cell help. In adoptive B cell transfer models, low-affinity B cells that normally form GCs alone are entirely outcompeted when co-transferred with high affinity B cells recognizing the same epitope, implying the presence of a limiting factor governing GC entry (Porto et al., 2002; Schwickert et al., 2011). The amount of antigen presentation by individual B cells, however, does not change in the presence of higher-affinity B cells. In addition, increasing the antigen dose fails to rescue the relative disadvantage of low-affinity cells in entering GCs, indicating that antigen is not limiting, at least at conventional doses used for immunization (Schwickert et al., 2011). On the other hand, increasing T cell help to a subset of B cells is sufficient to increase their entry into the GC relative to identical B cells not receiving additional help (Schwickert et al., 2011). These experiments show T cell help is limiting at the level of GC entry and, thus, describe the first bottleneck that determines the clonality of a B cell response.

The GC drives affinity maturation

The GC is the site of B cell clonal selection and affinity maturation. Once in the GC, B cells couple proliferation with somatic hypermutation mutation (SHM) of their BCRs via the action of an enzyme called activation-induced cytidine deaminase (AID). AID selectively deaminates cytosine residues to generate deoxy-uracil which can trigger several DNA damage repair pathways resulting a spectrum of characteristic SHM mutations in proximity to the initial lesion. SHM occurs at a rate of ~10^{-3} base pairs per generation, which is approximately a million-fold higher than the accumulation of genomic mutations during normal cell replication (Chaudhuri et al., 2014). Mutagenesis of V(D)J and VJ exons along with continued proliferation results in a panel of cells in which each member of a B cell clone differs only slightly in its ability to bind antigen. The GC is segregated into two anatomical zones, the dark zone and the light zone. SHM and proliferation occur predominantly in the dark zone, while selection occurs in the light zone. GC B cells test the affinity of their new BCRs in the light zone, where they bind to antigen found tethered to follicular dendritic cells (FDCs). As mutations are produced randomly, GC B cells that happen to accumulate affinity increasing mutations are more competitive at acquiring antigen from FDCs and presenting peptide to T follicular helper (T_{FH}) cells also present in the light zone. The strength of T_{FH} cell help, which is proportional to the peptide-MHCII density on the B cell surface, determines the extent of proliferation of B cells upon dark zone re-entry (Victora et al., 2010; Gitlin et al., 2014; Gitlin et al., 2015). Within the light zone, GC B cells can also be exported as memory B cells, which are primed for activation in response to re-challenge with

homologous antigen, or as antibody secreting plasma cells, which can home to the bone marrow and secrete antibody systemically (Kometani & Kurosaki, 2015). This iterative cycle of proliferation and mutation in the dark zone followed by selection and export in the light zone forms the basis of affinity maturation, the process by which humoral responses bind better to antigen overtime (Victora and Nussenzweig, 2022). As both memory B cells and plasma cells can be long-lived, the GC reaction provides protection not only during the duration of an initial response but also for future encounters with the same or similar pathogens.

Most of our knowledge of affinity maturation in the GC comes from studying anti-hapten responses (Bereke et al., 1991; Jacob et al., 1991). A hapten is a small chemical group that elicits immune responses only when conjugated to a larger carrier protein (Landsteiner & Scheer, 1931). A hapten alone cannot prime B cell responses for two reasons; it cannot cross-link multiple BCRs on the surface of individual B cells and it does not have a peptide component necessary to recruit T cell help. Haptens are convenient model antigens because they elicit highly reproducible responses across mice. For example, a large fraction of GC B cells responding to the hapten NP harbor the VH186.2 heavy chain and an Igλ light chain (Jacob et al., 1993). Effectively biasing the GC response towards one specificity is akin to tracking one GC B cell clone over time and has allowed immunologists to develop a deep understanding of somatic hypermutation and affinity maturation. With NP responses, for example, a W33L mutation in VH186.2 alone results in a 10-fold enhancement in affinity for NP (Allen et

al., 1988). The accumulation of this mutation is highly reproducible, and BCRs harboring W33L become heavily enriched among NP binders throughout the course of a response. As such, conclusions about GC dynamics have been dominated by findings from hapten-carrier systems.

Clonal selection in the GC

Compared to the molecular mechanisms of affinity maturation, clonal selection in the GC remains poorly understood. Hapten models establish affinity as a main parameter driving clonal selection in the GC. However, while these models are valuable for studying *intra*clonal selection, they fail to address *inter*clonal selection. Although the number varies depending on the antigen used, it is estimated that on the order of 100 distinct B cell clones enter a single GC following immunization (Tas et al., 2016). In single-protein immunizations, each B cell clone draws upon the same pool of T cell help. Therefore, the assumption based on hapten models is that clones that develop the highest affinity will dominate the GC pool, as these cells will be able to obtain the most T cell help. In reality, clonal selection in the GC is far more complicated. A fate-mapping study in which GC B cells were randomly labeled at the onset of a reaction with a combination of ten possible colors revealed that, overtime, many GCs become dominated by one color, or one clone (Tas et al., 2016). However, even within the same node there exist GCs that maintain their initial color diversity, and these demonstrate far more polyclonality. GCs dominated by a single color are defined by clonal bursts, wherein one variant of a B cell clone undergoes a massive proliferation event resulting

in multiple daughter cells that overtake the GC. Cells undergoing clonal bursts are invariably higher-affinity than their unmutated ancestors – however, it is not always the case that the highest-affinity cell in the GC is the one that bursts. Furthermore, GCs that do not undergo clonal bursts and retain their polyclonality still achieve efficient affinity maturation. These findings are incompatible with affinity as a sole driver for *inter*clonal selection in the GC. Therefore, there must exist other parameters governing *inter*clonal competition during a humoral response.

Antibody-mediated feedback

One such potential parameter is antibody-mediated feedback, which is the phenomenon by which immunoglobulin modulates B cell responses through binding antigen. This regulatory role was first observed in the early 1900s with humoral responses to diphtheria toxin in mice, as researchers found increasing the anti-toxin to toxin ratio during immunization had a suppressive effect on endogenous antibody production (Smith, 1909). The following century was marked by many efforts to decipher the mechanisms of antibody feedback, and important developments in the field and examples of antibody feedback are discussed in the following sections.

Prevention of maternal alloimmunization with anti-RhD immunoglobulin

The most clinically pertinent example of antibody feedback comes from the prevention of maternal alloimmunization to Rh antigen groups present on fetal erythrocytes. When an RhD^- mother conceives with an RhD^+ father, there is potential for an antigenic

mismatch between the mother and fetus. During childbirth or miscarriage, the mother is exposed to fetal red blood cells (RBCs), resulting in the priming of an anti-RhD response by maternal B cells. Although this rarely impacts the first child, the consequences for subsequent RhD+ pregnancies are dire, as maternal anti-RhD IgG can cross the placenta, gain access to fetal circulation and lead to the destruction of fetal RBCs (Kumpel, 2006). This results in a condition called hemolytic disease of the newborn, which is often lethal.

Hemolytic disease of the newborn has become a rare disease due to intervention with anti-RhD immunoglobulin. In RhD^- mothers at risk of alloimmunization, polyclonal anti-RhD IgG is administered around 28 weeks of gestation and shortly after childbirth; this prevents the mother from developing her own anti-RhD response and spares future RhD+ fetal RBCs from destruction. Although anti-RhD therapy is highly efficacious, its exact mechanism is poorly understood. Epitope masking, the direct blocking of RhD specific B cells from binding their antigen, seems to be an unlikely explanation, as it is estimated only 5% of D epitopes are bound by anti-D (Brinc and Lazarus, 2009). Another possibility is that IgG coated fetal RBCs engage FcγRIIb on RhD specific B cells and inhibit their response. In animal models with sheep red blood cell (SRBC) immunization however, Fc-independent suppression has been observed, calling a FcγR mechanism into question (Heyman, 2000). The most likely mechanism is clearance of fetal RBCs by the injected antibody. In fact, there is a clear correlation between antigen clearance and the anti-D response in the setting of polyclonal anti-D administration.

However, the same correlation does not always apply in studies with monoclonal RhD antibodies, and in some cases responses to RhD are even enhanced despite efficient antigen clearance (Kumpel, 2007). This likely results from differential FcγR involvement and is based on the Fc configuration dictated by both the isotype and glycan. Studies investigating multiple Fcs while keeping Fab regions constant will be needed to shift anti-Rh therapy to a more accessible and scalable monoclonal approach.

Passive maternal immunity

Antibody feedback is also evident from another mother-neonate interaction. Maternal IgG from placental transfer and IgA from breastfeeding provide passive immunity to newborns who are highly susceptible to disease due to immune inexperience. In fact, maternal immunization against pertussis, tetanus, and influenza results in a significantly lower rate of infant hospitalization and death (Benowitz et al, 2010; Kachikis & Englund, 2016). However, multiple clinical studies also exist that link high neonatal maternal antibody titers with diminished infant vaccination responses, resulting in higher risk of developing certain diseases during infancy, even following immunization (Borràs et al., 2012; Englund et al., 1995; Kurikka et al., 1995; Maertens et al., 2017). One such study establishes an inverse correlation between antigen specific IgG titers present at birth and IgG titers 4 weeks after immunization with pneumococcus, tetanus, pertussis and HiB, although nearly all infants reach protective levels of antibody (Jones et al., 2014). In addition, infants of mothers who receive a pneumococcal vaccine in the third trimester are at increased risk of developing acute otitis media during the first six

months of life (Daly et al., 2014). These observations may be explained by the potential mechanisms of antibody feedback discussed previously. A clever mouse model of early life immunization demonstrates that pre-existing maternal antibodies completely inhibit formation of neonatal IgG titers to influenza HA, without affecting total $CD4^+$ T cell responses. Although maternal antibody does not impact the formation of GC responses, it inhibits memory and plasma cell output from GCs. Furthermore, the presence of maternal antibodies alters the V gene usage pattern of immunization-induced GCs, indicating that existing antibody repertoires can qualitatively impact the process of clonal selection into or within the GC (Vono et al., 2019). A better understanding of antibody feedback in the context of passive maternal immunity is required to optimize the timing of neonatal vaccination regimes.

Administration of exogenous antibody during immunization

The most common approach to investigating antibody feedback has been via administration of antigen-specific antibody during or around the time of immunization. This has yielded varied and sometimes contradictory results, which are summarized in the following paragraphs.

IgM predominantly enhances antibody responses, although reports of suppression at higher concentrations also exist. Intravenous (IV) injection of anti-SRBC IgM shortly before IV immunization with SRBCs increases the production of antibody forming cells in the spleen by four to five-fold and improves serum IgG titers by three-fold. This

phenomenon is dependent on fixation of complement, as administration of cobra venom factor (which depletes circulating C3 to <5%) and utilization of mutant IgM unable to activate complement prevent enhancement (Heyman et al., 1988). In addition, IgM enhancement is rarely seen with soluble protein immunogens – this is likely due to the conformational change IgM must undergo to activate complement, which can only be achieved when epitopes are arrayed in an ordered fashion on particulate antigens. IgM enhancement is also seen with monoclonal preparations of anti-NP IgM in the context of NP-coupled SRBC immunization. However, increasing the dose of the anti-NP IgM mAb to 100 μg results in an inhibition of the NP response (Bruggemann and Rajewsky, 1982). It is likely that epitope masking dominates at very high antibody to antigen ratios, as this increases the probability NP epitopes are inaccessible to circulating B cells. IgM mediated suppression is also observed when anti-SRBC IgM is administered 2-48 hours following immunization, even when the same preparation administered prior to immunization leads to enhancement (Wason, 1973). This may be explained by the localization of antigen at the time of antibody administration, as a significant proportion of antigen reaches splenic follicles withing hours of immunization, which alters the dynamics of immune complex formation. Enhancement of the humoral response by pre-existing IgM has led to the suggestion that natural IgM present in the absence of antigenic exposure can act as an adjuvant to promote B cell activation (Boes, 2000).

The effect of IgG administration on humoral responses varies based on the immunization antigen used. The most documented effect of IgG is suppression, as

production of primary IgM and IgG against haptenated SRBCs is decreased by up to 100-fold in the presence of exogenous IgG (Heyman, 1990). This suppression correlates with both the dose and the affinity of the IgG preparation used. There are three main possible explanations for IgG mediated suppression of humoral responses: 1) antibodies accelerate antigen clearance and thereby limit its access to B cells (Brinc & Lazarus, 2009), 2) antibodies present in immune complexes engage the inhibitory FcγRIIB receptor found on the surface of B cells and dampen responses to the same antigen (Bournazos et al., 2017), or 3) antibodies mask epitopic sites on the antigen and inhibit binding and activation of B cells that recognize the same, or overlapping, epitopes (Bergström et al., 2017). The first two mechanisms are Fc-dependent and predict suppression occurs *at the level of the whole antigen*, while the third mechanism is Fc-independent and predicts suppression is *epitope specific* (Figure 4). Whole antigen clearance is unlikely, as other immune parameters such as T cell priming remain the same in the presence and absence of exogenous IgG (Kappler et al., 1971). The suppressive effect of IgG is maintained in mouse FcγR knock-out models, implying suppression is Fc-independent (Karlsson, 1999). Although there exist conflicting reports regarding the effects of $F(ab)_2$ fragments on B cell responses, impaired suppression is likely due to their decreased half-life as compared to full length IgG (Cerottini et al., 1969; Enriquez-Rincon & Klaus, 1983). Epitope masking is observed in cases when hapten-specific IgG antibodies are able suppress plasmablast responses to hapten but not to the SRBC carrier (Bergström et al., 2017; Möller, 1985). While studies also exist showing suppression is not epitope specific, this is likely due to the density of hapten on

the SRBC – higher densities bind more antibody which can then sterically hinder carrier specific B cells from binding their targets. Therefore, the inhibition still seems to occur via blocking, and not the Fc.

Figure 4: Three Models of IgG Mediated Feedback
i) Antigen clearance. Circulating IgG bound to antigen engages FcγRs present on phagocytic innate immune cells, resulting in clearance of antigen from the periphery and sequestration from potentially responsive B cells. This form of inhibition is on the level of the entire antigen.
ii) FcγRIIb engagement. FcγRIIb is an inhibitory FcγR found on the surface of B cells. When bound to IgG found in immune complex, FcγRIIb dampens BCR signaling and can inhibit activation of B cells binding the same antigen. As with clearance, this form of inhibition is non-epitope specific.
iii) Epitope masking. Antibody competes for binding to antigen only with B cells that bind the same, or overlapping epitopes. This form of inhibition is epitope specific, as an antibody can only inhibit responses to its own epitope.

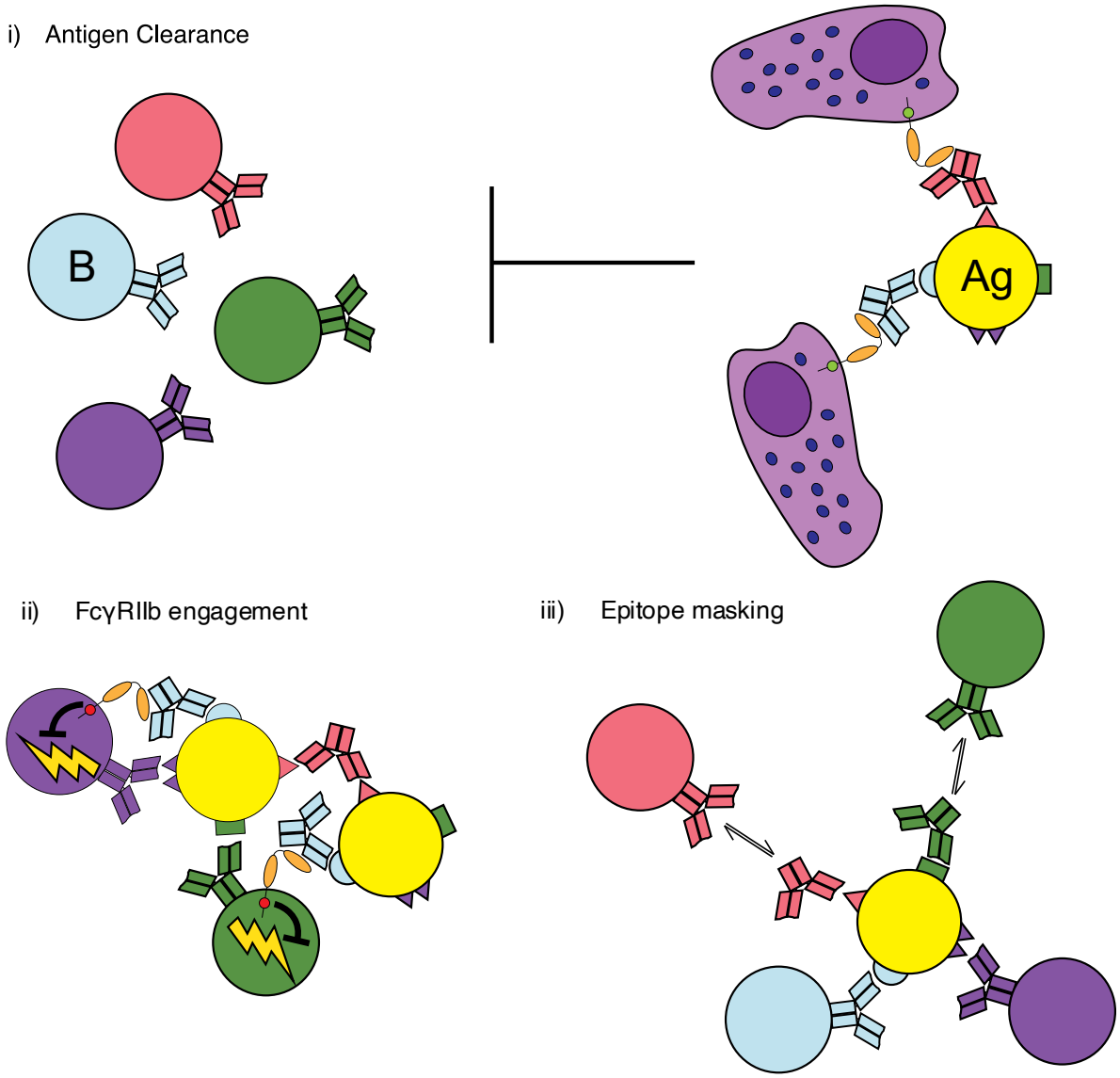

Figure 4: Three Models of IgG Mediated Feedback

Instances of IgG enhancement have also been documented, usually in response to immunization with soluble hapten-carrier antigens. In fact, the same anti-TNP IgG monoclonal suppresses B cell responses when TNP is conjugated to SRBCs but enhances responses when TNP is conjugated to KLH (Enriquez-Rincon & Klaus, 1983). This discrepancy likely results from the nature of the immunogen, as SRBCs are large and particulate while KLH is a relatively small soluble protein, altering the types of immune complexes than can be formed. IgG enhancement is dependent on the antibody Fc, as this effect is not seen with FcγR-deficient mice which have a functional complement system (Wernersson, 1999).

Pre-existing antibody influences B cell entry into GC responses

Studies performed throughout the 20th century convincingly demonstrate antibody can both suppress and enhance B cell responses in toto. However, the influence of pre-existing antibody on the clonality of the GC, memory, and plasma cell compartments is just beginning to be understood. Many early experiments were performed with hapten-carrier immunogens, which focus B cell responses onto one epitope and severely limit the extent of interconal competition. The transition to the use of complex antigens and infection models has resulted in an appreciation of how pre-existing antibody influence the clonality of B cell responses.

B cell receptor knock-in mice have greatly advanced our understanding of antibody feedback by enabling investigation of epitope specific responses to complex antigens. In a pre-clinical mouse model of HIV protein immunization, priming mice with gp160 protein suppresses the entry of gp160 specific B cells into secondary GCs; this effect was phenocopied by transferring IgG formed during the primary response prior to immunization (Tas et al., 2022). Furthermore, entry of the transgenic BCR clone into the GC was inversely proportional to both the quantity and the affinity of a monoclonal antibody administered prior to immunization, but only when the antibody was specific for the same epitope. Interestingly, in the same study, entry of BCR knock-in B cells specific for S protein of SARS-CoV2 into secondary GCs was enhanced when mice were primed. This incongruence was attributed to the differences in the diversity of the antibody response to both immunogens. In the case of HIV protein, serum titers following immunization are focused on one epitope, while serum titers to S-protein are far more polyclonal. Therefore, it is possible that at high levels of antibody, epitope masking dominates, and the overall effect is suppression, while at lower levels of antibody immune complex formation may increase B cell antigen acquisition and deposition onto FDCs.

Antibody feedback is also evident from immunization regimens against malaria. In humans, protective anti-circumsporozoite (CSP) protein titers plateau after the first boost with radiation-attenuated *P. falciparum* sporozoites (McNamara, 2020). The same saturation is observed in mice harboring a fixed heavy chain against the

immunodominant, repeat region of CSP. Anti-CSP transgenic memory B cells do not enter secondary GCs, and this effect is phenocopied during a primary response by the transfer of serum antibody from immunized mice. In the case of malaria, antibody suppression occurs at levels below those that are required for protection, implying the antibody formed during the primary response is a hinderance in developing protective humoral immunity. However, high titers against the immunodominant region of CSP diversifies antibody responses towards other less explored, subdominant epitopes. Therefore, although antibody feedback places a suboptimal ceiling on the amount of antibody directed towards a specific epitope, it may prevent over-focusing of responses onto immunodominant epitopes. In fact, a strong pattern between pre-existing antibody and responses also exists in the case of influenza infection. In humans, who have preexisting immunity to influenza due to multiple exposures throughout their lifetimes, there is a clear negative correlation between pre-existing strain-specific titers and the detection of activated plasmablasts following immunization with the homologous strain (Andrews et al., 2015a). Furthermore, while certain individuals developed broadly cross-reactive antibodies targeting the stem region of hemagglutinin upon first exposure to the 2009 pandemic strain, this subset was not boosted upon revaccination the following year (Andrews et al., 2015b), implying that high pre-existing stem titers may negatively impact the future success of B cell clones targeting stem epitopes.

Pre-existing antibody also affects B cell recruitment into the memory B cell compartment. This is seen in humans, as patients receiving a combination of two

therapeutic anti-S protein monoclonal antibodies prior to SARS-CoV-2 mRNA vaccination generate memory responses that shift away from epitopes targeted by the exogenous mAbs (Schaefer-Babajew et al., 2023). In addition to shaping the clonality of B cell responses, antibody can also influence the affinity threshold for B cell recruitment. In the same study, administration of antibody lowers the affinity of anti-S memory cells produced via immunization. In both SARS-CoV2 and HIV mouse immunization models, pre-existing antibody enables the recruitment of lower-affinity B cells into GCs (Hägglöf et al., 2023). This effect may be explained by the ability of antibody to form multimeric immune complexes that increase the avidity of interaction with lower affinity B cells, thus allowing them to partake in the response.

GC self-regulation via antibody feedback

It has become evident that antibody existing prior to antigenic challenge influences the participation of B cell clones into *de novo* responses, with implications for vaccination regimes with multiple boost requirements. However, the question remains whether antibody produced by an ongoing response can feedback onto a contemporaneous GC reaction, acting as a driver of clonal selection and affinity maturation. When exogenous antibody is transferred prior to antigenic challenge the observed effects on the B cell response mostly result from interference of signaling at the T-B border, the first step at which B cells are instructed to differentiate into GC B cells or extrafollicular plasmablasts. For example, high titers of antibody against a specific epitope will restrict access of antigen by B cells specific for the same epitope. These B cells will not be able

to acquire sufficient antigen to presentation to T cells and will therefore not be selected at the T-B border, allowing for participation of B cells with different specificities. Whether a similar process occurs within GCs, where antigen is acquired in multimeric form from the surface of FDCS, is largely unknown.

Mathematical modeling of the GC reaction identifies epitope masking via antibody as an important mechanism for maintaining upwards directionality of affinity maturation and placing a timely end to the GC. This model assumes dynamic re-entry of antibody produced by a response into the GC – as higher affinity antibody is produced it outcompetes and replaces the lower affinity antibody present on immune complexes on FDCs. This allows for efficient, directional affinity maturation, as GC B cells compete for access to antigen with recently produced antibody. Only those cells with higher affinity than the soluble antibody will be selected, ensuring affinity increases overtime, in a classic “traveling wave” model. After some time, the antibody produced by the GC will reach its maximal affinity, and the reaction will cease. *In vivo* experiments support some of these predictions. Mice unable to produce the secreted form of antibody undergo less affinity maturation and have longer-lasting GCs in response to immunization with NP-OVA. IV administration of anti-NP IgM during the GC results in its accumulation onto FDCs in an affinity dependent manner, as higher affinity IgM is more resistant to replacement by endogenous antibody (Zhang et al., 2013). IgM injection also reduces the percentage of NP-binding B cells in the GC through the induction of apoptosis. Despite this, serum affinity maturation is enhanced, particularly when IgM of high affinity

is administered three days after immunization. In this case, the presence of high-affinity antibody acts as a selection threshold for GC B cells, and only those with higher affinity than the antibody escape apoptosis to remain in the GC and ultimately become plasma cells. Therefore, while the total number of NP-binding GC B cells decreases, these are significantly enriched in high affinity cells. However, administration of high-affinity IgM five days post-immunization had no effect on serum affinity. There are two possible explanations for this discrepancy between administration at 3 days and 5 days. The first possibility is that, at the later time point, the IgM is not of high enough affinity to outcompete endogenous antibody already present in the GC, and therefore it cannot exert its influence on selection. The second possibility is that administration at day 3 is early enough to influence fate decisions at the T-B border, indicating the affinity enhancing effect may be a result of differential recruitment into the GC rather than selection within the GC.

While it is clear IV that administered antibody can gain access to the GC, the use of exogenous immunoglobulin inherently precludes investigation of a mechanism that is supposedly self-regulating. In addition, it is unknown whether similar results would be obtained with other isotypes, as IgM is known to have an enhancing effect when administered prior to immunization. Finally, as discussed previously, the use of hapten as a model antigen severely limits the assessment of clonality, as there is absence of *inter*clonal competition. A loss-of-function model is better suited to study a process that is self-regulated, as this would circumvent administration of arbitrary amounts of

antibody. A CD138-DTR genetic mouse model was used to test the hypothesis that antibody is responsible for the shift of specificity from Wuhan to Omicron S protein following consecutive boosts with an mRNA vaccine. In this model, administration of diphtheria toxin results in the killing of any $CD138^+$ cell, including plasma cells, leading to the depletion of serum antibody (Vijay et al., 2000). When antibody was depleted during an ongoing response to mRNA vaccination, cross-reactivity to Omicron decreased in the primary GC and in the plasmablast compartment following boost, despite the maintenance of total numbers of Wuhan S-protein binders (Inoue et al., 2022). This implies that antibody formed during a B cell response can modify the trajectory of the same response by shifting specificities towards epitopes that are less favored at the onset. However, the exact effect this has on the clonality of the B cell response and affinity maturation was not explored.

In the studies described above, antibody is proposed to exert its effect on selection in the GC through epitope masking. However, Fc dependent modes of antibody regulation have also been demonstrated. In humans vaccinated against influenza, anti-HA IgG1 serum antibodies undergo dynamic changes within their glycan structure through the addition or removal of certain sugar moieties. One week following immunization, there is an increase in sialylated and fucosylated IgG1, followed by a relative depletion of these glycans at week 3. Sialylated and fucosylated glycans bias the binding of IgG1 to the immunomodulatory type II FcγRs, DC-SIGN and CD23. In the case of influenza vaccination, sialylated antibodies in immune complex with HA bind to CD23 present on

GC B cells and upregulated their expression of FcγRIIb. By doing so, the affinity threshold of selection in the GC increases, as BCR signaling must overcome inhibitory FcγRIIb signaling to prevent cell death. In mice, immunization with HA in immune complexes containing sialylated antibody resulted in significantly higher serum IgG affinity than immune complexes containing asialylated antibody or HA alone – this was also dependent on the presence of CD23 (Wang et al., 2015). Furthermore, by an incompletely understood mechanism, sialylated antibody increased both the reactivity and the affinity to the conserved stem domain of HA, serving as another example of how understanding the mechanisms by which antibody influences selection in the GC can help inform vaccine design.

Here, we report the development of a simplified loss-of-function genetic mouse tool to clarify the mechanisms of antibody feedback during a contemporaneous humoral response. Our model allows for the deconvolution of epitope specific effects, mediated by antibody masking, from epitope non-specific effects, mediated by antigen clearance and FcγRIIb ligation. We find that antibody-mediated feedback acts predominantly via epitope masking during ongoing GC responses, limiting the expansion of B cells clones binding to the same epitope, which occurs both in adoptive B cell transfer systems and polyclonal responses. However, while antibody helps guide clonal selection within the GC, it has no discernable effect on its average affinity. Thus, feedback from a traveling wave of antibody of increasing affinity is not required to drive GC *intra*clonal selection and affinity maturation.

CHAPTER 2: Designing a Loss-of-Function System to Study Antibody Feedback

To investigate antibody-mediated feedback as a method for self-regulation of a contemporaneous GC reaction we created an oligoclonal transgenic B cell system with the ability for temporally controlled ablation of plasma cells, and thus, removal of antibodies produced by specific clones. In wild-type mice immunized with complex multi-epitope antigens, an average of ~100 clones enter each individual GC (Tas et al., 2016). Determination of the specificities of these clones is costly and time-consuming and any antibody driven effects on GC maturation can only be retrospectively inferred. Creating an oligoclonal GC reaction wherein B cell specificities are predetermined allows for tracking of specific clones over time and provides a tool for developing an *a priori* understanding of antibody feedback. Crucial to this model is that the B cell clones bind to distinct, non-overlapping sites on the same antigen – this allows us to separate epitope-specific effects, mediated by antibody masking, from epitope-agnostic effects, mediated by FcγRIIb ligation and antigenic clearance. Depletion of epitope-specific titers during an ongoing humoral response and interrogation of the ensuing clonal dynamics of the GC reaction provides a loss-of-function approach to understand how antibody influences clonal selection and affinity maturation of B cell responses. The following sections describe the genetic tools we have produced towards this effort.

Characterization of anti-HA BCR specificities

We chose influenza virus hemagglutinin (HA) as a model antigen for our oligoclonal B cell system. HA is the membrane protein responsible for viral binding and entry into host cells, and thus is a major target for neutralizing antibody titers. In fact, the efficacy of vaccines against influenza is primarily determined via hemagglutination inhibition assays, which read out the ability of serum antibodies to prevent HA from binding its sialic acid targets. HA has been intensively studied, and five major antigen sites on the head domain of PR8 HA have been identified by the characterization of antibody escape mutants (Gerhard et al., 1981; Caton et al., 1982). The minimal antibody footprints of these binding sites do not overlap, making HA an ideal candidate for which to develop an oligoclonal B cell response to which B cells recognize different epitopes on the same antigen (Figure 5A). Most of the antibody response in both mice and humans is directed towards the five antigenic sites, increasing the likelihood these specificities would also be successful in a transgenic BCR system. To obtain candidate B cell specificities directly from GC reactions, we infected C57BL/6 mice with 33 PFU of mouse-adapted PR8 influenza virus and single-cell sorted HA tetramer-binding GC B cells 21- and 45-days post-infection (Figure 5B). We sequenced the *Igh* and *Igk* loci of each cell and selected 20 expanded clones from which we recombinantly produced the antibodies of one of their members. All antibodies detectably bound HA in ELISA, confirming the validity of our approach using tetramer to detect HA binding GC B cells (Figure 5C). We then determined the epitope specificities of the mAbs in two ways; by assaying them against a panel of five PR8 HA mutants each with only one of their

antigenic sites intact, and by competing them all with one another to ascertain binding patterns of groups of antibodies. Several clones bound predominantly to one of the HA variants, serving as good candidates for further characterization (Figure 5D). Competition ELISAs demonstrated a high degree of mutually exclusive binding among the assayed mAbs (Figure 5E). While there were multiple pairs of mAbs that did not compete with one another, we failed to identify three that could simultaneously bind HA. There are two main reasons for this. First, an antibody (~150 kDa) is nearly the same size as an HA trimer (~180 kDa). Although antibody contact footprints may not overlap, steric hinderance from Fc portions may interfere with binding of antibodies to distinct sites. Second, anti-HA antibody responses predominantly target the immunodominant head domain at the expense of the stalk, resulting in excessive crowding of antibodies at one end of the antigen.

Figure 5: Identifying candidate B cell clones for BCR knock-in mice
A) Crystal structure of PR8 HA (PDB ID 1RUZ) viewed from the side and the top, with five major antigenic sites highlighted.
B) C57BL/6 mice were infected with PR8 influenza virus and mediastinal GC B cells were assayed by flow cytometry 21 and 45 days later. HA tetramer binding B cells were single cell sorted, their *Igh* and *Igk* loci were sequenced, and monoclonal antibodies were produced from members of 20 expanded clones.
C) Titration curves of candidate mAbs binding to recombinant PR8 HA via ELISA.
D) ELISA of mAbs binding to five Δ4 mutants, in which all but one of the five antigenic sites are mutated. Antibodies were assayed at a concentration of 1 μg/mL.
E) ELISA competition matrix between each antibody with itself and other mAbs. Biotinylated antibodies were competed with unlabeled antibodies, and competition was measured as intensity of biotin signal as compared to the biotinylated antibody alone. The competing mAb was used in five-fold excess to increase detection sensitivity.

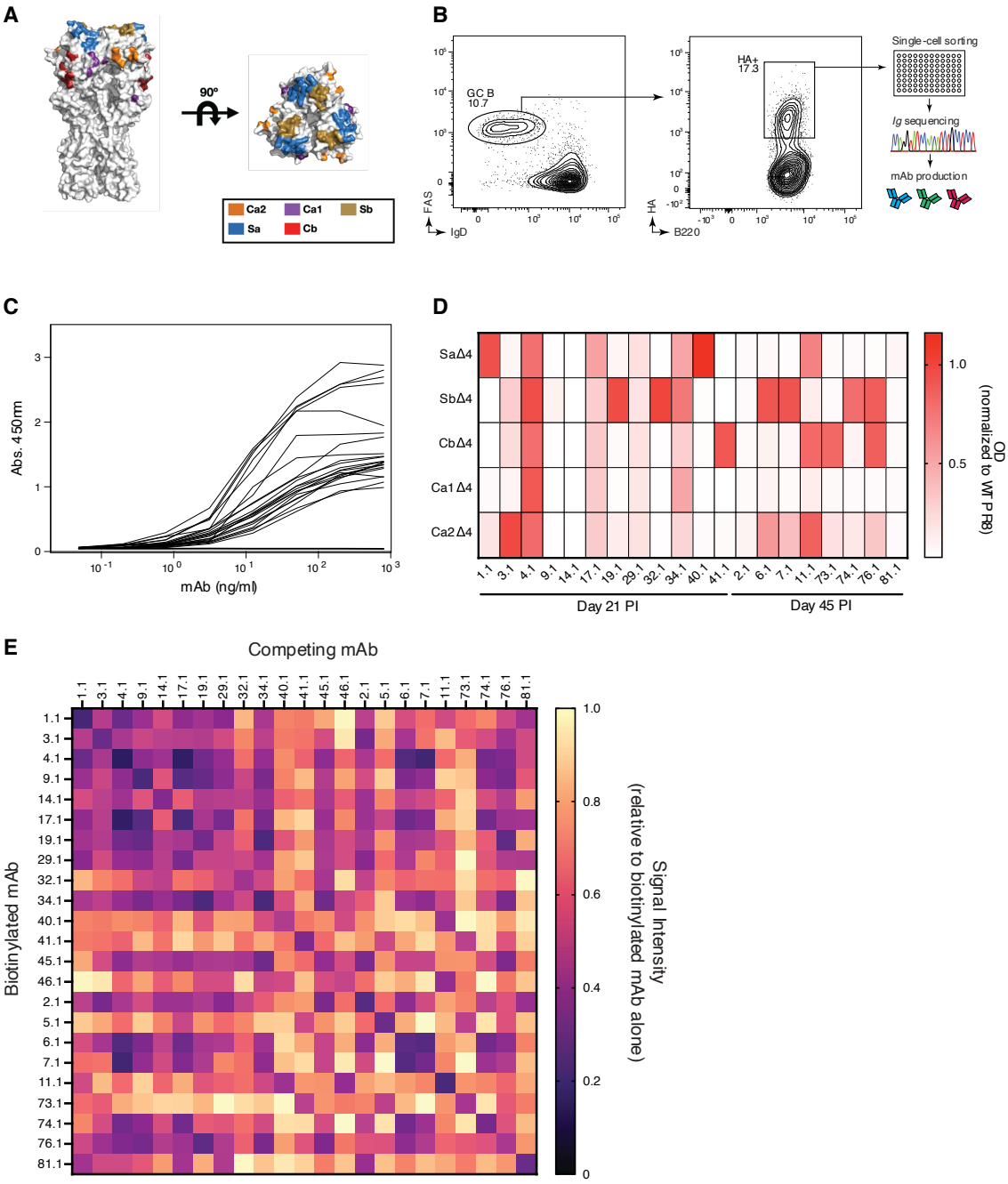

Figure 5: Identifying candidate B cell clones for BCR knock-in mice

From our panel of 20 mAbs, we selected non-competing clones 1.1 and 73.1, which bound antigenic sites Sa and Cb, respectively. Sa and Cb are both immunodominant epitopes in the context of immunization and infection, increasing the likelihood transgenic B cells specific for these epitopes will engage in GC responses to HA (Angeletti et al., 2017). For a third specificity, we turned to a previously characterized B cell clone that binds the stalk domain of HA. Clone C179 is the first described murine stem binding antibody and was discovered from hybridomas produced after i.p. immunization with and H2N2 influenza virus strain (Okuno et al., 1993). We solved cryo-EM structures of fabs 1.1 and 73.1 bound to PR8 HA, confirming binding to the Sa and Cb sites, which are entirely distinct from the binding site of fab C179 (Figure 6). For the remainder of this text, clones 1.1 and 73.1 will be referred to by their respective binding sites, Sa and Cb.

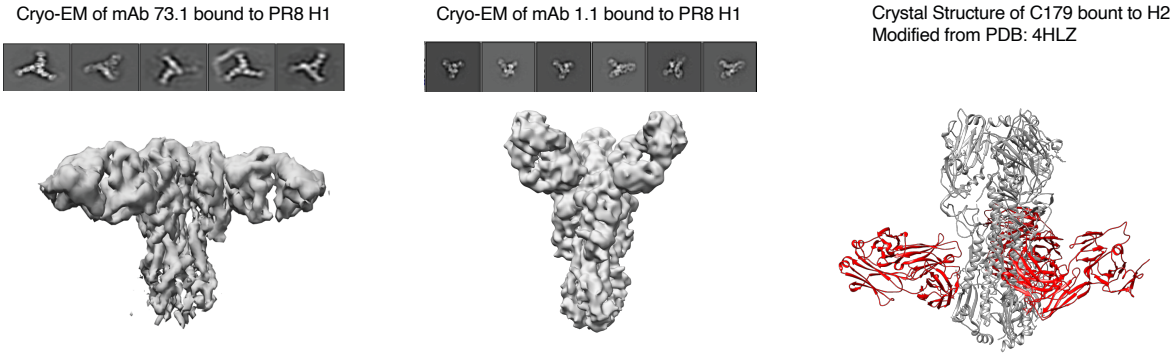

Figure 6: Structures of fabs 73, 1, and C179 complexed with HA
(Left) 2D class averages and 5.5 angstrom cryo-EM structure of Fab 73 (Cb) bound to PR8 HA. (Middle) 2D class averages and 6.7 angstrom cryo-EM structure of Fab 1 (Sa) bound to PR8 HA. (Right) Cystal structure of Fab C179 bound to H2. Adapted from PDB ID 4HLZ.

To further characterize the three clones, we performed competitive ELISA titration assays. We found mAbs do not compete for binding to HA, even at 100-fold differences in concentration (Figure 7A). In addition, non-competing mAbs did not prevent further mass accumulation onto HA-bound sensors in a highly sensitive bio-layer interferometry assay (Figure 7B). Finally, overlaying the cryo-EM structures of fabs Sa and Cb bound to HA with the crystal structure of fab C179 bound to HA demonstrates the distinct, non-overlapping specificities of the three clones (Figure 7C). B cells experience their first affinity-dependent selection bottleneck at the TB border. With transgenic B cells specific for the same epitope, co-transfer of high and low affinity B cells inhibits the GC differentiation of the low affinity clone, which is otherwise capable of forming a GC when transferred alone (Schwickert et al., 2011). T cell help at the TB border has been shown to be the limiting factor for competition at the level of GC entry. As B cells internalize entire antigen upon BCR engagement, it is reasonable to assume affinity dependent selection into the GC also occurs with multi-epitope systems. Therefore, it was crucial to ensure the affinities of the three clones were within the same order of magnitude. As mAbs, clones Sa, Cb and C179 bind HA very similarly in ELISA (Figure 7D). Bio-layer interferometry kinetics assays indicate the dissociation constants (K_Ds) of the three clones are approximately 3 x 10^{-8} M, or 30 nM, increasing the likelihood they would simultaneously participate in a GC response (Figure 7E). Although all clones share similar K_Ds, they exhibit different binding kinetics, particularly clone C179, which has both slower on- and off-rates. It is unknown whether binding kinetics can influence selection of B cells with similar nominal affinities. It is possible that BCRs with slower

off-rates can exert greater pulling forces on antigen when it is complexed on FDCs (Tolar et al., 2014). In fact, GC B cells have been shown to remove portions of the FDC membrane when they internalize antigen (Suzuki et al., 2009), and it would be interesting to investigate whether off-rate serves as a more accurate parameter for selection in the GC.

As C179 binds the conserved stalk domain of HA, it demonstrates cross-reactivity with a drifted H1 variant and H5, which clones Sa and Cb fail to bind (Figure 7F). Several studies in humans show stem-binding monoclonal antibodies are often poly- and/or autoreactive, leading to the hypothesis that humoral responses against the stem are rare because these B cell specificities are counterselected (Guthmiller et al., 2020). However, C179, as well as the two head-directed clones, did not bind any members of a conventional polyreactvity panel (Figure 7G). In conclusion, clones Sa, Cb and C179 are suitable to create an oligoclonal GC system because they target non-overlapping epitopes, are similar in nominal affinity, and do not exhibit polyreactivity.

Figure 7: mAbs Sa, Cb, and C179 bind distinct sites on PR8 HA
A) Competitive ELISA titration curves. Biotinylated antibodies were co-incubated with unlabeled competing mAbs in wells coated with PR8 HA. Competition is measured as reduction of biotin signal intensity.
B) ELISA titration curves of mAbs Sa, Cb, and C179 binding to PR8 HA.
C) Bio-layer interferometry analysis of binding kinetics between Fabs Sa, Cb, and C179 and PR8 HA.
D) Overlay of cryo-EM structures of Fabs Sa and Cb bound to PR8 HA with crystal structure of Fab C179 bound to H2 (PDB ID 4HLZ).
E) Epitope binning matrix via bio-layer interferometry. Binding of one mAb to PR8 HA was followed by binding with another, and binding to distinct sites is indicated by continued mass accumulation onto the sensor.
F) Area under curve analyses of ELISAs of mAbs Sa, Cb, and C179 binding to drifted strains of HA.
G) Polyreactivity assays of mAbs Sa, Cb, and C179. ED038 and MG053 were used as positive and negative controls, respectively.

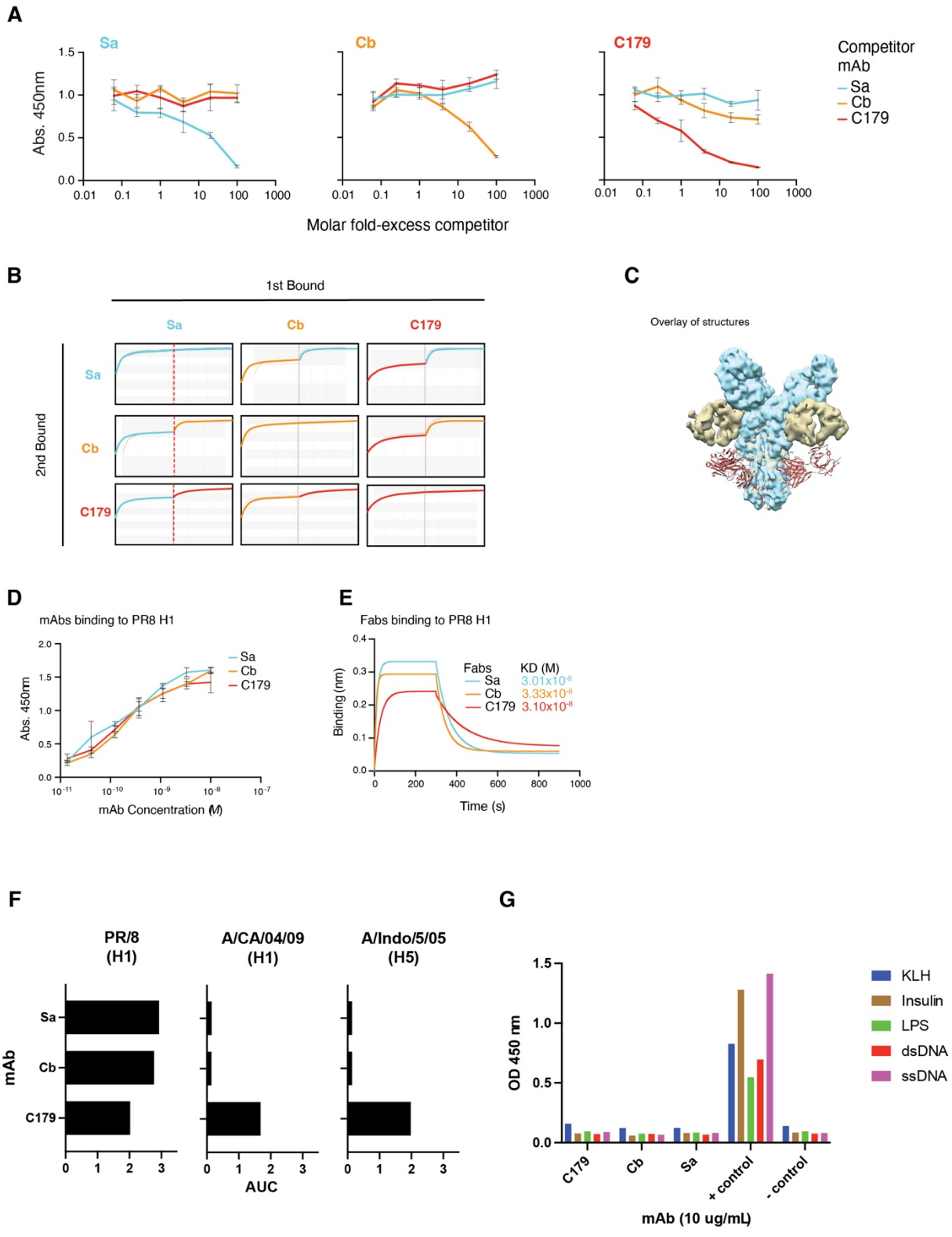

Figure 7: mAbs Sa, Cb, and C179 bind distinct sites on PR8 HA

Generation of BCR knock-in mice

To obtain a continuous source of monoclonal B cells, we produced BCR knock-in (KI) mice using the VDJ and VJ sequences of clones Sa, Cb and C179. We utilized CRISPR-Cas9 zygote microinjections to generate heavy chain and kappa light chain transgenic mouse lines. Our approach involved excising the J segments of both the heavy chain and light chain loci by flanking them with guide RNAs, and then providing the prearranged V-gene sequences as templates for homology directed repair (Figure 8A). In doing so, we replaced the J segments of the heavy and kappa light chain loci with the VDJ and VJ sequences of the three HA-binding clones. When integrated into the *Ig* loci, the BCR can undergo further somatic hypermutation and class switch recombination (Taki et al., 1993; Pelanda et al., 1996). In addition, BCR expression levels are far more likely to resemble those of naïve B cells from a wild-type mouse.

Compared to wild-type mice, the peripheral, naïve B cell compartment of all three BCR KI mice have a significant proportion of HA-tetramer binding B cells, indicating efficient allelic exclusion of the non-rearranged heavy and light chain (Figure 8B). $Igh^{Cb/+}$.$Igk^{Cb/+}$ (Cb) and $Igh^{C179/+}$.$Igk^{C179/+}$ (C179) mice both contained a clearly separate population of HA-binding B cells. However, the $Igh^{Sa/+}$.$Igk^{Sa/+}$ mice contained B cells with a range of HA-binding avidities, seen as a smear by flow cytometry. We reasoned this was due to accumulation of B cells with rearranged endogenous *Igk* alleles, given that allelic exclusion is less strict in the antibody light chains than in *Igh* (Vettermann et al., 2010). To prevent endogenous *Igk* rearrangements, we used CRISPR/Cas9 editing to produce

an *Igk* knock-out mouse by creating an indel in the kappa constant region (Hartweger et al., 2019). Crossing mouse Sa to our $Igk^{-/-}$ mouse ($Igh^{Sa/+}.Igk^{Sa/-}$) yielded mice with a distinct high HA-binding population. All BCR KI mice thus displayed >80% of B cells specific for HA. Although our biochemical assays show the three mAbs do not compete with one another, we tested whether mAbs can outcompete the binding to HA to a B cell. Since the surface of each B cell is coated with many BCRs, there is a much larger opportunity for steric hinderance from the cell to interfere with binding of antibodies to different epitopes. To assess this, we tested the ability of each mAb to interfere with HA tetramer staining of naïve B cells from the three KI mice. Similar to the biochemical assays, each mAb efficiently competed with its cognate B cell clone for binding to the HA tetramer. However, at high concentrations, mAbs Sa and Cb slightly interfered with HA binding of Cb and Sa, respectively, indicating steric hinderance effects do come into play in settings where mAbs are competing with entire B cells (Figure 8C). However, this binding inhibition is modest compared to the effect of the antibody on the cognate clone, implying that effects due to steric hinderance will be negligible compared to those of cognate competition. In summary, we have successfully generated three monoclonal BCR KI mice that bind to distinct sites of HA.

Figure 8: Generation of B cell receptor knock-in mice
A) Schematic of *Igh* and *Igk* locus editing. CRISPR guides flanking J gene segments along with repair templates harboring prearranged V(D)J sequences of clones Sa, Cb and C179 with ~200 bp of homology results in the replacement of J segments with V(D)J sequences.
B) (Left) Flow cytometry panels of peripheral B cells from WT and BCR KI mice binding to PR8 HA tetramer. Panels are pre-gated on $B220^{+}$ $TCRb^{-}$ lymphocytes. (Right) Quantification of HA binding from circulating B cells of BCR KI mice.
C) Flow-cytometry competition assays between KI B cells and soluble mAbs for binding to HA tetramers. mAbs were co-incubated with tetramer at increasing concentrations, and inhibition of B cell staining was assessed. Proportion of HA+ is normalized to binding of HA in the absence of competing antibody.

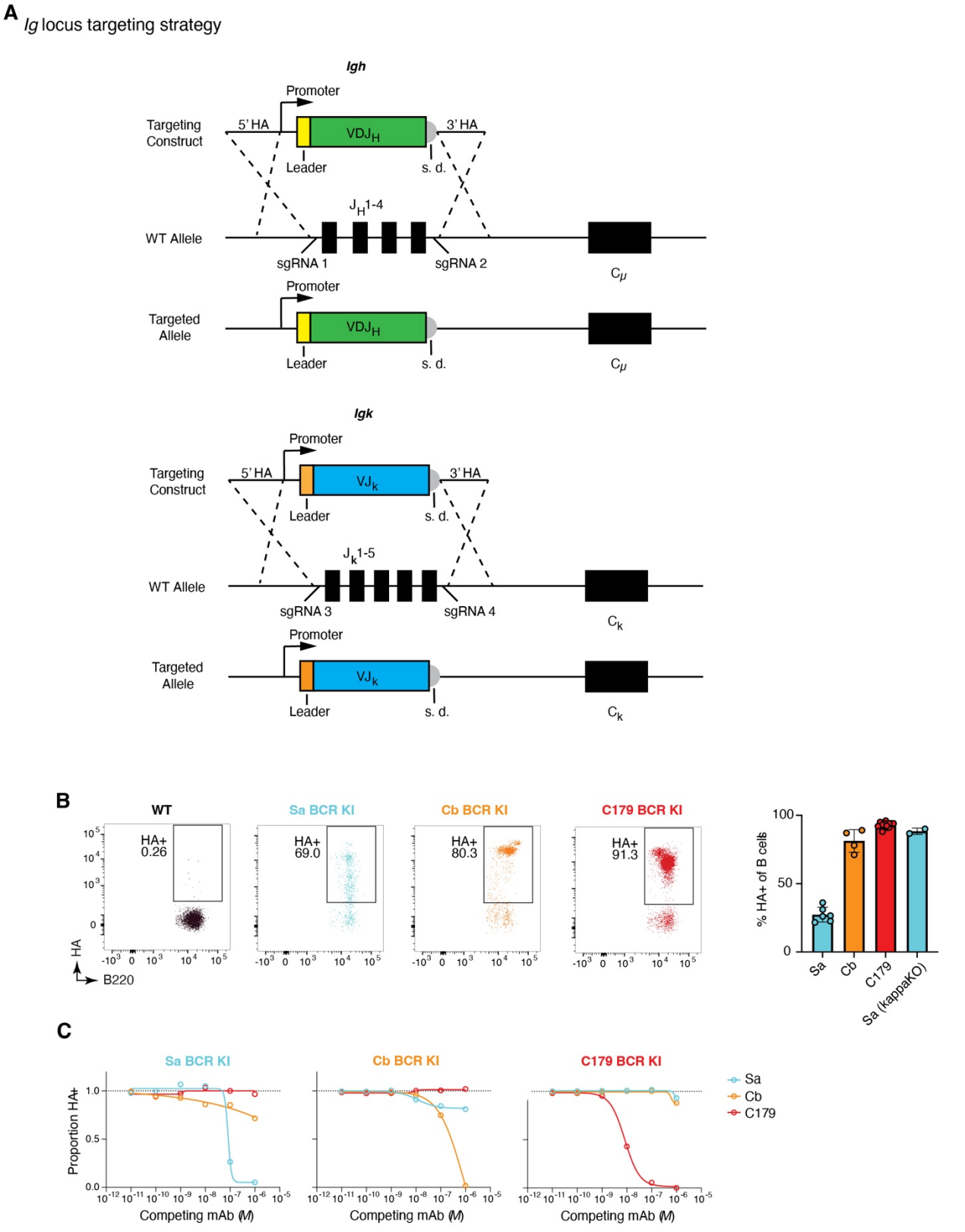

Figure 8: Generation of B cell receptor knock-in mice

Considerations for a plasma cell loss-of-function system

To study the effect of antibody feedback on a contemporaneous GC response in a way that circumvents administration of exogenous antibody, we looked to utilize a loss-of-function approach that relies on the removal of endogenous antibody. While gain-of-function approaches based on IV injection of antigen specific monoclonal and polyclonal antibodies have been useful in understanding antibody feedback, conclusions drawn from these studies are based on several variables that are either arbitrary or not well standardized. For example, the quantity of immunoglobulin administered can dramatically affect the outcome of B cell responses. However, it is difficult to gauge the amount of antibody that is physiologically relevant during a humoral response. Furthermore, antigens differ in their ability to elicit plasma cell responses, and various adjuvants can also influence the outcomes of B cell responses – each response likely produces a different amount of epitope specific antibody that cannot be standardized. In addition, variables such as isotype, the timing of antibody administration, and the glycan structure of antibodies have been shown to influence the outcome of antibody feedback. Above all, administration of exogenous antibody to interrogate clonal selection and affinity maturation in the GC precludes investigation of a process that is hypothesized to be self-regulating. A loss-of-function model is advantageous in this regard, as the system is allowed to proceed naturally, without the introduction of extraneous variables. One candidate for such a system is a *Prdm1*$^{flox/flox}$ (Blimp1-flox) genetic mouse model. When crossed to a B cell specific Cre, Blimp-1, the transcription factor required for plasma cell induction and maintenance, is excised from the genome, resulting in the

inability to differentiate into plasma cells and, therefore, produce antibody. To test whether a Blimp-1-flox model would be suitable for our anti-HA monoclonal system, we crossed *Prdm1*$^{flox/flox}$ to *Cd79a*$^{Cre/+}$ (Mb1-Cre) and *Igh*$^{B1\text{-}8hi/+}$ (B1-8hi) mice. Mb1, also known as CD79a, is an essential component of the BCR signaling machinery, and is expressed on all B cells starting at the inception of their development from precursor cells. The B1-8hi allele encodes a BCR heavy chain that binds to the hapten NP when it is paired with a naturally occurring lambda light chain, which occurs approximately 5-15% of the time in mice (Sonoda et al., 1997). Combining these alleles together yields a source of antigen specific B cells that cannot produce antibody due to their inability to become plasma cells.

We co-transferred equal numbers of Mb1-Cre; *Prdm1*$^{flox/flox}$; B1-8hi (Blimp-1-KO) and Mb1-Cre; *Prdm1*$^{flox/flox}$; B1-8hi (Blimp-1-WT) cells into *Igh*$^{LMP2A/LMP2A}$ (LMP2A) hosts, and immunized mouse footpads with NP-OVA complexed in alhydrogel the following day (Figure 9A). LMP2A mice have circulating B cells that lack BCRs, preventing their participation in humoral responses, allowing for isolated analysis of the transferred cells (Casola et al., 2004). On day 7 post immunization, we looked at the proportion of Blimp-1-KO to Blimp-1-WT B cells in the naïve, GC and PC compartments. As expected, the PC compartment was completely devoid of Blimp-1-KO cells (Figure 9B). In addition, compared to the transfer cells in the naïve compartment, which were composed of 70% Blimp-1-KO cells, Blimp-1-KO cells were enriched in the GC compartment (~87%). This implies there is biased entry into the GC of Blimp-1-KO cells. The initial fate decision of

individual B cells into the GC or PC compartments occurs at the T-B border. When a B cell cannot differentiate into a plasma cell, as is the case with Blimp-1-KO cells, it becomes biased towards the alternate fate (Figure 9C). This altered fate decision probability explains the enrichment of Blimp-1-KO cells in the GC compartment and renders the Blimp1-flox model unsuitable for investigating the effects of antibody feedback on an ongoing GC. A GC-specific Cre would result in a similar problem, as GC B cells unable to differentiate into PCs would remain in the GC and undergo further rounds of proliferation. In this case, clonal composition of the GC results from skewed fate decisions rather than from the depletion of antibody.

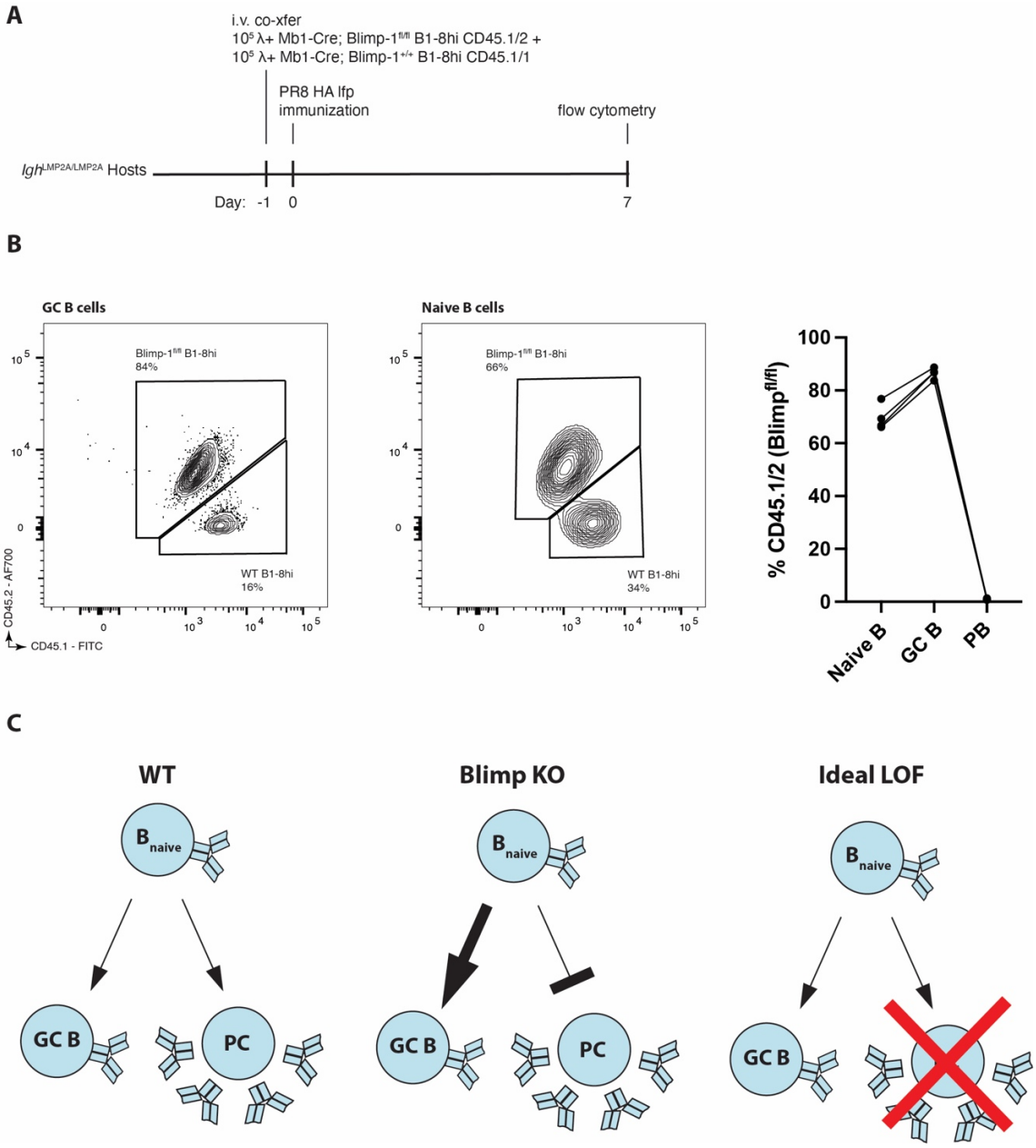

Figure 9: The Blimp-1-flox genetic model is unsuitable to assess antibody-mediated feedback

A) Experimental setup.

B) (Left) Flow cytometry panels of cell transfer populations in the GC and naïve B cell compartment. (Right) Proportion of Blimp-1-deficient B cells in the naïve B, GC B, and plasmablast compartments. Lines connect points from the same mouse.

C) Schematic of an ideal loss-of-function model to study Ab feedback. (Left) Naïve B cells can become GC B cells or plasma cells. (Middle) When Blimp-1 is knocked out, B cells cannot become plasma cells and are skewed towards the GC B cell fate. (Right) The ideal loss-of-function system is one where plasma cells are depleted following their formation. This prevents biasing of cell fate decisions.

Generation of the Blimp-1-DTR mouse

The ideal loss of function system would enable the depletion of antibody titers without influencing B cell fate decisions. One way to accomplish this is to allow B cells to differentiate into plasma cells as they would naturally, and then deplete the plasma cell population once it has formed. For this purpose, we developed a "stopped" Blimp-1-DTR (*Prdm1*$^{LSL\text{-}DTR}$) allele. Downstream of the final exon of *Prdm1* is a P2A sequence in frame with the coding sequence for the diphtheria toxin receptor (DTR). Separating *Prdm1* from the P2A-DTR is a stop codon that is flanked by two loxP sites. In the presence of Cre activity, the stop codon is floxed and DTR is co-translated along with Blimp-1 (Figure 10A). As mice do not express DTR, administration of DT leads to ablation only of cells that are Blimp-1^{+}. Unlike a Blimp-1-KO model, using Blimp-1-DTR to deplete PCs after they have been formed prevents the skewing of B cell fate decisions and allows for an unbiased investigation of the effect on antibody depletion on the GC.

An alternative approach would have been to develop the same mouse with the coding sequence for DTA in the place of DTR. DTA is the active component of DT, and it is has been shown that one molecule of DTA is sufficient to induce cell death (Yamaizumi et al., 1978). Using DTA in place of DTR would result in the automatic killing of plasma cells after they have been formed, which would both obviate the need for DT and ensure complete depletion. However, the use of DTA would yield a system far too sensitive to leaky Blimp-1 expression that would likely result in depletion of unwanted

cell populations. Additionally, one study claims GC B cells upregulate Blimp-1 to undergo proliferative bursts in the dark zone (Radtke & Bannard, 2019). If this is the case, using DTR allows for the titration of DT, enabling the identification of a DT concentration that results in selective depletion of plasma cells without directly affecting the GC compartment.

To characterize the Blimp-1-DTR mouse, we crossed it to CD23-Cre, which drives Cre expression in B cells. At steady state, administration of 1 μg of DT to these mice results in efficient depletion of plasmablast and plasma cell populations, in the mesenteric lymph nodes and bone marrow, respectively (Figure 10B). To determine the minimal effective dose of DT, we assessed various concentrations and routes of administration to find 200 ng intraperitoneal injections sufficed to deplete most plasma cells in both compartments (Figure 10C). The amount of plasma cell depletion reaches a peak two days following DT administration, after which plasma cells begin to recover if DT is not continuously provided (Figure 10D). Furthermore, there is no evidence of isotype bias, as IgA, IgM, and non-IgA/IgM plasma cells undergo similar rates of depletion and recovery following DT (Figure 10E). As plasma cells are continuously generated, continuous administration of DT is required to deplete serum immunoglobulin. To test this, we administered DT to Blimp-1-DTR; CD23-Cre mice daily for two weeks and measured serum IgM and IgG at days 0, 4, 7 and 14.

While total IgM and IgG remained stable in WT mice after DT administration, they are both gradually depleted in Blimp-1-DTR; CD23-Cre mice. Depletion of IgM occurs at a faster rate than IgG due to its considerably shorter half-life. Daily DT administration resulted in a maximal average IgM and IgG depletion of 35- and 8-fold, respectively (Figure 10F). Interestingly, serum IgM increased slightly in concentration after day 7 despite continued DT administration. One possibility is repeated exposure to DT induces an antibody response that neutralizes the toxin and prevents further plasma cell depletion; however, we could not detect anti-DT reactivity at any timepoint via ELISA (data not shown). Overall, Blimp-1-DTR is an effective model for plasma cell and immunoglobulin depletion.

Figure 10: Generation of the Blimp-1-DTR mouse
A) Schematic of the Blimp-1-DTR allele. Downstream of the final exon of *Prdm1* is a P2A-DTR sequence separated by a stop codon flanked by two loxP sites. In the presence of Cre activity, the stop codon is floxed, and DTR is co-translated with Blimp-1. **B)** (Left) Flow cytometry panels of plasma cells in mesenteric lymph nodes and bone marrow in CD23-Cre and CD23-Cre; Blimp-1-DTR mice given DT one day prior. (Right) Quantification of plasma cells in mesenteric lymph nodes and bone marrow with and without plasma cell depletion.
C) Dosing and route of DT administration necessary for efficient depletion of plasma cells. CD23-Cre; Blimp-1-DTR mice were given DT and plasma cells were analyzed in mesenteric lymph nodes and bone marrow one day later.
D) Kinetics of plasma cell re-seeding. 200 ng of DT was administered i.p. to CD23-Cre; Blimp-1-DTR mice and plasma cells in the bone marrow and mesenteric lymph nodes were analyzed 1, 2, and 3 days later.
E) Same as D, but plasma cell isotypes are included.
F) CD23-Cre; Blimp-1-DTR or WT mice were given 200ng of DT i.p. daily and bled at days 0, 4, 7, and 14. Midpoint serum titers of total IgM and IgG were determined via ELISA.

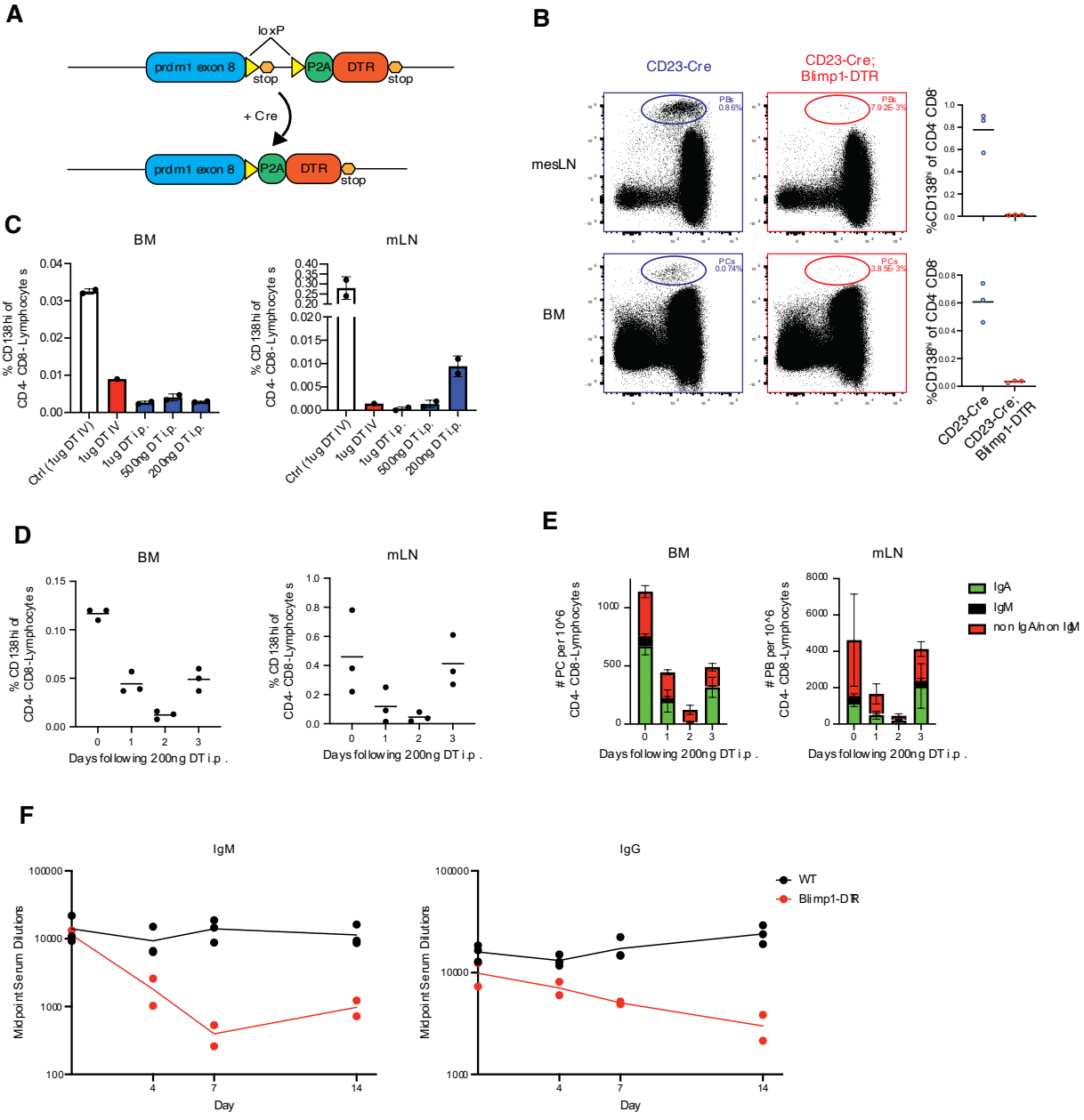

Figure 10: Generation of the Blimp-1-DTR mouse

CHAPTER 3: Investigating the Effect of Antibody on Clonal Selection in the GC

HA specific BCR KI cells dominate early GC but decay rapidly following immunization

To characterize the response kinetics of our transgenic B cells, we separately transferred 10^5 HA-binding B cells from each KI mouse into C57BL/6 hosts and, one day later, immunized them in the footpad with PR8 HA in alhydrogel. From day 7 to day 21, total GC size was stable at around 2% of total B cells, regardless of the clone that was transferred. At day 7 of the response, the transferred cells of each clone dominated the GC compartment, forming on average 80% of total GC B cells. This was expected, as the transferred cells have relatively high affinity and outnumber naïve HA binders, which provides them with a competitive advantage for GC entry. Unexpectedly, the proportion of transferred cells in the GC decreased as early as day 9 and continued to decay until day 21. For example, although clone Sa comprised 76% of the GC at day 7, by days 9, 14, and 21 it had decreased to 38, 20, and 16% of the GC (Figure 11A). This depletion was not an idiosyncrasy of one clone, as it was preserved among all three clones (Figure 11B,C). Each of the three clones readily differentiated into plasmablasts at day 7, a time point at which they also dominated this compartment in the lymph node (Figure 11D). As in the GC, the number of plasmablasts derived from the transferred cells steadily decreased over time. As lymph node plasmablasts later in the response more accurately represent export from the GC, the lower number of transferred cells in this compartment likely reflects lower amounts in the GC. Bone marrow plasma cells from the transferred population were not detected at any timepoint following

immunization – this is most probably due to the relatively small magnitude of responses induced by footpad immunization, as transferred cells were detected as bone marrow plasma cells following infection with influenza virus (data not shown).

Figure 11: BCR KI B cell clones contract in the GC after immunization with HA
A) 10^5 HA-binding B cells from clone Sa BCR KI mice were transferred into C57BL/6 mice, and hosts were footpad immunized with PR8 HA in alhydrogel the following day. GCs were analyzed via flow cytometry at days 7, 9, 14, and 21 after immunization. (Left) Representative flow plots of total GCs (top) and composition of GCs (bottom). Top panels are pre-gated on B cells and bottom panels are pre-gated on GC B cells. (Right) Quantification of GC size (top) and proportion of clone Sa in the GC (bottom) over time.
B) Same experimental setup as in A, but with transfer of clone Cb. (Left) Quantification of total GC size over time. (Right) Proportion of clone Cb in the GC over time.
C) Same experimental setup as in A, but with transfer of clone C179. (Left) Quantification of total GC size over time. (Right) Proportion of clone C179 in the GC over time.
D) Proportion of clones Sa, Cb, and C179 in the lymph node plasmablast compartment following footpad immunization with HA.

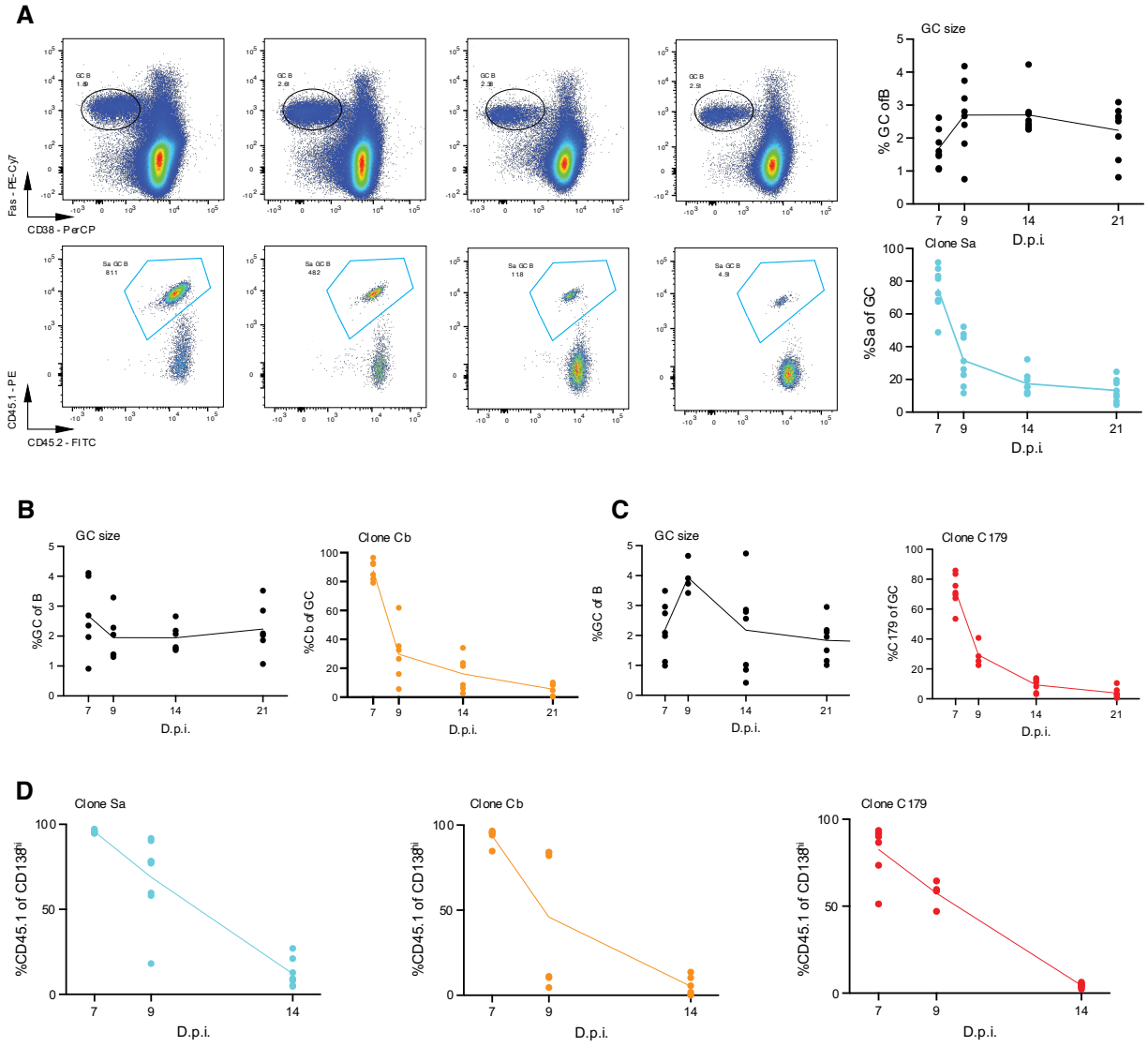

Figure 11: BCR KI B cell clones contract in the GC after immunization with HA

To rule out that the decay of our KI clones in the GC was an artifact of the number of cells transferred, we repeated the experiment with 10-fold greater and 10-fold fewer cells of clone Cb (Figure 12A,B). Regardless of the number of cells transferred, the transfer population became depleted within the GC compartment two weeks after immunization. With transfer of 10,000 cells, the level of GC entry was poorly reproducible, likely due to increased competition from endogenous B cells. However, decay still occurred at this more physiologic precursor frequency. Interestingly, amounts of epitope-specific antibody did not directly correlate with the number of cells transferred (Figure 12C,D). In fact, transfer of 10^6 Cb B cells resulted in lower endpoint titers at day 7 compared to transfer of 10^5 and 10^4 cells. This is likely due to saturation of T cell help at the T-B border – the number of antigen-specific T cells is likely to remain roughly the same regardless of the number of B cells transferred, so individual B cells receive less help when transferred in large numbers. This explains why both titers and number of plasma cells are lower under conditions of excess cell transfer.

Clonal decay is not specific to HA responses, as another BCR KI mouse model specific for chicken IgY also becomes depleted in the GC after immunization at a similar rate as the anti-HA clones (Figure 12E). In addition, HA BCR KI clones are not depleted in the GC following infection, ruling out that lack of competitiveness in the GC results from peculiarities of our monoclonal mouse design (Figure 12F).

Figure 12: Clonal contraction is not an artifact of experimental approach or mouse design

A) 10^6, 10^5, and 10^4 HA-binding cells from clone Cb BCR KI mice were transferred into C57BL/6 hosts, and mice were immunized one day later with HA. GC size was followed over time.

B) Proportion of clone Cb within the GC with different transfer numbers.

C) Cb serum endpoint dilution titers with different transfer amounts of clone Cb.

D) Number of lymph node plasma cells derived from the transfer population, quantified over time following immunization.

E) 10^5 B cells from a BCR KI mouse against chicken IgY were transferred into C57BL/6 hosts and mice were immunized the following day with chicken IgY in alhydrogel. Shown is the proportion of transfer cells in GCs 7- and 13-days following immunization.

F) Response of clone Sa to infection with influenza virus. 10^5 HA-binding B cells from clone Sa BCR KI mice were transferred into C57BL/6 hosts and mice were infected with PR8 intranasally the following day. (Left) GC size at 2-, 3-, and 4-weeks following infection. (Right) Proportion of clone Sa in the GC at 2, 3, and 4 weeks after infection.

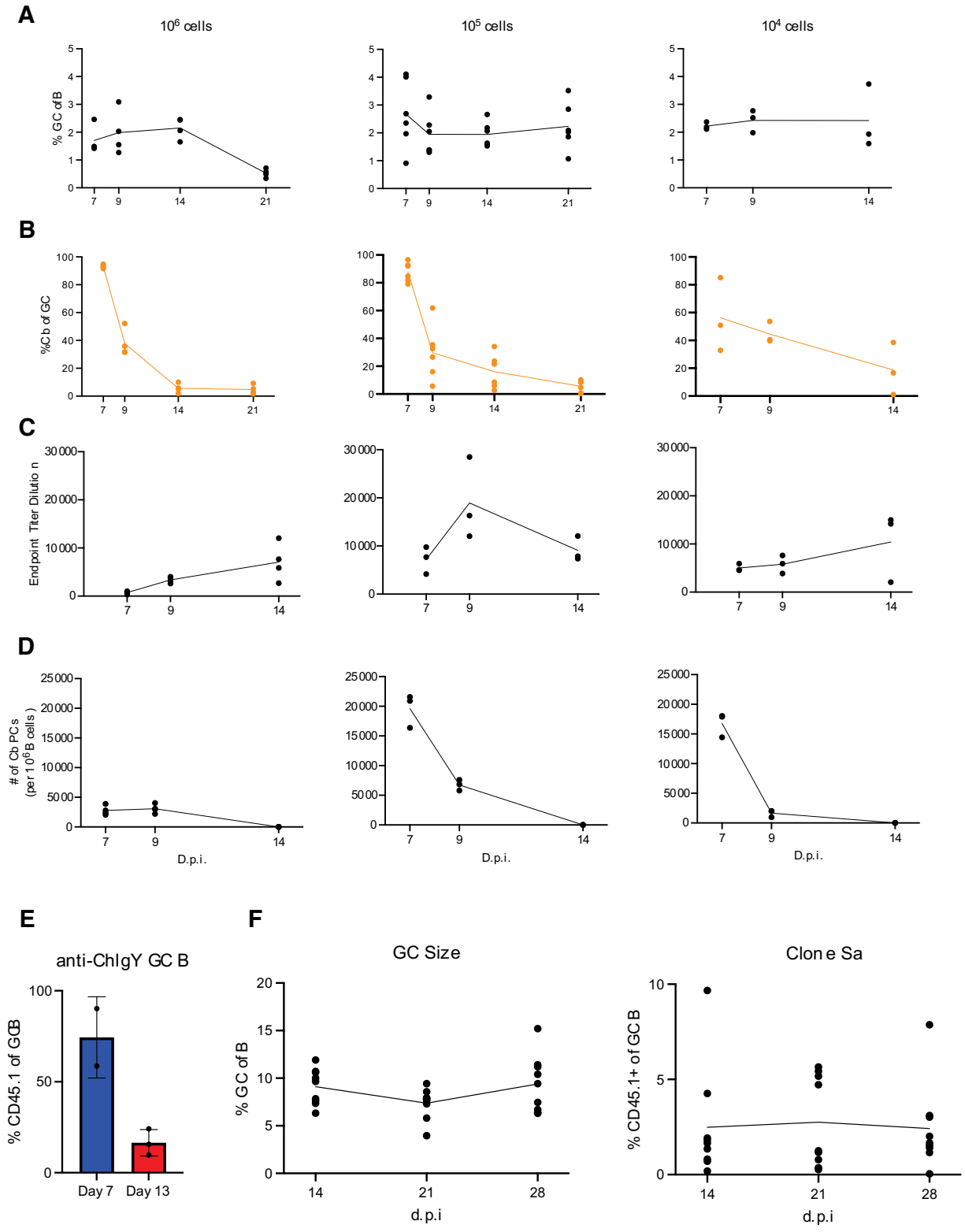

Figure 12: Clonal contraction is not an artifact of experimental approach or mouse design

Interestingly, concurrent with the decay of transferred clones in the GC was the enrichment of HA-tetramer binders among endogenous GC B cells (Figure 13). For example, with transfer of clone Sa, endogenous B cell HA binders were undetectable in the GC at day 7 post immunization but rose to 7 and 12% at days 14 and 21. The appearance of HA specificity among endogenous B cells over time makes excessive antigen consumption an unlikely explanation for the decay of the transferred cells; it is likelier that these cells are being outcompeted by endogenous GC B cells over time.

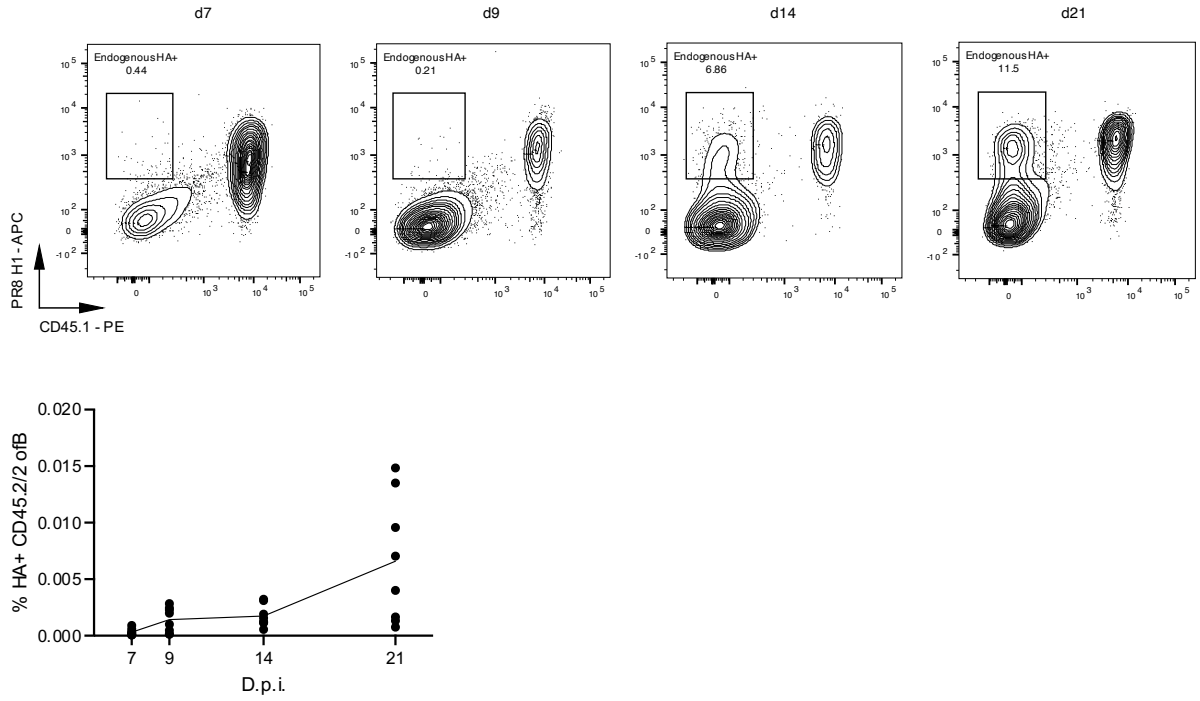

Figure 13: Endogenous GC B cells exhibit increased HA binding with time
(Top) Representative flow plots of endogenous cells binding to HA tetramer upon transfer with clone Sa and immunization with HA. (Bottom) Quantification of endogenous HA binders.

Compared to immunization of wild type mice, HA-specific IgG antibody titers over a timespan of 21 days were on average 9- and 40-fold greater upon adoptive transfer of Sa and Cb B cells, respectively (Figure 14A). This difference is most pronounced early in the response, when HA titers from clone Sa are 12-fold higher than WT at days 7 and 10, and titers from clone Cb are 103- and 20-fold higher at days 7 and 10, respectively, likely indicating the excess antibody is predominantly derived from the extrafollicular response (Figure 14B). The increased titers are derived from the transferred cells themselves, as the extra serum antibodies produced react to the same epitopes recognized by the transferred clones (Figure 14C). Additionally, when cells are transferred, nearly all IgG HA serum reactivity is derived from the transferred cells, as the epitope-specific titers are virtually identical to the total HA titers (Figure 14D). The early antibody dominance of the transferred clones indicates they outcompete WT naïve B cells for T cell help at the T-B border and within the GC. Although the clones quickly decay in the GC over time, any effect in the serum would be delayed due to the long half-life of IgG. Nevertheless, a decay in epitope-specific titers can be seen in transfer of clone Cb, as epitope specific titers are approximately 10-fold lower than total HA titers at later timepoints after immunization. The massive production of antibodies from the transferred cells led us to hypothesize that high levels of epitope-specific antibody titers feedback onto the GC and limit the competitiveness of cognate clones in the ongoing reaction.

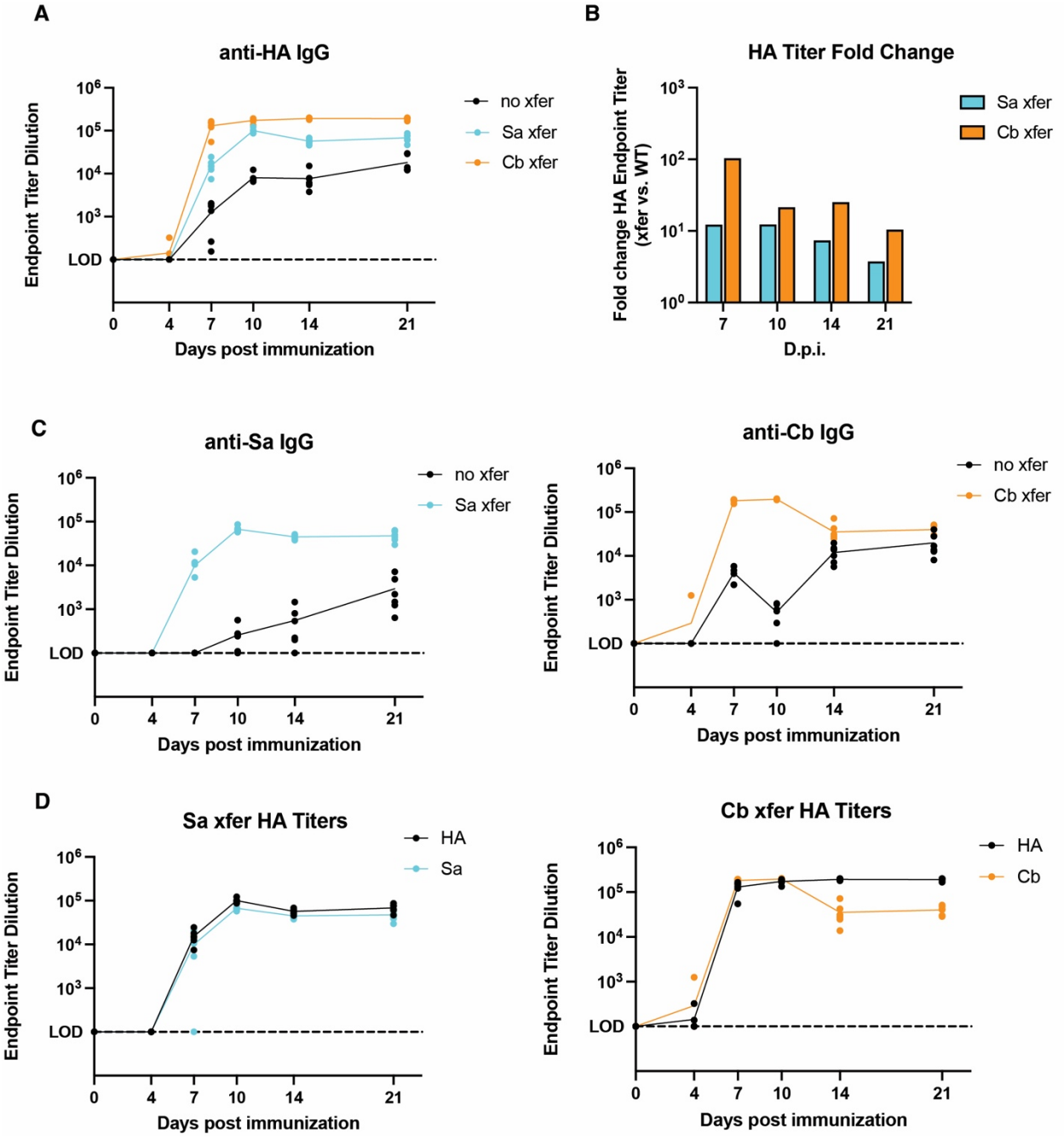

Figure 14: Transfer of monoclonal B cells prior to immunization produces large anti-HA antibody titers

A) Time course of anti-HA IgG endpoint titers in response to immunization in WT mice or in mice receiving 10^5 HA-binding Sa or Cb B cells one day prior.

B) Fold change of HA IgG titers in transfer conditions vs. non-transfer conditions.

C) Site specific HA IgG titers in transfer and non-transfer conditions (Sa on left and Cb on right).

D) Site specific and total HA IgG titers in transfer mice, for both Sa (left) and Cb(right).

Antibody-mediated feedback accelerates clonal decay

To formally test the hypothesis that antibody feeds back onto the GC to limit expansion of clones harboring the same specificities, we crossed our BCR KI mice to a germline excised version of Blimp1-DTR, where expression of DTR is constitutive in all Blimp-1-expressing cells. Since HA-binding B cells are transferred into WT mice, administration of DT solely depletes antibodies from the transferred cells without affecting secretion of endogenous antibody. We separately transferred clones Sa and Cb into C57BL/6 hosts, immunized them with PR8 HA one day later, and began administering DT daily four days post immunization (Figure 15A). In our transfer system, mice begin producing antigen specific titers at day 5 post immunization, and dosing with DT beginning at day 4 prevents the formation of these titers. Daily dosing is required for the remainder of the experiment, as plasma cells are constantly being produced throughout the response. Depletion of lymph node plasmablasts was highly efficient, as transferred cells were virtually absent from the plasmablast compartment 7 days post-immunization when mice were treated with DT (Figure 15B). As expected, endogenous plasma cells did not increase in numbers early in the response – likely because the number of transferred and endogenous B cells that enter the plasmablast compartment is determined at the TB border, prior to the initiation of treatment with DT. Since DT acts only after a cell has differentiated, it does not influence the fate decisions of other cells, precluding a compensatory increase in endogenous plasma cells. With transfer of clone Sa, plasma cell depletion translated into an approximately 50-fold depletion in epitope-specific antibody at day 18 post immunization. The non-depleted epitope-specific antibody at

day 18 most likely represents the fraction produced by endogenous B cells, although it may also reflect incomplete depletion of the transferred clone.

In the case of clone Sa, antibody depletion did not affect the size of the GC at any timepoint after immunization. With clone Cb, antibody depletion resulted in a larger GC at day 9, but this difference was not significant 18 days after immunization. As with Blimp-1-WT cells, Blimp-1-DTR cells dominated GC entry, but decayed quickly with time. For both clones, antibody depletion did not affect entry into the GC. Although it is known that pre-existing antibody influences entry into the GC, this is only true if antibody is present at the time B cells interact with T cells at the TB border, which occurs within 24-48 hours after immunization. Since HA titers begin to form at day 5 in our system, there is no pre-existing antibody before the initial T cell help phase required for differentiation into GC B cells. Despite not influencing entry of transferred cells into the GC, depletion of antibody partially rescued the decay within the GC compartment (Figure 15C,E). For both clones Sa and Cb, this rescue was most striking at day 9 after immunization and persisted at later time points. The enrichment of transferred cells in the GC upon DT administration is not a result of DT itself, as administration of DT to Blimp-1-WT cells did not increase their representation in the GC (Figure 15D). Therefore, antibody produced by plasma cells derived from adoptively transferred clones accelerates the decay of their counterparts in the GC.

Figure 15: Depletion of epitope specific antibody slows contraction of cognate clone in the GC

A) Experimental setup. 10^5 HA-binding B cells from clone Sa and Cb BCR KI mice harboring the Blimp-1-DTR allele were transferred into C57BL/6 hosts, and mice were immunized one day later with HA. Starting at day 4 post immunization, mice were given daily DT or PBS. Mice were analyzed at days 7, 9, 14, and 18 following immunization.
B) (Left) Number of plasmablasts derived from clone Sa 7 days after immunization. (Right) Sa IgG1 antibody titers 18 days after immunization. Black dots represent mice treated with PBS. Red dots are mice treated with DT.
C) Time courses of GC size (left) and proportion of clone Sa in the GC (right) following immunization. Black lines are mice treated with PBS and red lines represent mice treated with DT.
D) Same setup as in A, except clone Sa does not have the Blimp-1-DTR allele. GC was analyzed for percent of clone Sa 18 days after immunization.
E) Time courses of GC size (left) and proportion of clone Cb in the GC (right) following immunization. Black lines are mice treated with PBS and red lines represent mice treated with DT.

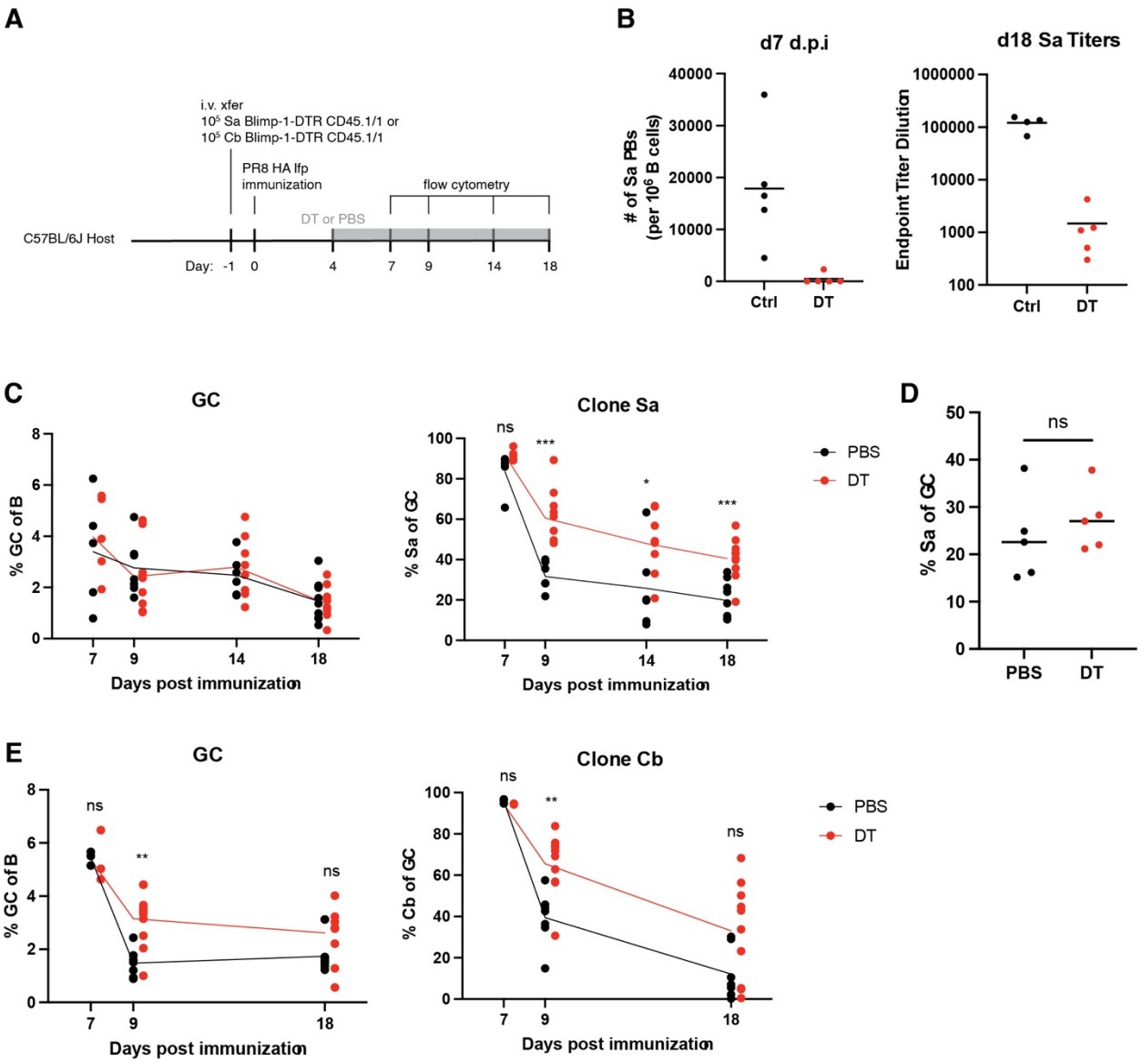

Figure 15: Depletion of epitope specific antibody slows contraction of cognate clone in the GC

Although the rate of clonal decay was slowed upon antibody depletion, the rescue was not complete, as transferred cells still became less represented in the GC over time. There are several explanations for this. It is possible that non-depletable antibody from endogenous cells is significant enough to produce an inhibitory effect. Another possibility is that DT directly kills GC B cells, leading to two simultaneous opposing effects of releasing antibody inhibition and ablation of transferred cells directly in the GC that results in an incomplete rescue of clonal decay. To rule out that DT was directly eliminating GC B cells, we devised an experiment in which we compared the GC frequency of the same B cell clone with or without the Blimp-1-DTR allele after administration of DT. We co-transferred 10^5 C179 Blimp-1-WT and 10^5 C179 Blimp-1-DTR B cells into C57BL/6 hosts and immunized them one day later. Four days following immunization, we administered DT or PBS daily, and we compared GCs at day 7 post immunization (Figure 16A). In this experiment, both populations of transferred cells are from the same clone. Administration of DT will eliminate the Blimp-1-DTR cells that enter the plasma cell compartment without affecting the Blimp-1-WT cells. Therefore, the antibody depletion that ensues will be experienced equally by Blimp-1-DTR and Blimp-1-WT C179 GC B cells. If DT directly depletes GC B cells, the ratio of the Blimp-1-DTR to Blimp-1-WT cells would decrease when DT is given. However, despite a complete depletion of the Blimp-1-DTR clone in the lymph node plasmablast compartment, the ratio of Bimp-1-DTR:Blimp-1-WT cells in the GC remained the same in the presence and absence of DT (Figure 16B,C). This indicates that DT is not directly

killing GC B cells, and therefore cannot explain the incomplete rescue of clonal decay upon antibody depletion.

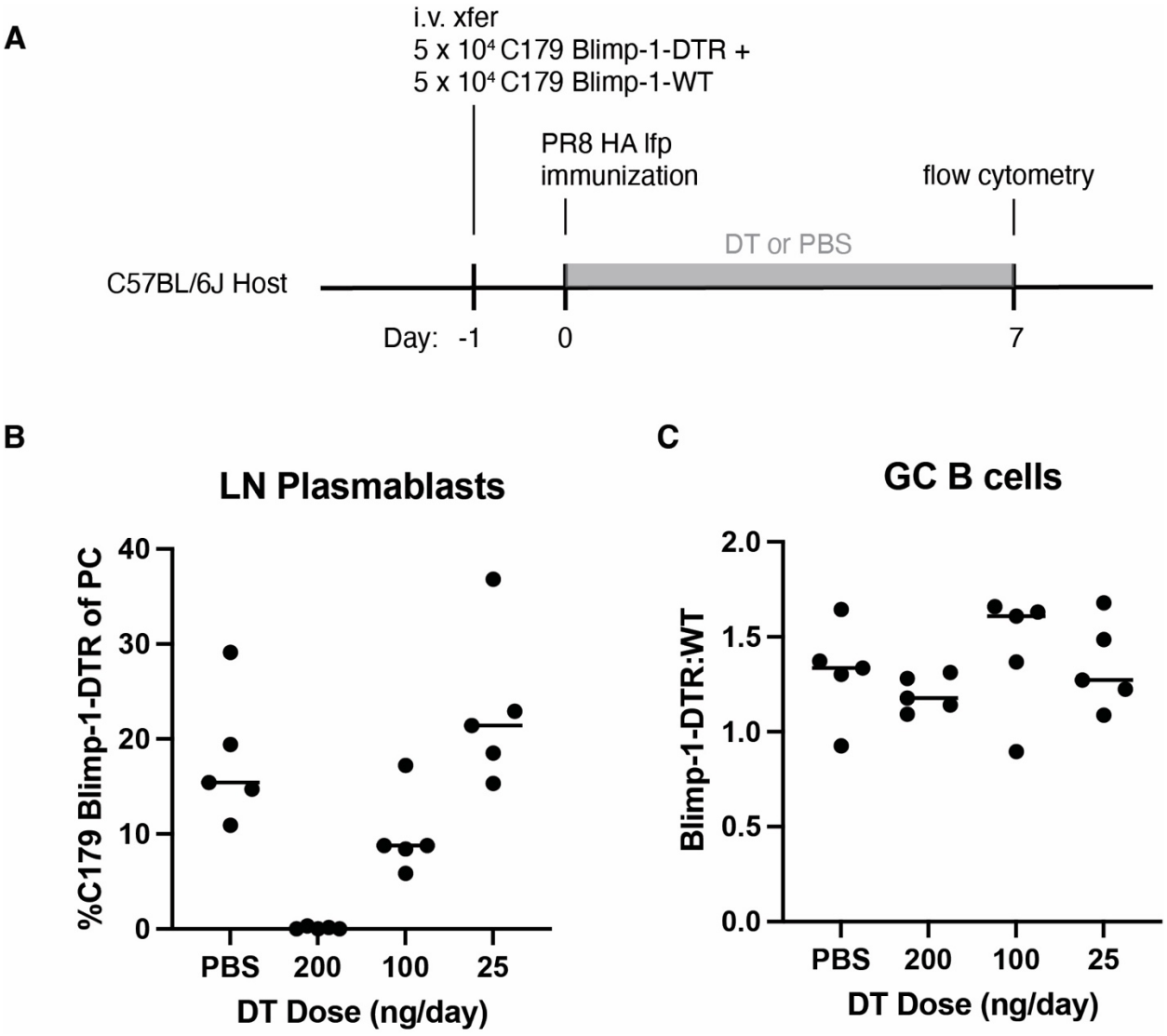

Figure 16: DT does not directly kill Blimp-1-DTR GC B cells
A) Experimental setup. HA-binding cells from C179 BCR KI harboring the Blimp-1-DTR allele were co-transferred with C179 BCR KI Blimp-1-WT cells in a 1:1 proportion into C57BL/6 hosts. Mice were footpad immunized with HA one day later and given daily PBS or DT. Mice were sacrificed for flow cytometry analysis 7 days after immunization.
B) Proportion of C179; Blimp-1-DTR clone in the lymph node plasma cell compartment with different doses of daily DT administration.
C) Ratio of Blimp-1-DTR to Blimp-1-WT clone in the GC with different doses of DT.

Antibody inhibition is epitope-specific

Depletion of epitope specific antibody titers slows the decay of transferred cells in the GC without significantly influencing total GC size. This implies antibody feedback within the GC acts mostly via an epitope specific mechanism, as endogenous GC B cells are not significantly affected. To formally test this hypothesis, we sought to establish a model in which GCs are composed solely of two transferred clones that bind non-overlapping epitopes. Essential to this is a host containing B cells unable to enter the GC reaction. Three candidate hosts we evaluated for this system were MD-4, Eμ-LMP2A, and CD23-Cre; *Bcl6*$^{fl/fl}$ mice. MD-4 mice are transgenic for a hen egg lysozyme (HEL) specific BCR, with 99% of B cells being HEL-specific (Goodnow et al., 1988). As this BCR does not bind HA, host B cells will not participate in a HA or influenza driven immune response. Latent membrane protein 2A (LMP2A) is a protein encoded by the Epstein Barr virus (EBV) that inhibits BCR signal transduction, and transgenic mice with LMP2A insertions in the immunoglobulin locus produce BCR-deficient B cells that maintain their ability to survive in the periphery (Casola et al., 2004). As in the MD-4 model, these host cells will not respond to immunization with HA or infection with influenza because they lack any antigen reactivity. Finally, as BCL6 is required for initiation and maintenance of the GC program, the CD23-cre*; Bcl6*$^{fl/fl}$ mouse has a population of B cells that cannot enter the GC reaction, although they can still engage in normal extrafollicular responses. Unlike the other two hosts, the CD23-cre*; Bcl6*$^{fl/fl}$ mice will also have natural antibody that may be important for the initiation of GC responses. We tested the ability of all three hosts to produce GCs composed of transferred B cells.

While all three hosts supported formation of GCs, LMP2A and MD-4 hosts failed to sustain GCs longer than 10 days (data not shown). In the case of LMP2A hosts, it is possible that transferred B cells are rejected upon activation due to introduction of BCRs not present in the host. However, considering GCs are also difficult to maintain in MD-4 hosts which are tolerized to the BCR, it is more likely that GC longevity is hampered by the lack of natural antibody in both LMP2A and MD-4 hosts. Natural antibody, especially IgM, is enriched in polyreactivity and weak binding to self-antigens, and it has been proposed to be important in deposition of antigen onto FDCs in the absence of pre-existing antigen specific titers (Palma et al., 2018). Therefore, in LMP2A and MD-4 mice, it is possible the transfer cells can adopt the GC fate upon binding to soluble HA in the follicle but cannot maintain the GC program due to inefficient antigen access on FDCs resulting from suboptimal amounts of natural antibody. In CD23-Cre; *Bcl6*$^{fl/fl}$ mice, which can produce natural antibody, GC responses persist past 10 days.

We used CD23-Cre; *Bcl6*$^{fl/fl}$ mice to establish a co-transfer model to produce GCs consisting of only two clones. Since clones Sa and Cb bind separate antigenic sites on HA, this setup allows for the deconvolution of epitope specific and epitope agnostic effects of antibody on the GC response. If antibody feedback operates via an epitope-specific mechanism, depletion of immunoglobulin produced by one clone will relieve inhibition solely on that clone, without affecting the other. Alternatively, if antibody feedback operates predominantly via an epitope-agnostic mechanism, depletion of immunoglobulin from one clone will relieve a general suppression of the GC response,

and both clones in the system will be affected. Into CD23-Cre; *Bcl6*$^{fl/fl}$ hosts we transferred 10^5 cells of clone Sa harboring the Blimp-1-DTR allele along with 10^5 cells of clone Cb, and immunized mice in the footpad one day later (Figure 17A). Four days after immunization, we administered DT daily. As only clone Sa expressed the Blimp-1-DTR allele, only Sa titers were depleted, while Cb titers remained unchanged (Figure 17B). Depletion of Sa antibody titers did not significantly affect GC size 14 days after immunization. However, the composition of the GC was significantly altered, as clone Sa became heavily enriched upon depletion of its antibody (Figure 17C). In the PBS condition, clone Sa comprised on average 20% of the GC, with the remainder composed of clone Cb. Upon depletion of Sa titers, clone Sa expanded to on average 50% of the GC. This enrichment was a result of expansion of clone Sa and not a contraction of clone Cb. In fact, total numbers of clone Cb in the GC remained similar in both conditions, indicating antibody inhibition operates specifically on GC B cells clones with similar specificities (Figure 17D). Therefore, in this two-clone system, antibody feedback inhibition is predominately epitope-specific.

Altogether, these data indicate that high antibody titers limit expansion of GC B cell clones that bind to the same or overlapping epitopes. At the level of clonal selection in the GC, antibody acts via a negative feedback mechanism that favors exploration of epitopes poorly targeted by the antibody response. Thus, antibody produced during a humoral response can help guide GC clonal dynamics in real-time.

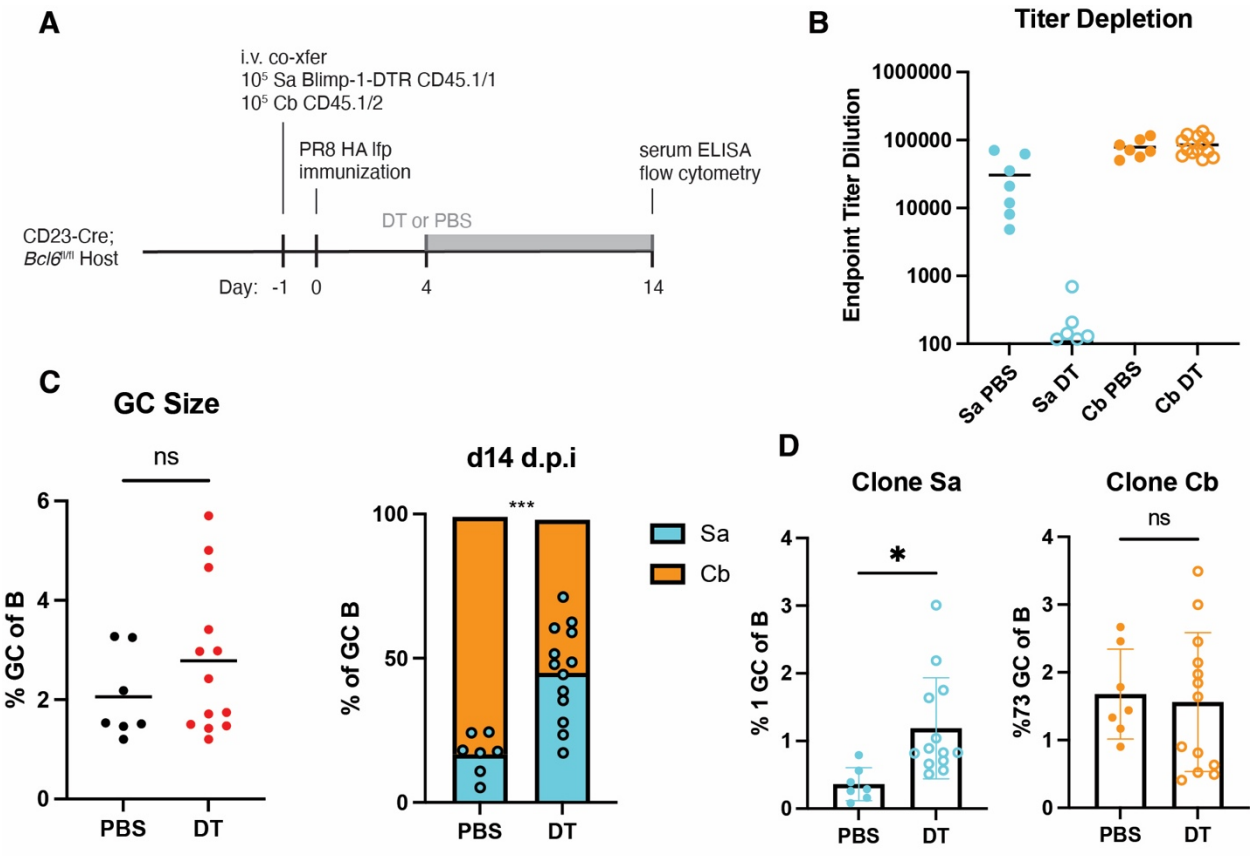

Figure 17: Antibody feedback inhibition is epitope specific

A) Experimental setup. 10^5 HA-binding cells from Sa BCR KI mice harboring the Blimp-1-DTR allele were co-transferred with 10^5 Cb BCR KI Blimp-1-WT cells into CD23-Cre; $Bcl6^{fl/fl}$ hosts. Mice were immunized in the footpad with HA one day later and given daily PBS or DT beginning 4 days after immunization. Mice were sacrificed 14 days after immunization.

B) Endpoint dilution titers of antibodies derived from clone Sa (blue) and clone Cb (orange) with or without DT administration.

C) (Left) Quantification of GC size 2 weeks after immununization. (Right) Proportion of clone Sa (blue) and clone Cb (orange) within the GC 2 weeks after immunization.

D) Proportion of clone Sa (left) and clone Cb (right) relative to total B cells in the lymph node.

CHAPTER 4: Investigating the Effect of Antibody on Affinity Maturation in the GC

Our data suggest that high titers of endogenously-produced antibody limit expansion of GC B cell clones harboring overlapping specificities. We next sought to investigate whether antibody plays a role in the affinity maturation process within the GC. It has been proposed that antibody acts as a rising selection threshold that dictates the directionality of affinity maturation during a humoral response. As plasma cells are continuously exported from the GC, higher affinity antibodies replace lower affinity ones on immune complexes deposited on FDCs, creating a “traveling wave” scenario where the affinity of circulating antibody increases over time. In our depletion model, B cells no longer compete with soluble antibody for antigen acquisition, and therefore obtain more T cell help to proliferate in the GC. This increase in expansion, however, may be accompanied by a decreased rate of affinity maturation, as the affinity threshold for GC B cells to acquire antigen is lower in the absence of antibody. Therefore, the “traveling wave” model predicts that selection of affinity enhancing mutations over time will be impaired when epitope specific antibody is depleted. The following experiments are aimed at testing this model.

Antibody does not affect accumulation of affinity enhancing mutations

To measure affinity maturation in our monoclonal B cells, we sequenced the *Igh* loci of transferred Sa and Cb GC B cells eighteen days after footpad HA immunization (Figure 18A). Clone Sa acquired an average of ~3 *igh* mutations in both mice we sequenced, with 26% and 18% of cells containing 5 or more mutations (Figure 18B). Although the number of mutations accumulated was not large considering the time spent in the GC, the input cells are already moderately mutated, which can lead to loss of AID mutation hotspots (Dosenovic et al., 2015). Of all mutations in the BCRs of clone Sa, three of the most frequent involved the asparagine at position 66. As N66 is the first amino acid after the CDR2 region of the antibody, it is likely to contribute to HA binding, especially considering it is heavily mutated in both mice. The most common N66 mutations were N66I, N66K and N66V. When combined, these three mutations were found in 66% and 78% of clone Sa GC B cells, implying the existence of a heavy selection pressure for the replacement of asparagine at that position. Two other common mutations were S63N and Y109F, detected on average at 6.5% and 3.5% of clone Sa GC B cells (Figure 18B). To test whether the most frequently accumulated mutations in clone Sa were affinity-enhancing, we produced single mutations as Fabs and measured their binding to PR8 HA via biolayer interferometry. Not surprisingly, all N66 mutations resulted in an affinity increase. N66K and N66V mutations resulted in a 2.6 and 2.9-fold increases in affinity, respectively. N66I led to a drastic increase in affinity, a 10.7-fold over the starting BCR (Figure 18C). The increase in affinity was heavily driven by the decrease in off-rate of the interaction with HA (Figure 18D). Off-rate translates into the

strength with which a B cell can pull on antigen tethered to FDCs and is likely a driving parameter for selection with a GC (Batista et al., 1998). The final mutation, Y109F, also enhanced affinity by 2.6-fold. Clone Cb accumulated an average of 3 and 4 mutations per heavy chain in both mice, with 23% and 37% of cells containing 5 or more mutations. Unlike clone Sa, the mutations of clone Sa were not shared as frequently between mice. This is best exemplified by mutations at position S35, which were found in 25% of cells in one mouse but were absent from the other (Figure 18E). Since clone Cb tended not to accumulate common mutations in different mice, we did not produce any of the mutations in fabs, as the irreproducibility of these mutations renders them difficult to consistently detect.

Figure 18: Single mutations in BCR KI clones result in affinity maturation
A) Experimental setup. 10^5 HA-binding B cells from Sa BCR; Blimp-1-DTR or Cb BCR; Blimp-1-DTR mice were transferred into C57BL/6 hosts. Mice were footpad immunized with HA one day later and given daily PBS or DT beginning 4 days after immunization. 18 days after immunization, GC B cells from the transfer population were single cell sorted and their *igh* loci were sequenced.
B) (Left) Number of nucleotide mutations per cell in clone Sa 18 days after immunization. (Right) Frequency of specific mutations in clone Sa 18 days following immunization. Each bar represents the frequency of the indicated mutation in one of the two mice.
C) Fold-change in affinity of most frequent mutations found in clone Sa assessed via bio-layer interferometry.
D) Binding kinetics curves of starting Sa sequence and N66I mutation Fabs as measured by bio-layer interferometry. Fabs were assayed at concentrations of 160, 120, 80 and 40 *nM*.
E) (Left) Number of nucleotide mutations per cell in clone Cb 18 days after immunization. (Right) Frequency of specific mutations in clone Cb 18 days following immunization.

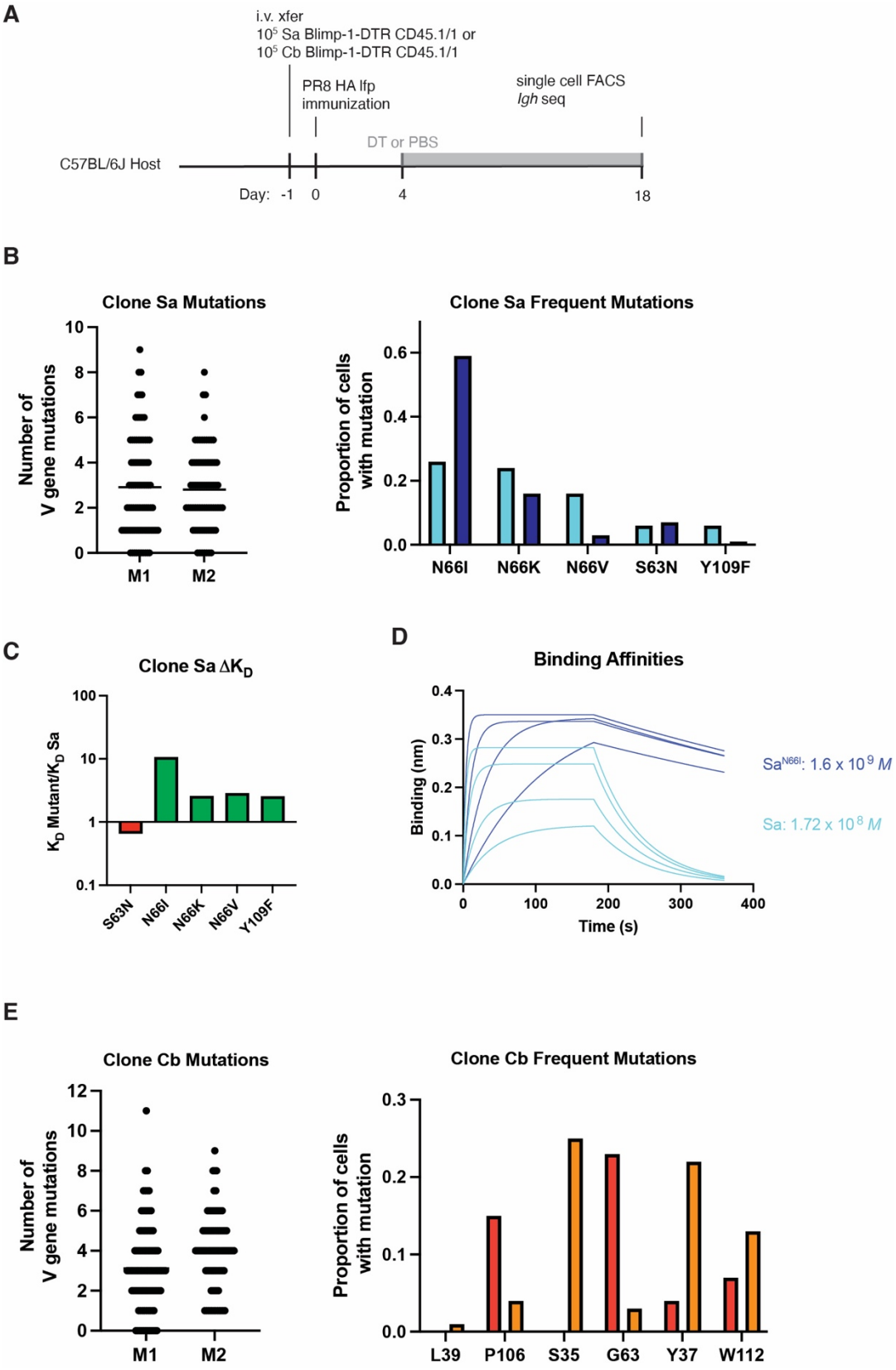

Figure 18: Single mutations in BCR KI clones result in affinity maturation

To test whether antibody plays a role in the accumulation of affinity enhancing mutations of clone Sa, we utilized our co-transfer model into CD23-Cre; *Bcl6*$^{fl/fl}$ mice to deplete antibodies from clone Sa following immunization with HA (Figure 19A). Two weeks after immunization Sa GC B cells harbored the same number of *Igh* mutations regardless of whether its secreted antibody was present (Figure 19B). In addition, the frequency of N66I and N66K was not altered when antibody was depleted, and neither was the frequency of all affinity-enhancing mutations combined (Figure 19C). These mutations were not detected earlier in the response, making it unlikely that excessive time has passed to detect an initial acceleration in their accumulation (data not shown). Therefore, despite influencing clonal selection within the GC, antibody does not accelerate affinity maturation of B cell clones recognizing the same epitope in an adoptive transfer system.

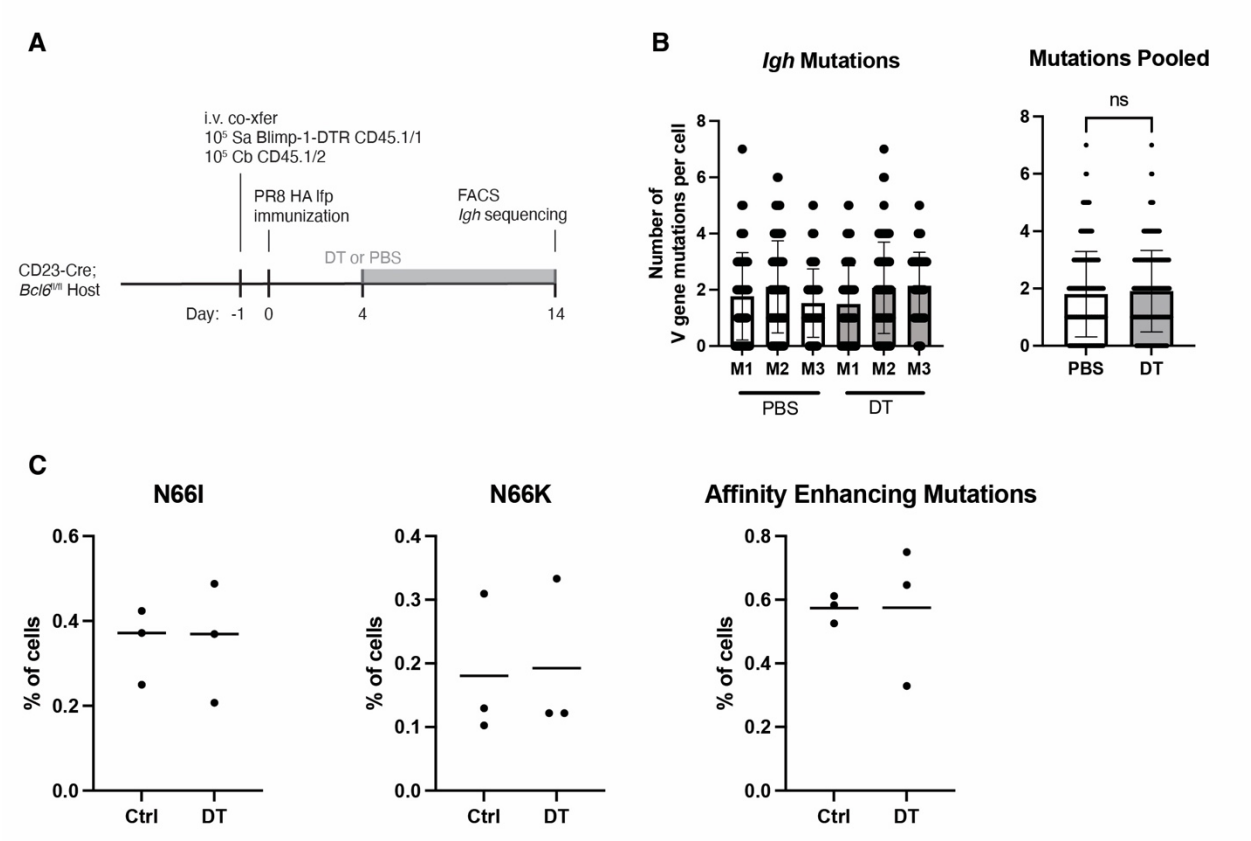

Figure 19: Depletion of antibody fails to impact accumulation of affinity increasing mutations in clone Sa

A) Experimental setup. 10^5 HA-binding cells from Sa BCR KI mice harboring the Blimp-1-DTR allele were co-transferred with 10^5 Cb BCR KI Blimp-1-WT cells into CD23-Cre; $Bcl6^{fl/fl}$ hosts. Mice were footpad immunized with HA one day later and given daily PBS or DT beginning 4 days after immunization. Mice were sacrificed 14 days after immunization, and the *Igh* loci of Sa GC B cells were sequenced.

B) (Left) Number of mutations per cell of each mouse from control and experimental groups. (Right) Pooled number of mutations per cell.

C) Proportion of Sa GC B cells harboring N66I (left), N66K (middle) and a combination of all affinity enhancing mutations (N66I + N66K + N66V + Y109F, right).

Antibody does not affect affinity maturation of polyclonal responses

Whereas adoptive cell transfers are valuable for discovery of mechanisms, they invariably introduce potential artifacts into a model. For example, in our system the precursor frequency of epitope-specific cells is far greater than would ever be present in the WT mouse, and this is further exacerbated by the supraphysiological titers of epitope-specific antibody that are produced upon immunization. Therefore, we wanted to extend our findings on antibody feedback to an unbiased polyclonal system. For this, we utilized the full-length version of the Blimp-1-DTR allele. As Blimp-1 is expressed in other cell populations such as certain subsets of T cells, we could not use the pre-excised version of the allele outside of a B cell transfer setting. The full-length version of Blimp-1-DTR has the stop codon between the final exon of *Prdm1* and DTR flanked by two loxP sites, and using a tamoxifen inducible Cre confers the ability to flox the stop codon at a specific timepoint. Therefore, we crossed Blimp-1-DTR to an AID-CreERT2 mouse. Upon administration of tamoxifen, all activated B cells within a 4-day window will produce the floxed version of the Blimp-1-DTR allele. It follows that any plasma cell derived from these B cells can then be depleted with DT. However, other plasma cells, whose B cell precursors were not activated in the time window of tamoxifen administration, remain untouched. We immunized AID-CreERT2; Blimp-1-DTR with HA and administered tamoxifen via gavage on days 2, 5, 8, and 11 to ensure maximal recombination of ensuing GC B cells (Figure 20A). We also began administering daily DT at day 4 following immunization. At day 14, anti-HA IgG titers were depleted approximately 40-fold with DT, but total IgG concentrations remained the same, as

plasma cells not produced during the HA response are not depleted (Figure 20B). GC size, HA specificity, and HA avidity (tetramer gMFI) were not affected when antibody was depleted (Figure 20C). Unlike in the transfer system where epitope specific antibodies can be depleted, in polyclonal systems only total HA titers are depletable. Therefore, the percentage of HA binding in the GC does not change despite the removal of inhibitory antibody. Another possibility is that antibody titers are not high enough during a primary response in mice with WT B cell repertoires to produce the inhibitory effect seen with the adoptive transfer conditions. Regardless, we detected no differences in GCs in the absence of antigen specific antibody.

To address whether antibody helps accelerate affinity maturation in this polyclonal system, we made use of NB-21 feeder cells to culture single GC B cells and assess the affinities of their antibodies. NB-21 cells support the proliferation and differentiation of GC B cells into plasmablasts that secrete their antibodies into the culture well, allowing for isolation of supernatants for downstream binding assays (Nojima et al., 2011; Kuraoka et al., 2016). As plasmablasts within each well are derived from a single GC B cell, the resulting antibodies are monoclonal. Therefore, the use of NB-21 feeder cells allows us to interrogate the affinities of individual GC B cells in a high-throughput manner (Kuraoka et al., 2016). On day 14 post immunization, we single-cell sorted GC B cells onto NB-21 feeder cells. After culturing the cells for one week, we collected supernatants from each well and assessed their concentrations and binding to HA. Upwards of 90% of the antibodies produced were of the IgG1 isotype, consistent with

the use of alhydrogel as the adjuvant for immunization (data not shown). To establish accurate IgG1 concentrations from each well, we used recombinantly produced mouse Cb IgG1 monoclonal antibodies to generate standard curves for total IgG1. Once we determined the concentration of IgG1 in each well, we assayed the antibodies against HA in ELISA and compared their OD values to a standard curve of clone Cb binding to HA. As a proxy for affinity maturation, we calculated the difference between experimentally obtained OD values and the OD values interpolated from the standard curve of Cb. A cell with higher affinity than Cb will have an OD value greater than that of Cb binding to HA at the same concentration, while a cell with lower affinity than Cb will have a smaller OD value when concentration is constant. We term this calculation the avidity index (Figure 20D). We calculated the avidity indexes of antibodies produced from sorted cells. As expected, most antibodies had a negative avidity index, indicating they were generally lower in affinity than mAb Cb, which was originally isolated from late GCs in response to flu infection and boasts a 30nM affinity. We saw no difference in avidity indexes between cells when HA titers were depleted (Figure 20E). In addition, there was no difference in the average avidity index of GC B cells of each mouse. These data indicate that antibody does not drive or accelerate affinity maturation in a polyclonal setting.

Figure 20: Affinity of polyclonal responses to HA is not affected by depletion of antibody

A) (Top) Schematic of Blimp-1-DTR allele. The full-length version of the allele was utilized for all experiments involving polyclonal B cell repertoires. (Bottom) Experimental setup. AID-CreERT2 mice were immunized with HA and gavaged with tamoxifen at days 2, 5, 8, and 11 after immunization. In parallel, mice were dosed daily with at day 4 with DT. Animals were sacrificed at day 14 and processed for serum titers and single cell sorting.

B) Total IgG concentrations (left) and anti-HA IgG titers (right) in WT and antibody depleted mice.

C) GC size (left), percentage of HA binders in the GC (middle), and gMFI of HA binders (right).

D) Schematic demonstrating calculation of avidity index. Black curve represents binding of reference mAb Cb to HA in ELISA. mAbs with better binding than Cb will be higher than the curve (green dot), while mAbs with decreased binding will be lower (red dot).

E) (Left) Pooled avidity indexes from cells from 6 mice per group. (Right) Average avidity indexes from single GC B cells of each mouse.

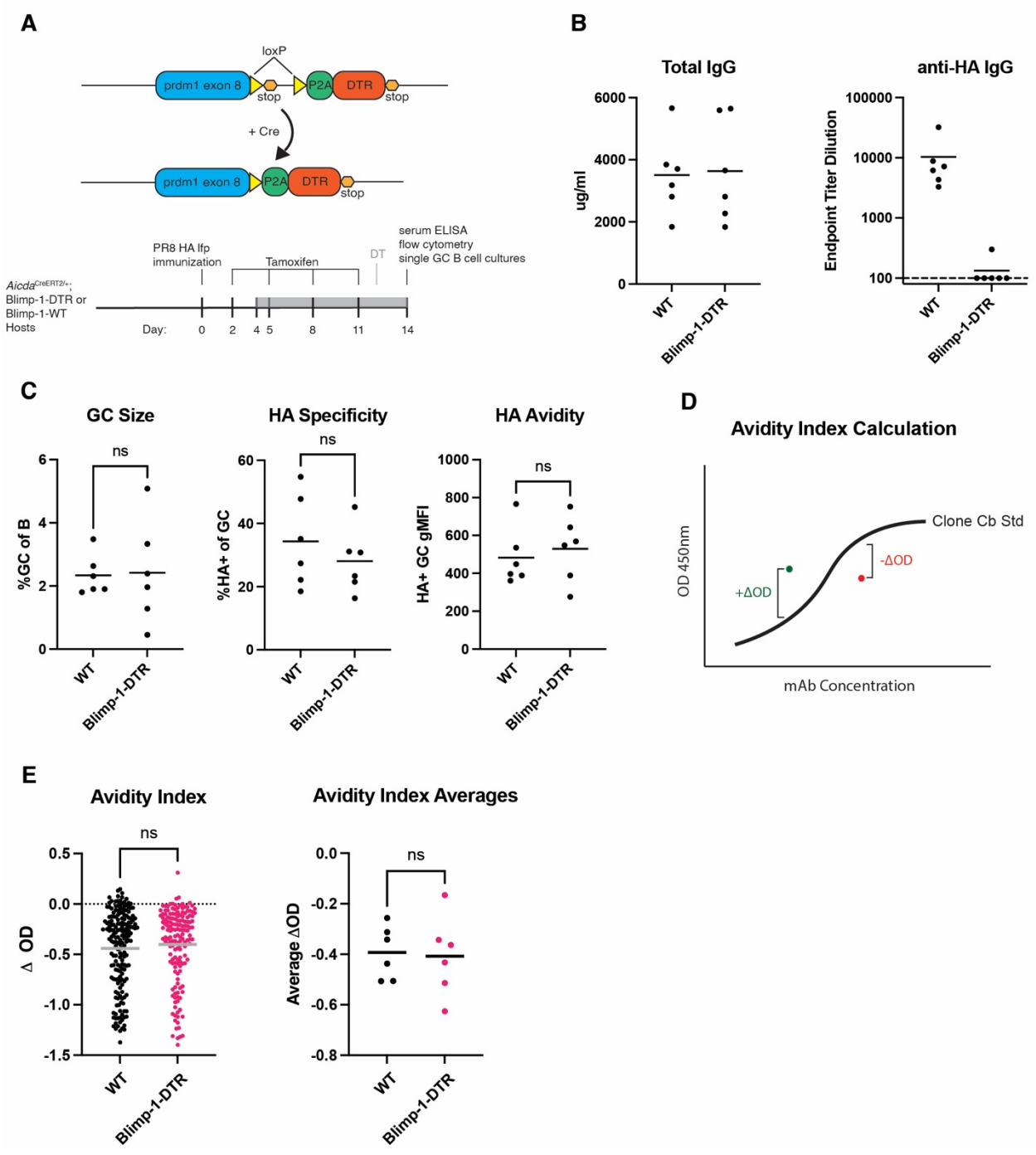

Figure 20: Affinity of polyclonal responses to HA is not affected by depletion of antibody

Although our data indicate that antibody plays no role in affinity maturation, it is possible that measuring binding via ELISA is not sensitive enough to detect subtle differences in affinity between the two groups. Therefore, we tested antibody feedback with polyclonal repertoires in response to another antigen, NP-OVA. As discussed previously, NP is a small molecule that only elicits B cell responses when linked to a carrier protein. Immunization with NP produces highly stereotyped and reproducible responses in which a majority of NP-reactive BCRs are produced by the VH1-72 gene segment pairing with an Igλ light chain. In addition, a 10-fold increase in affinity of the BCR occurs when the tyrosine at the 33rd position of VH1-72 is mutated to a leucine (W33L). Therefore, immunization with NP-OVA enables convenient detection of epitope specificity in the GC along with affinity maturation of GC B cells. We immunized AID-CreERT2 mice with NP-OVA in the footpad and followed the same tamoxifen and DT administration protocol as with HA immunization (Figure 21A). At day 14 titers to NP-OVA were approximately 10-fold depleted with administration of DT (Figure 21B). While the GC as a whole was not affected, we observed a shift in specificity towards NP. Since B cells harboring an Igλ light chain are rare within the naive repertoire (5-10% in mice), the enriched Igλ$^+$ population in GCs responding to NP is predominately NP-specific. Using Igλ as a surrogate for NP binding, we detected an increase in NP binding in the GC upon depletion of antibody, corroborating our results from adoptive transfers with B cells from BCR KI mice (Figure 21C). We are in the process of sequencing Igλ$^+$ GC B cells and analyzing the proportion of VH1-72 bearing rearrangements that accumulate the W33L

affinity enhancing mutation, which will provide a highly sensitive method to further investigate the effect of antibody on affinity maturation in a polyclonal WT system.

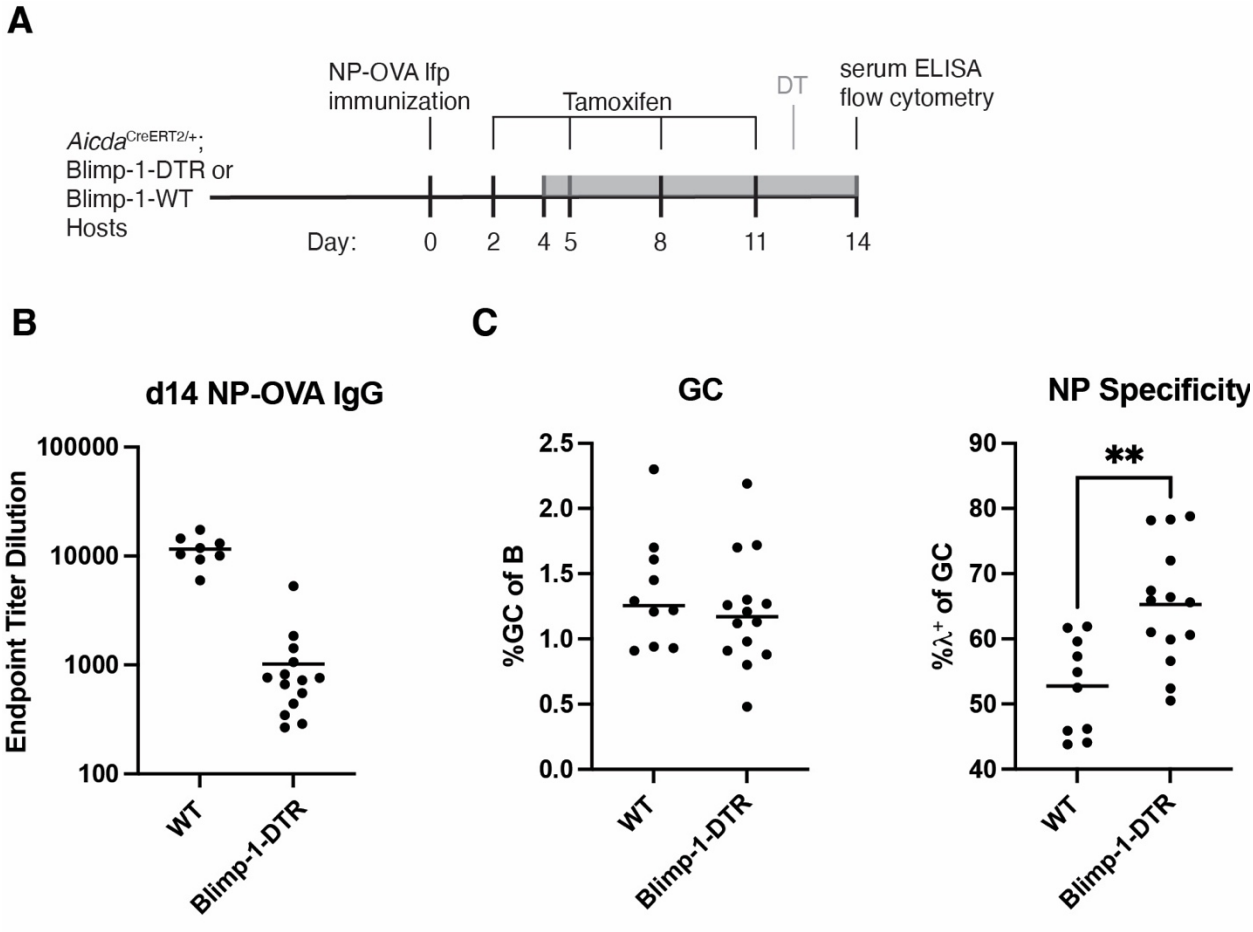

Figure 21: Epitope masking is evident in polyclonal responses to NP
A) Experimental setup.
B) NP-OVA IgG titers 14 days after immunization, measured via ELISA.
C) GC size (left), and percentage of lambda+ B cells in the GC (right).

CHAPTER 5: Discussion and Future Directions

Developing a complete understanding of the output of primary B cell responses is important for effective vaccine development. Affinity and polyclonality are two essential features of protective antibody responses, and improved control over these factors will be beneficial towards generating effective humoral immunity in the human population. Whether B cell responses are regulated by their own antibodies remains a highly debated topic and represents a gap in our knowledge of adaptive immunity. It has been proposed that antibody can feedback onto contemporaneous humoral responses and modulate the diversity and affinity of primary GC reactions in real-time (Zhang et al., 2013). However, a lack of available loss-of-function tools to study antibody feedback precludes the investigation of antibody feedback as a *bona fide* self-regulatory process. Here, we have designed a loss-of-function genetic mouse tool allowing us to deplete plasma cells, and therefore, antibody, upon administrated of diphtheria toxin. In parallel, we have developed BCR knock-in mice whose B cells bind to distinct epitopes on influenza HA. Combining these tools has allowed us to study the effect antibody from a primary response on clonal selection and affinity maturation within ongoing GCs. As our HA-binding clones bind to different epitopes on the same protein, our model allows us to deconvolute epitope specific and epitope non-specific mechanisms of antibody feedback. We find that high titers of antibody produced during an ongoing response inhibit expansion of GC clones specific for the same epitopes, implying that the predominant mechanism of antibody feedback is via epitope masking. This negative feedback loop likely encourages the GC to engage specificities that are not heavily

represented in the serum antibody compartment. However, while antibody can influence the outcome of *inter*clonal competition within the GC, it does not play a major role in driving affinity maturation within individual B cell clones.

Antibody suppresses ongoing GC responses via feedback inhibition in an epitope specific manner

Adoptively transferred BCR knock-in cells quickly decay in the GC despite dominating the early reaction. This decay is in part mediated by the high levels of epitope-specific antibody titers produced by the transferred cells, as depletion of these titers slows the turnover of the transferred population. Removal of antibodies secreted by the transferred clones, however, did not significantly affect the size of the total GC. Instead, the antibody suppressed the transferred cells that bound to the same epitope without affecting endogenous cells in the GC, suggesting epitope masking is the predominant mechanism of antibody feedback in this system. If antibody exerted epitope non-specific effects on the GC, total GC size would increase upon antibody depletion, as a general suppressor of the entire response would be removed. Observations from single clone transfer experiments into WT hosts were corroborated by co-transfer experiments with different B cell clones into mice whose endogenous cells could not form GCs. We found that depletion of antibody from one of the two clones resulted in a concurrent expansion of the same clone within the GC, without significantly affecting GC size or cell numbers of the other clone. In this set-up, if antibody exerted epitope non-specific effects, the entire GC would expand, including the clone whose antibody was not depleted (Figure 22).

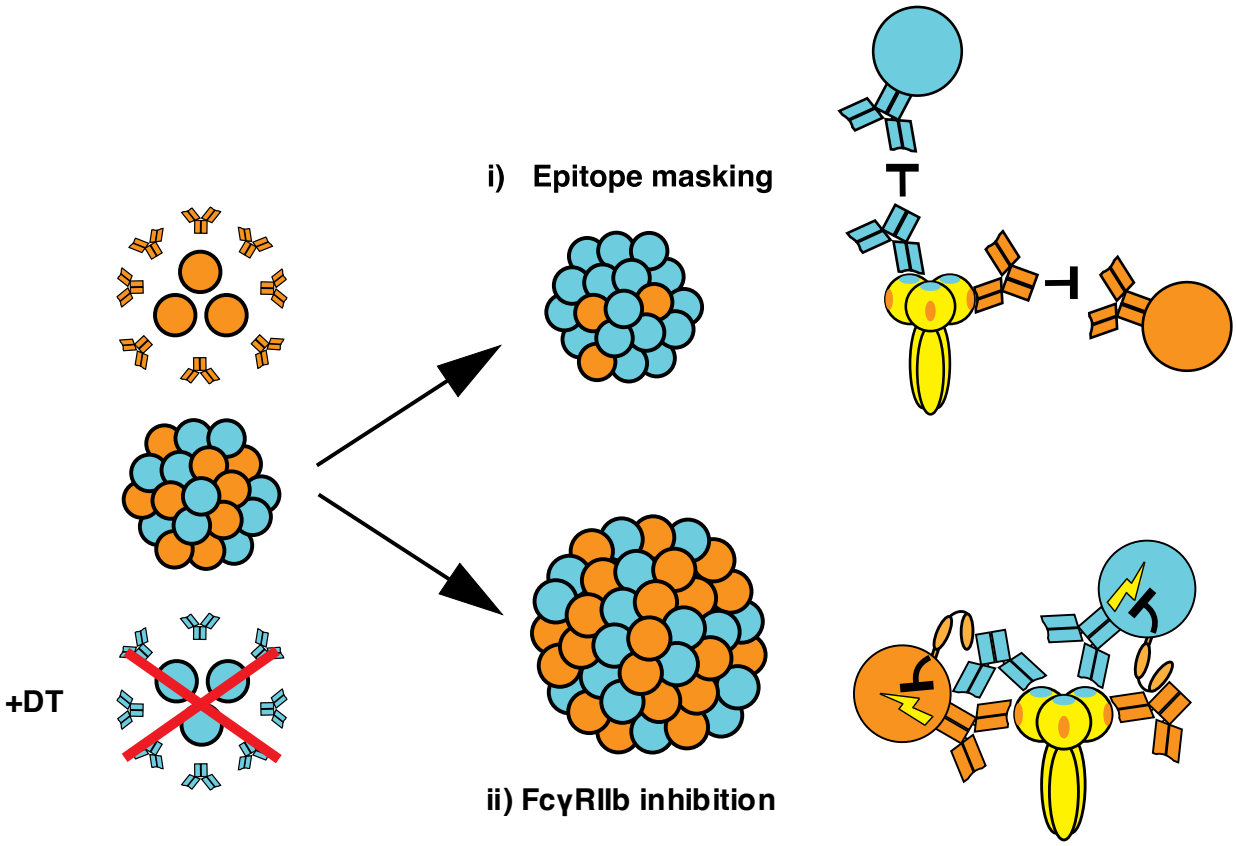

Figure 22: Hypothetical outcomes of antibody depletion
i) With epitope masking, removal of antibody from one clone will only affect the cognate clone in the GC.
ii) With FcγRIIb-mediated inhibition, removal of antibody secreted by one clone will remove a general suppressor of the GC reaction, and the entire GC will expand.

Therefore, our model predicts that epitope masking is the dominant mechanism of antibody feedback during an ongoing GC response. This epitope specific negative feedback loop has major implications for *inter*clonal selection in the GC. Negative feedback loops are commonly employed within homeostatic pathways to maintain important parameters within a narrow value range (Chakravarty et al., 2023). In a simple negative feedback loop, the output that is produced in response to a stimulus can slow

or completely inhibit the further production of that output. Examples of negative feedback loops can be found in the majority of metabolic pathways, where the accumulation of final or intermediary products can reversibly inhibit enzymes throughout the pathway and thereby slow it down. On a more macroscopic level, negative feedback loops are important in maintaining blood glucose levels and regulating body temperature and blood pressure. In a similar fashion, antibody feedback via epitope masking regulates the clonality of primary B cell responses in real-time. During a GC response, B cell clones that are heavily expanded will have more opportunities to differentiate into plasma cells than clones that are rare. Once antibody titers from these expanded clones reach high enough levels, they begin to suppress the further expansion of the dominant clone in the GC by binding to its epitope and limiting its access to antigen. This process allows subdominant clones in the GC to remain in the GC, further expand, and have more opportunities to contribute to the plasma cell compartment. Therefore, antibody-mediated suppression via epitope masking may be an important mechanism in guiding the development of primary GC responses towards epitopes that are poorly represented in the serum antibody compartment.

Several observations can be explained in light of this this model of antibody feedback in ongoing GCs. GC B cell responses to HA change in specificity over time. For example, 14- and 21-days following infection with influenza virus, all HA-binding GC B cells bind either the Cb or the Sa epitopes, while reactivity to other epitopes is undetectable. 4 weeks after infection, however, a significant proportion of GC B cells bind the Sb, Ca1,

and Ca2 epitopes (Angeletti et al., 2017). This can be explained by epitope masking, as Cb and Sa specific antibodies produced early in the response inhibit the further expansion of Sa- and Cb-binding B cell clones, allowing other specificities to access antigen and gain a competitive advantage in the GC. We also observe antibody regulating GC *inter*clonal selection in a polyclonal system in response to immunization with NP-OVA. In the case of NP-OVA, the majority of the antibody response is directed towards the hapten, NP, while OVA is relatively inert. However, despite dominating the antibody compartment, only approximately 50% of GC B cells in the GC 14 days after immunization are NP-specific. This is likely due to feedback inhibition from NP-specific antibody onto NP-binding B cell clones in the GC. Indeed, upon depletion of antibody from the NP-OVA response, the percentage of NP-binding B cells in the GC significantly increases, indicating that high anti-NP antibody titers shift the specificity in the GC away from the hapten and likely towards OVA, the carrier protein. Taken together, these data imply that antibody feedback may play an important role in ensuring antibody responses maintain diversity throughout a GC reaction that predominantly selects for affinity.

While our loss-of-function system supports epitope masking as the dominant mechanism of antibody feedback, it fails to rule out FcγRIIb-mediated inhibition as an important factor in GC regulation. In WT, polyclonal systems, it is likely that both epitope masking and FcγRIIb-mediated inhibition contribute towards antibody feedback. However, in our BCR KI transfer system, the high antibody titers likely bias the system towards epitope-specific mechanisms of feedback. At very high antibody

concentrations, it is possible that the corresponding epitopes are completely bound, rendering most of the antigen inaccessible to GC B cells binding the same epitope. Therefore, when this antibody is depleted, the antigen becomes far more accessible to the cognate GC B cell clone, and the ensuing epitope specific expansion may mask potentially more subtle effects mediated by FcγRIIb-mediated inhibition. Therefore, our adoptive transfer models provide a proof of principle that antibody can regulate clonal selection within an ongoing GC (Figure 23), although it is unclear whether such high antibody titers can indeed be elicited in primary responses. Nevertheless, our observation of epitope specific suppression in polyclonal systems suggests that antibody feedback via epitope masking is an important parameter in regulating *inter*clonal selection in ongoing GC responses.

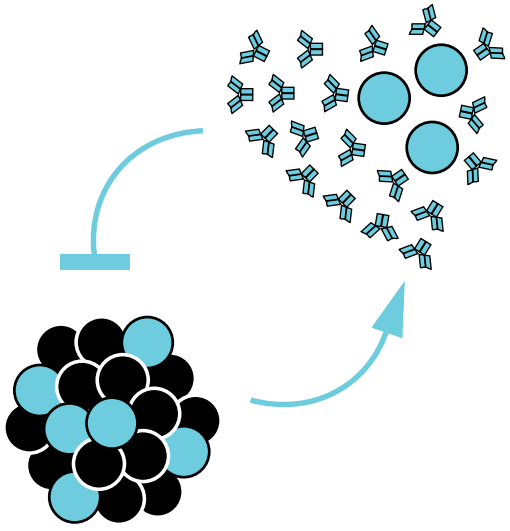

Figure 23: Antibody suppresses expansion of GC B cell clones binding the same epitope

Circulating antibody does not accelerate affinity maturation in the GC

A prediction derived from epitope masking models of antibody feedback is that circulating antibody helps guide the directionality of affinity maturation in the GC. Plasma cells exported from the GC are enriched in high-affinity BCRs so that, at a given time point, the average affinity of plasma cells is higher than the average affinity of GC B cells. Antibody produced by these plasma cells regains access to the GC and binds antigen found on FDCs. It follows that only GC B cells with higher affinity than the soluble antibody will be able to displace the bound immunoglobulin and internalize antigen for presentation to T_{FH} cells (Figure 24). Since plasma cells are continuously exported, the affinity of the antibody with which GC B cells must compete increases over time, and this "traveling wave" model is proposed to maintain the positive directionality of affinity maturation within the GC (Zhang et al., 2013).

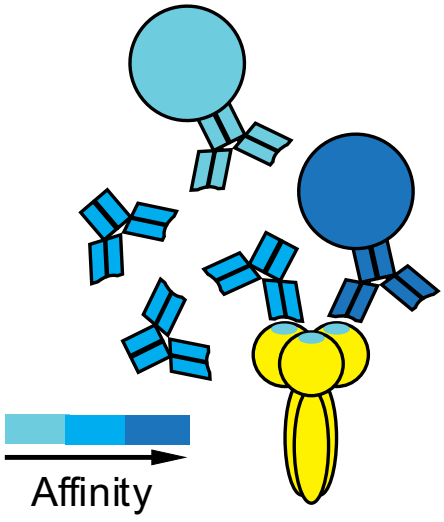

Figure 24: Proposed model of affinity maturation via epitope masking

In our BCR KI adoptive transfer model, depletion of antibody produced by clone Cb had no discernable effect on the accumulation of affinity-enhancing mutations in its GC counterparts. Additionally, we observed no difference in the avidity indexes of HA-binding GC B cells when antibody from the primary response was removed. An unchanged rate of affinity maturation may seem at odds with clonal expansion upon antibody depletion. These two observations can be reconciled by the limited availability of T cell help, which is not altered when antibody is removed. The amount of proliferation, and therefore mutation rate, of a GC B cell is governed by the strength of T cell help it receives. The relative amount of T cell help received, in turn, is directly dependent on the affinity of the BCR, which determines the amount of antigen that is processed and presented on MHCII (Schwickert et al., 2011). Regardless of the amount of antigen present, a B cell of higher affinity will always obtain more T cell help than a B cell with lower affinity. Epitope-specific antibody limits access of antigen only to those B cells clones specific for the same epitope. However, within a B cell clone, the relative amount of peptide presented by individual B cell variants remains the same in the presence or absence of antibody. For example, take a variant of clone Sa that has produced the N66I mutation that confers a >10-fold increase in affinity for HA and compare it to a variant of the same clone that has not produced this mutation. Assuming the relationship between antibody affinity and peptide presention is linear (Schwickert et al., 2011), the N66I variant will present ten times more antigen than its unmutated counterpart. In the absence of antibody, although the absolute amount of peptide presented will be higher on a per cell basis, the relative proportion of presentation

remains the same, and the higher-affinity B cell will still present 10-fold more peptide than the lower affinity variant. Therefore, within the same clone, the relative amount of T cell help to each variant remains the same, and the rate of affinity maturation is not affected. However, in the case of *inter*clonal comepetition, the depletion of epitope-specific antibody skews the ratio of peptide presentation between two clones. In our co-transfer system, when antibody Sa is depleted, the absolute amount of antigen presentation by clone Cb is not affected, while the absolute amount of antigen presented by clone Sa increases. Therefore, the ratio of antigen presentation between clone Sa and clone Cb increases, explaining the competitive advantage acquired by clone Sa when its antibody is removed. In essence, our system demonstrates that antibody affects *inter*clonal competition but has no consequence for *intra*clonal competition, explaining its lack of influence on affinity maturation.

HA stalk-binding B cell clones are subdominant even when present at equal precursor frequency

Although our oligoclonal B cell system was initially designed to investigate antibody feedback, it will also be helpful in addressing other questions in the field of GC biology and humoral immunity. One interesting insight from competing our three BCR KI clones is that clone C179 was reproducibly subdominant within the GC. Antibody responses against the stalk of hemagglutinin are broadly protective as they bind epitopes that are conserved between different subtypes and occasionally between different groups of influenza strains (Wu et al., 2019). However, despite their efficacy against a wide range

of influenza viruses, stalk responses are rarely found in the human population, and when present, they are difficult to sustain with boosting regimens (Fukuyama et al., 2020). The majority of universal influenza vaccine efforts have been geared towards eliciting anti-HA stem responses, but even so currently available vaccines only confer protection within actively circulating virus strains. There are several hypotheses for why HA stem responses are immuno-subdominant to responses to the HA head. The simplest explanation is that the stalk domain is more inaccessible to B cells than the head domain when HA is on the surface of a virion (Krammer et al., 2013). Although antibodies can burrow between HA molecules on the surface of a virion to bind the stem domain, it has been shown anti-stem antibodies bind virus-tethered HA with lower avidity than soluble HA (Andrews et al., 2015b). In addition, it is likely even more difficult for stem-reactive B cells to access their epitope, as they must also overcome the steric hinderance imposed by the B cell itself. However, the relative ease of access to the head and stalk domains does not explain why the stalk is also subdominant upon immunization with HA, where the stem and head domains should be equally accessible. Another explanation for the rarity of stalk responses is that the precursor frequency of stem-reactive B cells in the naïve repertoire is low. In humans, a significant proportion of stalk-reactive antibodies use VH1-69, which contacts the hydrophobic stem epitope via specific residues in its HCDR2 (Sui et al., 2009). VH1-69 is highly polymorphic in the human population, and alleles harboring a phenylalanine at position 54 in the CDR2 produce antibodies that are far more likely to bind the HA stalk. In fact, a majority of VH1-69 anti-stalk antibodies identified contain Phe54, enabling individuals with this

polymorphism to produce anti-stem responses more readily (Pappas et al., 2014). The significant VH gene and polymorphism restriction of anti-stalk antibodies implies that solutions to produce BCRs against this epitope are extremely rare. Further contributing to their scarcity is the fact that these antibodies may also be enriched for polyreactivity and autoreactivity, resulting in their gradual counterselection in the B cell repertoire. Overall, a lack of complete understanding of the subdominance of HA stem responses presents a barrier for universal influenza vaccine design.

Of the three BCR KI mice we produced, one of them, C179, is specific for the stem of HA. C179 is the first reported anti-stem antibody, and it was discovered in mice immunized with an H2N2 virus. Structural studies reveal C179 binds to a similar epitope as VH1-69-restricted human antibodies, albeit with a different approach angle (Dreyfus et al., 2013). Nevertheless, C179 provides a good model for investigating human anti-HA stem responses. C179 binds PR8 HA with similar affinity to clones Sa and Cb, and it is capable of forming GCs when transferred in isolation (Figure 25A, data not shown). However, during co-transfer, clone C179 is outcompeted in the GC by the head binding clones, despite starting with an identical precursor frequency (Figure 25B). This defect cannot be readily explained by poly- or autoreactivity, as clone C179 did not bind any of a panel of common polyreactivity antigens. Therefore, when both head and stem B cell precursors exist, B cells specific for the head are preferentially recruited to respond. This phenomenon is similar to observations in humans. A subset of individuals produced robust anti-stem titers during infection with the 2009 H1N1 (Cal09) pandemic

strain, as the highly divergent shifted strain recruited crossreactive memory B cells into the primary response. However, upon boost of the same individuals with Cal09 HA, their recall responses were dominated by head reactivity, as memory responses to these epitopes were formed during primary infection (Andrews et al., 2015b). These observations demonstrate that B cell memory to stem is capable of being recalled, but only in the absence of memory to head epitopes, as is evident from our three-clone competition experiments.

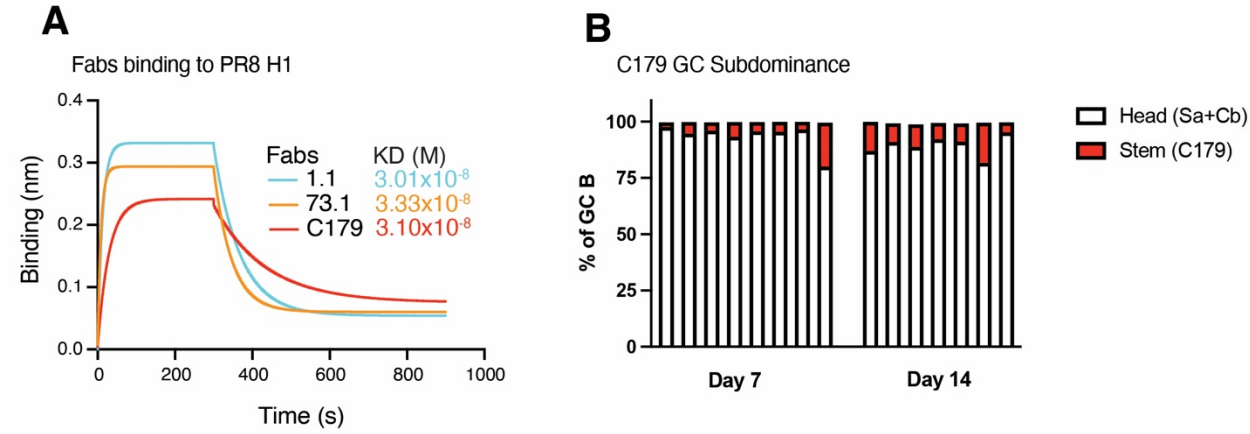

Figure 25: HA stem responses are subdominant even when affinity and precursor frequency are matched
A) Bio-layer interferometry analysis of binding kinetics between Fabs Sa, Cb, and C179 and PR8 HA.
B) Percentage of Sa + Cb (black) and C179 (red) clones in the GC following immunization with HA. Equal cell numbers of all three clones were transferred into CD23-Cre; $Bcl6^{fl/fl}$ hosts, whose endogenous cells cannot form GCs.

Entry of stem reactive B cell clones into secondary GCs is not suppressed by antibody

When we first designed our antibody depletion system, we tested its functionality by examining the effect of antibody on GC entry during recall responses. Numerous studies have shown antibody can suppress GC entry of naïve B cell clones harboring the same specificities, and this suppression is dependent on the amount and the affinity of pre-existing antibody (Tas et al., 2022). To this end, we proceeded to determine if depletion of antibody from a primary response results in increased entry of B cells during a recall response to the same antigen. We transferred HA-binding Cb B cells into C57BL/6 hosts, immunized the mice with HA in their left food pads the following day, and administered daily DT or PBS beginning at day 4 after immunization. 20 days after the prime, we transferred a new population of clone Cb, and boosted the mice with HA in their ipsilateral footpad (Figure 26A). At the time of boost, there are two main transferred B cell populations capable of responding: memory Cb B cells from the pre-prime transfer and naïve Sa B cells from the pre-boost transfer. As expected, entry of the naïve clones into secondary GCs at day 7 is lower than entry into a primary GC, as only ~25% of the secondary GC is composed of the transferred clone, in comparison to ~80% at day 7 of a primary GC. In agreement with previous studies, depletion of antibody resulted in increased entry of naïve Sa B cells into recall GCs, without significantly affecting memory re-entry (Figure 26B). Interestingly, we did not observe the same effect when repeating the prime boost experiment with clone C179, as

depletion of C179 antibody from the primary response did not alter the entry of naïve C179 into recall GCs.

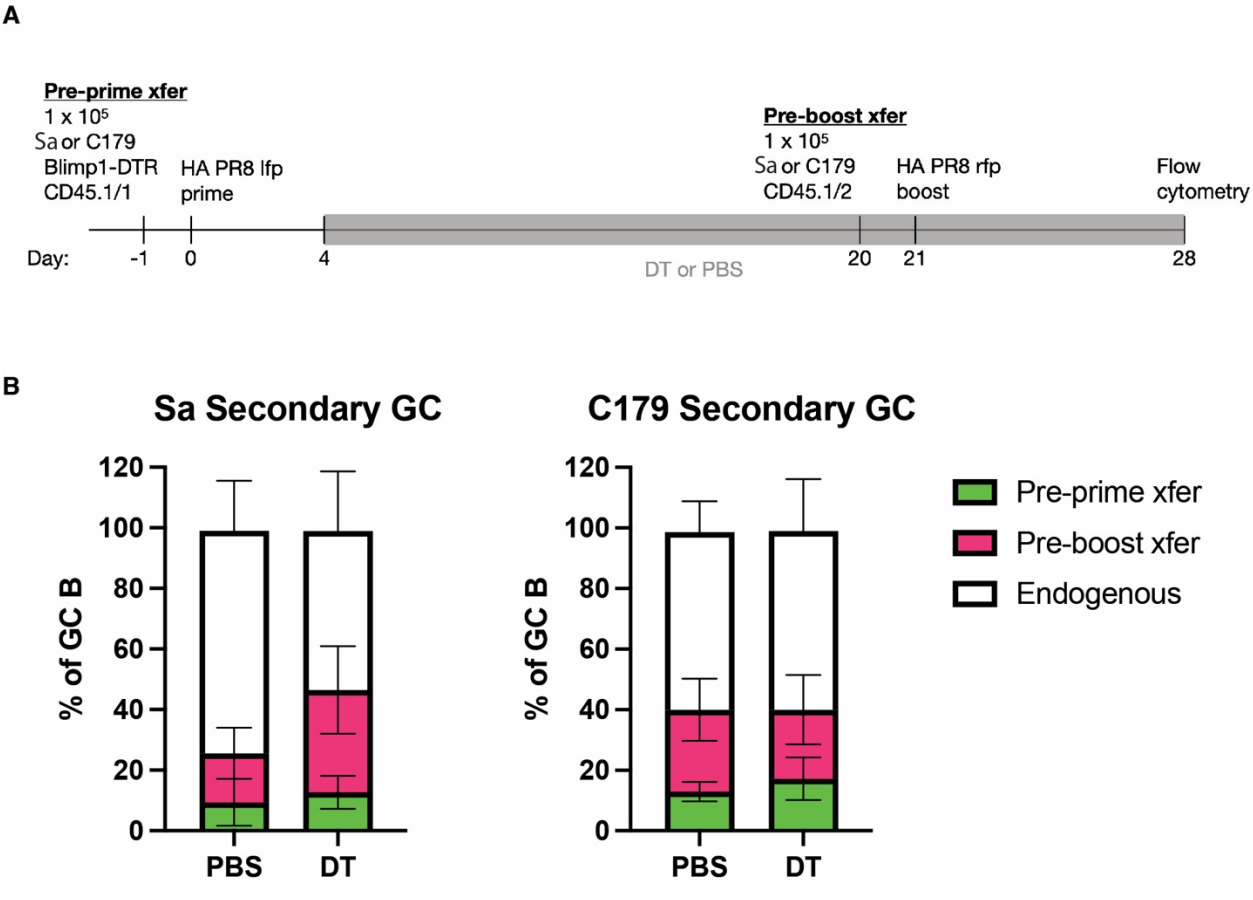

Figure 26: Antibody does not suppress entry of naïve stem reactive B cells into secondary GCs
A) Experimental setup, described in text.
B) Percentage of secondary GC occupied by pre-prime transfer and pre-boost transfer populations for clone Sa (left) and clone C179 (right).

Although these experiments are preliminary, they further support the notion that stem-reactive B cell clones do not follow the same rules as their head-binding counterparts. However, if stem responses are not suppressed by stem-specific antibodies, this is promising for the design of boost strategies that seek to recall stem reactive clones during B cell responses, as it implies that pre-existing antibody does not impose a barrier to propagating anti-stalk responses.

Immunization with HA and infection with influenza virus elicit variable B cell responses

The oligoclonal BCR KI system we have developed can also be used to understand differential anti-HA GC responses to immunization with HA and infection with influenza virus. Upon immunization, clone Cb dominated the initial response in all mice. However, upon infection of mice receiving an identical mix of the 3 clones, clone Sa B cells dominated GC entry (Figure 27). This may be explained by the relative accessibility of epitopes in each antigen. When HA is found on the surface of a virion, epitope Sa is more accessible to B cells than the Cb and stem epitopes, explaining why clone Sa dominates the reaction. As the 3 clones harbor similar nominal affinities, these experiments demonstrate affinity is not the only factor governing interclonal competition, and that epitope accessibility is an important parameter to consider in immunogen design.

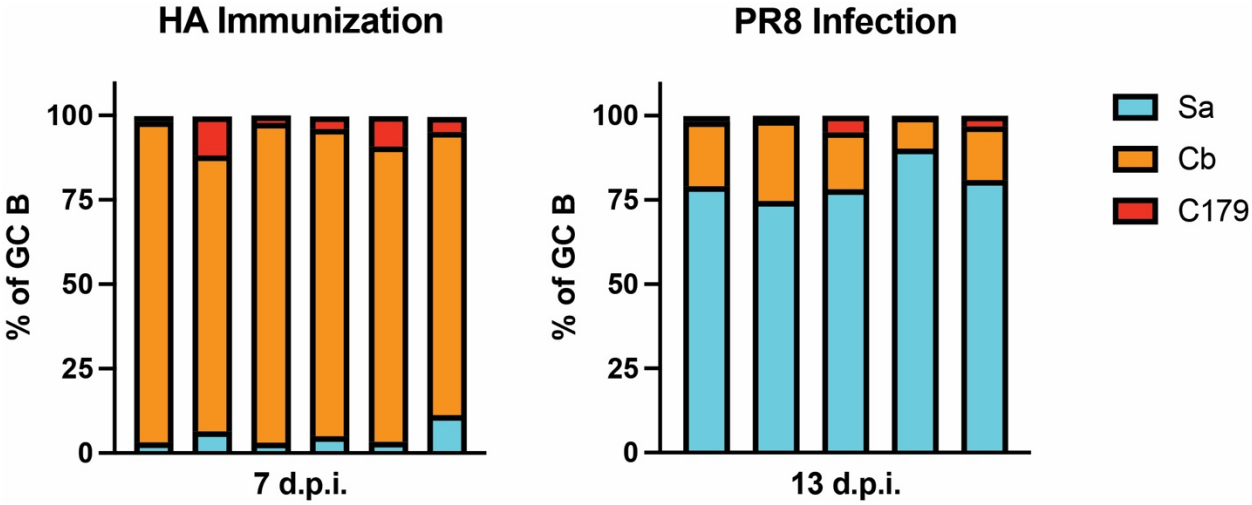

Figure 27: Specificity of HA responses varies with with infection vs. immunization
Clones Sa, Cb and C179 were transferred into CD23-Cre; Bcl6$^{fl/fl}$ hosts. One day later, mice were either immunized with protein HA or infected with PR8 infleunza virus. GCs were analyzed 7 days after immunization and 13 days after infection. Each bar represents one mouse.

Our oligoclonal B cell system is also valuable translational tool that can aid in the development of novel immunization strategies against HA. The inclusion of a subdominant stem-specific B cell clone allows for a simple read out of engagement of subdominant epitopes, and thus can be used to develop strategies that consistently bias the response towards the cross-reactive clone. Before testing HA immunogens in a polyclonal system, the quality of the ensuing responses can quickly be ascertained with this transfer model.

Conclusion

Understanding the parameters that dictate *inter*clonal selection within germinal center reactions is important for the design of immunization strategies geared towards biasing responses against desired epitopes. Here, we show that antibody produced from an

ongoing B cell response can feedback onto contemporaneous GCs and influence i*nter*clonal selection within this compartment (Figure 28). Through the design of Blimp-1-DTR, a plasma cell deleter mouse, along with BCR KI mice with specificities for non-overlapping epitopes on influenza hemagglutinin, we have shown that antibody suppresses only those GC B cell clones that bind to the same epitope, implicating epitope masking as the dominant mechanism of antibody feedback. However, while antibody can influence the outcome of *inter*clonal competition in the GC, it has no discernable effect on the rate of affinity maturation of individual B cell clones. We propose that antibody feedback provides a form of negative feedback by which GCs may diversify their specificities, diverting their focus to epitopes that are not heavily represented within the serum antibody compartment.

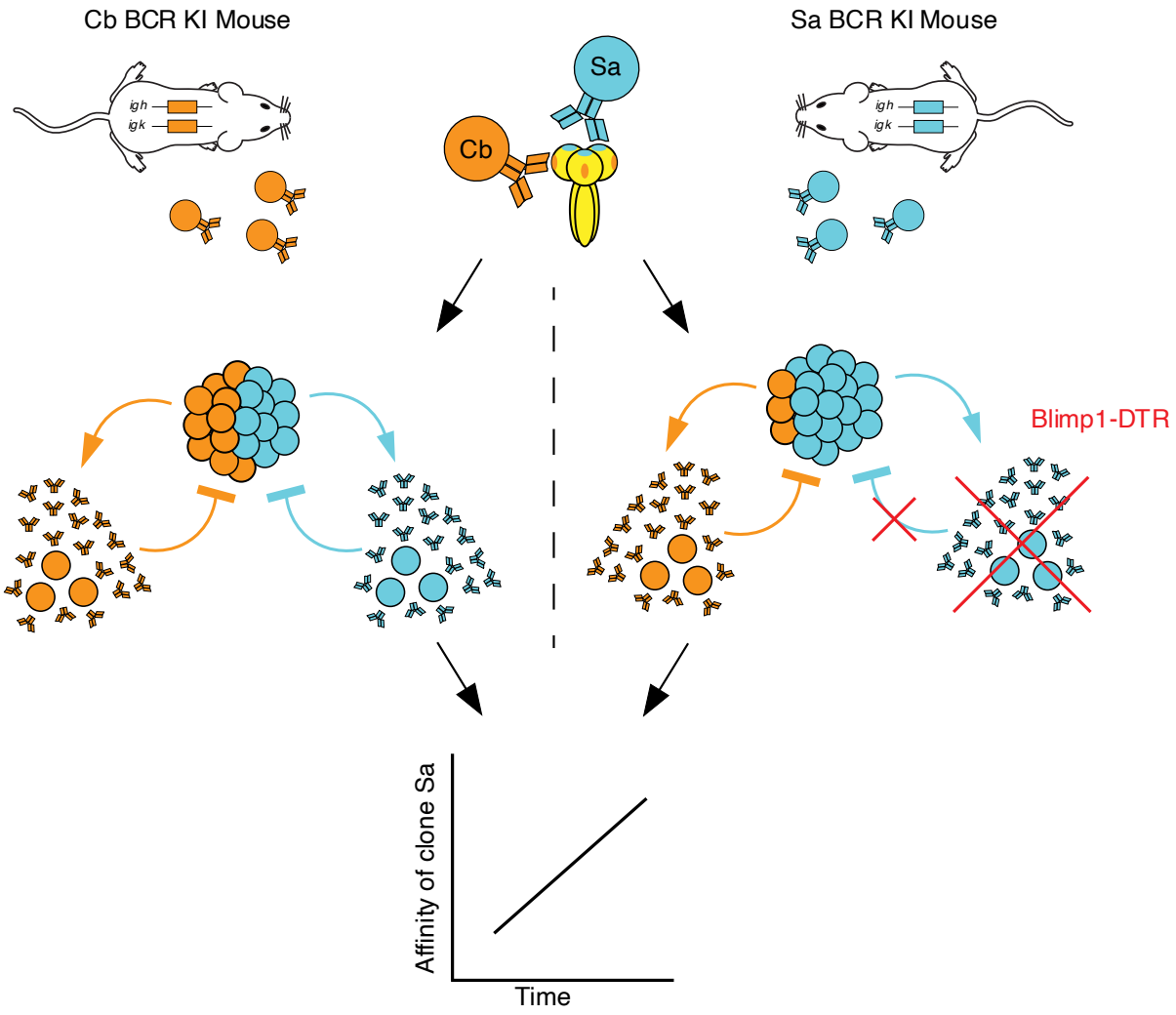

Figure 28: Graphical Abstract

- We report the design of a genetic mouse tool used to investigate antibody feedback during a contemporaneous GC response
- Depletion of antibody from a specific clone results in its isolated expansion in the GC, implicating epitope masking as the primary mechanism of action of antibody feedback
- Antibody feedback does not play major role in accelerating affinity maturation in the GC

METHODS

Monoclonal antibody production

mAb heavy and light chain sequences were assembled in Ig production plasmids by Twist Biosciences. Expi293 cells were transfected with plasmids, and mAbs and Fabs (with C-terminal his-tags) were purified with protein-G or Ni-NTA affinity chromatography. Briefly, supernatants from suspension cell cultures were batch incubated overnight at 4° C with 2 μl of resin for every 1 mL of culture. The following day, the supernatant resin mixture was transferred to a column, and the resin was allowed to settle. Flow through was allowed at a rate of 1mL/minute. After flow through had completed, columns were washed with 3x column volumes of buffer. Resin was then eluted with 1-2 mL of elution buffer. For protein G, mAbs were eluted with 100 mM glycine HCl, pH 2.7 and immediately neutralized with 1 M Tris-HCl, pH 9.0. For Ni-NTA, Fabs were eluted with buffer containing 20 mM sodium phosphate, 500 mM NaCl, 500 mM imidazole, pH 7.4. Following dilution, proteins were exchanged into PBS either via overnight dialysis or buffer exchange with Amicon Centrifugal filters.

Generation of *Ig* knock-in mice

J segments in the *Igh* and *Igk* loci were excised with a pair of CRISPR sgRNAs. The guide sequences used for *Igh* were TCTCTACTTCCTCATAGCTC and GGAGCCGGCTGAGAGAAGTT, and the sequences for *Igk* were CTGTGGTGGACGTTCGGTGG and AAGACACAGGTTTTCATGTT. Pre-rearranged V(D)J sequences of clones Sa, Cb and C179 were cloned into a plasmid containing

~200 bp homology arms that flanked the cut sites of the guides. From this plasmid, a strandase reaction was performed to produce ssDNA, which produced the template used for our microinjections. We followed the easiCRISPR protocol to generate all transgenic mice in the text.

ELISAs

ELISA plates were coated at 4° C overnight with 5 μg/mL of PR8 HA or SaΔ4 and CbΔ4 mutants in PBS. The following morning, plates were washed twice with PBS and blocked for two hours at RT with 2% BSA in PBS. For NB-21 single GC B cell cultures, total Ig was first assayed by coating plates with goat anti-mouse Ig at 1 μg/ml, and these were then used in HA ELISAs. In the case of monoclonal antibodies, calculated concentrations of mAb diluted in PBS supplemented with 1% BSA were incubated in each well. For serum, serial 3-fold dilutions were completed down the plate, with the top concentration being a 1/100 dilution. Antibodies were incubated on ELISA plates for two hours at RT. Plates were then washed 3x with PBS containing 0.05% of Tween (PBST), after which they were incubated with anti-isotype antibody conjugated to horse radish peroxidase diluted at 1:10,000 for 1 hour at RT. Plates were then washed 2x with PBST and 2x with PBS, after which they were developed with TMB. Absorbance at 450 nm was measured on a plate reader.

Bio-layer interferometry measurements

Bio-layer interferometry (BLI) was performed on an Octet RED96 instrument to determine the affinities of Fabs bound to PR8 influenza HA. Briefly, HA was biotinylated at its AviTag site with BirA via the manufacturer's instructions to enable single site biotinylation. Biotinylated HA was loaded onto High Precision Streptavidin (SAX) Biosensors until binding reached approximately 1 nm. Association was measured by submerging sensors into wells containing Fabs (160nM – 20nM in PBS, 0.1% BSA, 0.02% Tween20) for 400s, Disassociation was measured by transferring sensors into empty buffer solution for 500s. K_D values were calculated using the global fit 1:1 binding algorithm provided with the Octet data analysis software. For epitope binning, HA-bound sensors were submerged into buffer containing one antibody and immediately transferred into wells containing another antibody without any disassociation.

Flow cytometry and cell sorting

For flow cytometry and cell sorting, lymph nodes were mechanically disassociated with disposable micropestles into single cell suspensions into PBS. Cell suspensions were washed with 1mL of PBS and pelleted at 6,700 x g for 30s. Pellets were then resuspended in PBE 1x (PBS supplemented with 0.5% BSA and 1 mM EDTA) containing fluorescently conjugated antibodies and incubate 30 min on ice. Samples were washed with 1mL of PBE and filtered before analysis on FACS Symphony cytometers and sorting on FACS ARIA II cytometers. Analyses were performed using FlowJo v. 10 software.

Single cell *Ig* sequencing

Single GC B cells were index-sorted into 96-well plates containing 5 μl of TCL buffer supplemented with 1% β-mercaptoethanol. SPRI beads were used to extract nucleic acids. RT maxima reverse transcriptase with oligo(dT) as a primer was used for reverse-transcription into cDNA, and a forward primer mix comprising of consensus sequences for all V-regions and reverse primers for each isotype was used to PCR amplify *Igh* genes. *Igk* genes were amplified separately when needed to confirm clonality or for antibody production. Following the initial PCR, 5-nucleotide barcodes were introduced by PCR to label Ig-sequences with plate- and well-specific barcodes. A final PCR step was then performed to incorporate Illumina paired-end sequencing adapters into single-well amplicons. PCR products from all plates were pooled together and subsequently cleaned-up using a 0.7x volume ratio of SPRI beads. Sequencing was performed on the Illumina Miseq platform with a 500-cycle Reagent Nano kit v2 as per the manufacturer's instructions.

Analysis of sequencing data

PandaSeq was used to assemble paired-end sequences and processing was performed with the FASTX toolkit. Barcode sequences were used to assign the resulting demultiplexed and collapsed reads to their respective plates and wells. High-count sequences were analyzed for every single cell/well. To determine the V(D)J arrangements and the number of somatic mutations compared to putative germline precursors, Ig heavy chain and Ig light sequences were aligned to the online databases

(IMGT51; Vbase252). Sequences that shared VH/JH genes, had the same CDR3 lengths, and contained at least 75% CDR3 nucleotide identity were grouped and classified automatically into clonal lineages. Manual curation was performed based on features including V-region SHM patterns and stretches of mismatches at the junctional regions, resulted in further joining of sequences deemed to belong to the same clone, but which fell below 75% CDR3 nucleotide identity. For the few clones in which a rearranged *Igh* gene was not detected, the *Igk* sequence was used to establish clonality. Only cells with productively rearranged *Igh* genes were used for VH mutation analyses. GCtree was used to infer clonal lineage trees, with the unmutated V gene sequence of the V(D)J clonal rearrangement used for outgroup rooting.

Naïve B cell isolation and adoptive B cell transfers

Spleens from donor mice were mashed into single cell suspensions, red blood cells were lysed with ACK buffer, and resulting suspensions were filtered through a 70 μm mesh into PBE. Resting naïve B cells were obtained via negative selection by magnetic separation using anti-CD43 magnetic beads, as per the manufacturer's instructions. The number of cells to transfer was determined based on the percentage of HA-tetramer binding B cells, and cells were first stained and analyzed via flo cytometry to determine the number of HA-binding cells in each sample. The day before immunization, 100 μl of cells in PBS were transferred i.v. via retro-orbital injection.

Immunization with PR8 HA and infection with PR8 influenza

Mice were immunized with 25 μl containing 5 μg of recombinantly produced PR8 HA in alhydrogel subcutaneously in the footpads of their left hind limbs. To prepare the immunogen, HA was mixed with PBS and alhydrogel so that the adjuvant made up 1/3 of the total volume. The entire mixture was then pipetted up and down for 5 minutes at RT. For infection, mice were anesthetized with ketamine/xylazine diluted in sterile PBS and infected intranasally with 33 PFU of mouse-adapted influenza PR8 virus.

Single-GC B cell cultures

NB-21.2D9 feeder cells expressing CD40L, BAFF and IL-21 were seeded the day before B cell sorting into 96-well round bottom plates at a density of 2,500 cells per well. On the day of single GC B cell sorting, cultures were supplemented with 4 ng/ml of recombinant IL-4 and *Salmonella typhimurium* LPS. Supernatants were harvested on day 7 of culture.

REFERENCES

Ahmed, Alysia A. et al. “Structural Characterization of Anti-Inflammatory Immunoglobulin G Fc Proteins.” *Journal of Molecular Biology* 426.18 (2014): 3166–3179. Web.

Allen, D. et al. “Antibody Engineering for the Analysis of Affinity Maturation of an Anti-hapten Response.” *The EMBO Journal* 7.7 (1988): 1995–2001. Web.

Andrews, Sarah F et al. “High Preexisting Serological Antibody Levels Correlate with Diversification of the Influenza Vaccine Response.” *Journal of Virology* 89.6 (2015): 3308–3317. Web.

Andrews, Sarah F. et al. “Immune History Profoundly Affects Broadly Protective B Cell Responses to Influenza.” *Science Translational Medicine* 7.316 (2015): 316ra192-316ra192. Web.

Angeletti, Davide et al. “Defining B Cell Immunodominance to Viruses.” *Nature Immunology* 18.4 (2017): 456–463. Web.

Anvari, Sara et al. “IgE-Mediated Food Allergy.” *Clinical Reviews in Allergy & Immunology* 57.2 (2019): 244–260. Web.

Atta, Mohamed G., Sophie De Seigneux, and Gregory M. Lucas. “Clinical Pharmacology in HIV Therapy.” *Clinical Journal of the American Society of Nephrology* 14.3 (2019): 435–444. Web.

Batista, Facundo D, and Michael S Neuberger. “Affinity Dependence of the B Cell Response to Antigen: A Threshold, a Ceiling, and the Importance of Off-Rate.” *Immunity* 8.6 (1998): 751–759. Web.

Benowitz, Isaac et al. “Influenza Vaccine Given to Pregnant Women Reduces Hospitalization Due to Influenza in Their Infants.” *Clinical Infectious Diseases* 51.12 (2010): 1355–1361. Web.

Berek, C., A. Berger, and M. Apel. “Maturation of the Immune Response in Germinal Centers.” *Cell* 67.6 (1991): 1121–1129. Web.

Bergström, Joakim J. E., Hui Xu, and Birgitta Heyman. “Epitope-Specific Suppression of IgG Responses by Passively Administered Specific IgG: Evidence of Epitope Masking.” *Frontiers in Immunology* 8 (2017): 238. Web.

Boes, Marianne. “Role of Natural and Immune IgM Antibodies in Immune Responses.” *Molecular Immunology* 37.18 (2000): 1141–1149. Web.

Booth, Brian J. et al. “Extending Human IgG Half-Life Using Structure-Guided Design.” *mAbs* 10.7 (2018): 1098–1110. Web.

Borràs, E et al. “Measles Antibodies and Response to Vaccination in Children Aged Less than 14 Months: Implications for Age of Vaccination.” *Epidemiology and Infection* 140.9 (2012): 1599–1606. Web.

Bournazos, Stylianos, Hoa Thi My Vo, et al. “Antibody Fucosylation Predicts Disease Severity in Secondary Dengue Infection.” *Science* 372.6546 (2021): 1102–1105. Web.

Bournazos, Stylianos, Taia T. Wang, et al. “Signaling by Antibodies: Recent Progress.” *Annual Review of Immunology* 35.1 (2017): 285–311. Web.

Bournazos, Stylianos, and Jeffrey V Ravetch. “Diversification of IgG Effector Functions.” *International Immunology* 29.7 (2017): 303–310. Web.

Brinc, Davor, and Alan H. Lazarus. “Mechanisms of Anti-D Action in the Prevention of Hemolytic Disease of the Fetus and Newborn.” *Hematology* 2009.1 (2009): 185–191. Web.

Briney, Bryan et al. “Commonality despite Exceptional Diversity in the Baseline Human Antibody Repertoire.” *Nature* 566.7744 (2019): 393–397. Web.

Brüggemann, Marianne, and Klaus Rajewsky. “Regulation of the Antibody Response against Hapten-Coupled Erythrocytes by Monoclonal Antihapten Antibodies of Various Isotypes.” *Cellular Immunology* 71.2 (1982): 365–373. Web.

Casola, Stefano et al. “B Cell Receptor Signal Strength Determines B Cell Fate.” *Nature Immunology* 5.3 (2004): 317–327. Web.

Caton, Andrew J. et al. “The Antigenic Structure of the Influenza Virus A/PR/8/34 Hemagglutinin (H1 Subtype).” *Cell* 31.2 (1982): 417–427. Web.

Cerottini, Jean-Charles, Patricia J McConahey, and Frank J Dixon. “The Immunosuppressive Effect of Passively Administered Antibody IgG Fragments.” *The Journal of Immunology* 102.4 (1969): 1008–1015. Web.

Chakravarty, Suchana, Christian I. Hong, and Attila Csikász-Nagy. “Systematic Analysis of Negative and Positive Feedback Loops for Robustness and Temperature Compensation in Circadian Rhythms.” *npj Systems Biology and Applications* 9.1 (2023): 5. Web.

Chaudhuri, Jayanta et al. “Biological Function of Activation-Induced Cytidine Deaminase (AID).” *Biomedical Journal* 37.5 (2014): 269. Web.

Clynes, Raphael et al. “Fc Receptors Are Required in Passive and Active Immunity to Melanoma.” *Proceedings of the National Academy of Sciences* 95.2 (1998): 652–656. Web.

Clynes, Raphael A. et al. “Inhibitory Fc Receptors Modulate in Vivo Cytoxicity against Tumor Targets.” *Nature Medicine* 6.4 (2000): 443–446. Web.

Daly, Kathleen A. et al. “Maternal Immunization with Pneumococcal 9-Valent Conjugate Vaccine and Early Infant Otitis Media.” *Vaccine* 32.51 (2014): 6948–6955. Web.

Dosenovic, Pia et al. “Immunization for HIV-1 Broadly Neutralizing Antibodies in Human Ig Knockin Mice.” *Cell* 161.7 (2015): 1505–1515. Web.

Dreyfus, Cyrille, Damian C Ekiert, and Ian A Wilson. “Structure of a Classical Broadly Neutralizing Stem Antibody in Complex with a Pandemic H2 Influenza Virus Hemagglutinin.” *Journal of Virology* 87.12 (2013): 7149–7154. Web.

Ekiert, Damian C. et al. “Cross-Neutralization of Influenza A Viruses Mediated by a Single Antibody Loop.” *Nature* 489.7417 (2012): 526–532. Web.

Elsner, Rebecca A., and Mark J. Shlomchik. “Germinal Center and Extrafollicular B Cell Responses in Vaccination, Immunity, and Autoimmunity.” *Immunity* 53.6 (2020): 1136–1150. Web.

Englund, J A et al. “The Effect of Maternal Antibody on the Serologic Response and the Incidence of Adverse Reactions after Primary Immunization with Acellular and Whole-Cell Pertussis Vaccines Combined with Diphtheria and Tetanus Toxoids.” *Pediatrics* 96.3 Pt 2 (1995): 580–4. Print.

Enriquez-Rincon, F, and G G Klaus. “Differing Effects of Monoclonal Anti-Hapten Antibodies on Humoral Responses to Soluble or Particulate Antigens.” *Immunology* 52.1 (1984): 129–36. Print.

Fukuyama, Hidehiro, Ryo Shinnakasu, and Tomohiro Kurosaki. “Influenza Vaccination Strategies Targeting the Hemagglutinin Stem Region.” *Immunological Reviews* 296.1 (2020): 132–141. Web.

Garside, Paul et al. “Visualization of Specific B and T Lymphocyte Interactions in the Lymph Node.” *Science* 281.5373 (1998): 96–99. Web.

Gerhard, Walter et al. “Antigenic Structure of Influenza Virus Haemagglutinin Defined by Hybridoma Antibodies.” *Nature* 290.5808 (1981): 713–717. Web.

Gitlin, Alexander D. et al. “T Cell Help Controls the Speed of the Cell Cycle in Germinal Center B Cells.” *Science* 349.6248 (2015): 643–646. Web.

Gitlin, Alexander D., Ziv Shulman, and Michel C. Nussenzweig. “Clonal Selection in the Germinal Centre by Regulated Proliferation and Hypermutation.” *Nature* 509.7502 (2014): 637–640. Web.

Goodnow, Christopher C. et al. “Altered Immunoglobulin Expression and Functional Silencing of Self-Reactive B Lymphocytes in Transgenic Mice.” *Nature* 334.6184 (1988): 676–682. Web.

Guthmiller, Jenna J. et al. “Polyreactive Broadly Neutralizing B Cells Are Selected to Provide Defense against Pandemic Threat Influenza Viruses.” *Immunity* 53.6 (2020): 1230-1244.e5. Web.

Hägglöf, Thomas et al. “Continuous Germinal Center Invasion Contributes to the Diversity of the Immune Response.” *Cell* 186.1 (2023): 147-161.e15. Web.

Hartweger, Harald et al. “HIV-Specific Humoral Immune Responses by CRISPR/Cas9-Edited B Cells.” *Journal of Experimental Medicine* 216.6 (2019): 1301–1310. Web.

Heyman, Birgitta. “Regulation of Antibody Responses via Antibodies, Complement, and Fc Receptors.” *Annual Review of Immunology* 18.1 (2000): 709–737. Web.

---. “The Immune Complex: Possible Ways of Regulating the Antibody Response.” *Immunology Today* 11.9 (1990): 310–313. Web.

Inoue, Takeshi et al. “Antibody Feedback Contributes to Facilitating the Development of Omicron-Reactive Memory B Cells in SARS-CoV-2 MRNA Vaccinees.” *Journal of Experimental Medicine* 220.2 (2022): e20221786. Web.

J., Nabel Gary. “Designing Tomorrow’s Vaccines.” *New England Journal of Medicine* 368.6 (2013): 551–560. Web.

Jacob, J et al. “In Situ Studies of the Primary Immune Response to (4-Hydroxy-3-Nitrophenyl)Acetyl. III. The Kinetics of V Region Mutation and Selection in Germinal Center B Cells.” *The Journal of experimental medicine* 178.4 (1993): 1293–1307. Web.

Jacob, Joshy et al. “Intraclonal Generation of Antibody Mutants in Germinal Centres.” *Nature* 354.6352 (1991): 389–392. Web.

Jacobsen, Johanne T. et al. “One-Step Generation of Monoclonal B Cell Receptor Mice Capable of Isotype Switching and Somatic Hypermutation.” *Journal of Experimental Medicine* 215.10 (2018): 2686–2695. Web.

Jones, Chrissie, and Paul Heath. “Antenatal Immunization.” *Human Vaccines & Immunotherapeutics* 10.7 (2014): 2118–2122. Web.

Jung, David, and Frederick W Alt. “Unraveling V(D)J Recombination Insights into Gene Regulation.” *Cell* 116.2 (2004): 299–311. Web.

Kachikis, Alisa, and Janet A. Englund. “Maternal Immunization: Optimizing Protection for the Mother and Infant.” *Journal of Infection* 72 (2016): S83–S90. Web.

Kaneko, Yoshikatsu, Falk Nimmerjahn, and Jeffrey V. Ravetch. “Anti-Inflammatory Activity of Immunoglobulin G Resulting from Fc Sialylation.” *Science* 313.5787 (2006): 670–673. Web.

Kappler, John W., Michael Hoffmann, and Richard W. Dutton. “REGULATION OF THE IMMUNE RESPONSE.” *The Journal of Experimental Medicine* 134.3 (1971): 577–587. Web.

Karlsson, Mikael C. I. et al. “Efficient IgG-Mediated Suppression of Primary Antibody Responses in Fcγ Receptor-Deficient Mice.” *Proceedings of the National Academy of Sciences* 96.5 (1999): 2244–2249. Web.

Kemper, Claudia et al. “Complement: The Road Less Traveled.” *The Journal of Immunology* 210.2 (2023): 119–125. Web.

Kenter, Amy L., Saurabh Priyadarshi, and Ellen B. Drake. “Locus Architecture and RAG Scanning Determine Antibody Diversity.” *Trends in Immunology* 44.2 (2023): 119–128. Web.

Kometani, Kohei, and Tomohiro Kurosaki. “Differentiation and Maintenance of Long-Lived Plasma Cells.” *Current Opinion in Immunology* 33 (2015): 64–69. Web.

Krammer, Florian, and Peter Palese. “Influenza Virus Hemagglutinin Stalk-Based Antibodies and Vaccines.” *Current Opinion in Virology* 3.5 (2013): 521–530. Web.

Kumpel, B. M. “Efficacy of RhD Monoclonal Antibodies in Clinical Trials as Replacement Therapy for Prophylactic Anti-D Immunoglobulin: More Questions than Answers.” *Vox Sanguinis* 93.2 (2007): 99–111. Web.

Kumpel, Belinda M. “On the Immunologic Basis of Rh Immune Globulin (Anti-D) Prophylaxis.” *Transfusion* 46.8 (2006): 1271–1275. Web.

Kuraoka, Masayuki et al. “Complex Antigens Drive Permissive Clonal Selection in Germinal Centers.” *Immunity* 44.3 (2016): 542–552. Web.

Landsteiner, K., and J. van der Scheer. “On the Specificity of Serological Reactions With Simple Chemical Compounds (Inhibition Reactions).” *The Journal of Experimental Medicine* 54.3 (1931): 295–305. Web.

Lee, Juhye M et al. “Mapping Person-to-Person Variation in Viral Mutations That Escape Polyclonal Serum Targeting Influenza Hemagglutinin.” *eLife* 8 (2019): e49324. Web.

Lu, Lenette L. et al. “Beyond Binding: Antibody Effector Functions in Infectious Diseases.” *Nature Reviews Immunology* 18.1 (2018): 46–61. Web.

Madsen, Anders et al. “Human Antibodies Targeting Influenza B Virus Neuraminidase Active Site Are Broadly Protective.” *Immunity* 53.4 (2020): 852-863.e7. Web.

Maertens, Kirsten et al. “Pneumococcal Immune Response in Infants Whose Mothers Received Tetanus, Diphtheria and Acellular Pertussis Vaccination During Pregnancy.” *The Pediatric Infectious Disease Journal* 36.12 (2017): 1186–1192. Web.

McNamara, Hayley A. et al. “Antibody Feedback Limits the Expansion of B Cell Responses to Malaria Vaccination but Drives Diversification of the Humoral Response.” *Cell Host & Microbe* 28.4 (2020): 572-585.e7. Web.

Ng, Kevin W. et al. “B Cell Responses to the Gut Microbiota.” *Advances in Immunology* 155 (2022): 95–131. Web.

Nie, Jianhui et al. “Quantification of SARS-CoV-2 Neutralizing Antibody by a Pseudotyped Virus-Based Assay.” *Nature Protocols* 15.11 (2020): 3699–3715. Web.

Nimmerjahn, Falk, and Jeffrey V. Ravetch. “Divergent Immunoglobulin G Subclass Activity Through Selective Fc Receptor Binding.” *Science* 310.5753 (2005): 1510–1512. Web.

Nojima, Takuya et al. “In-Vitro Derived Germinal Centre B Cells Differentially Generate Memory B or Plasma Cells in Vivo.” *Nature Communications* 2.1 (2011): 465. Web.

Nurk, Sergey et al. “The Complete Sequence of a Human Genome.” *Science* 376.6588 (2022): 44–53. Web.

Okada, Takaharu et al. “Antigen-Engaged B Cells Undergo Chemotaxis toward the T Zone and Form Motile Conjugates with Helper T Cells.” *PLoS Biology* 3.6 (2005): e150. Web.

Okuno, Y et al. “A Common Neutralizing Epitope Conserved between the Hemagglutinins of Influenza A Virus H1 and H2 Strains.” *Journal of Virology* 67.5 (1993): 2552–2558. Web.

Palma, Joanna et al. “Natural Antibodies – Facts Known and Unknown.” *Central-European Journal of Immunology* 43.4 (2018): 466–475. Web.

Pappas, Leontios et al. “Rapid Development of Broadly Influenza Neutralizing Antibodies through Redundant Mutations.” *Nature* 516.7531 (2014): 418–422. Web.

Paus, Didrik et al. “Antigen Recognition Strength Regulates the Choice between Extrafollicular Plasma Cell and Germinal Center B Cell Differentiation.” *The Journal of Experimental Medicine* 203.4 (2006): 1081–1091. Web.

Pelanda, Roberta et al. “A Prematurely Expressed Igκ Transgene, but Not a VκJκ Gene Segment Targeted into the Igκ Locus, Can Rescue B Cell Development in Λ5-Deficient Mice.” *Immunity* 5.3 (1996): 229–239. Web.

Pollard, Andrew J., and Else M. Bijker. “A Guide to Vaccinology: From Basic Principles to New Developments.” *Nature Reviews Immunology* 21.2 (2021): 83–100. Web.

Porto, Joseph M. Dal et al. “Very Low Affinity B Cells Form Germinal Centers, Become Memory B Cells, and Participate in Secondary Immune Responses When Higher Affinity Competition Is Reduced.” *The Journal of Experimental Medicine* 195.9 (2002): 1215–1221. Web.

Radtke, Daniel, and Oliver Bannard. “Expression of the Plasma Cell Transcriptional Regulator Blimp-1 by Dark Zone Germinal Center B Cells During Periods of Proliferation.” *Frontiers in Immunology* 9 (2019): 3106. Web.

Robert, Marcus et al. “Obinutuzumab for the First-Line Treatment of Follicular Lymphoma.” *New England Journal of Medicine* 377.14 (2017): 1331–1344. Web.

Rodriguez, Oscar L. et al. “Genetic Variation in the Immunoglobulin Heavy Chain Locus Shapes the Human Antibody Repertoire.” *Nature Communications* 14.1 (2023): 4419. Web.

Schaefer-Babajew, Dennis et al. “Antibody Feedback Regulates Immune Memory after SARS-CoV-2 MRNA Vaccination.” *Nature* 613.7945 (2023): 735–742. Web.

Schroeder, Harry W. “Similarity and Divergence in the Development and Expression of the Mouse and Human Antibody Repertoires.” *Developmental & Comparative Immunology* 30.1–2 (2006): 119–135. Web.

Schwickert, Tanja A. et al. “A Dynamic T Cell–Limited Checkpoint Regulates Affinity-Dependent B Cell Entry into the Germinal Center.” *Journal of Experimental Medicine* 208.6 (2011): 1243–1252. Web.

Sicca, Federica et al. “Comparison of Influenza-Specific Neutralizing Antibody Titers Determined Using Different Assay Readouts and Hemagglutination Inhibition Titers: Good Correlation but Poor Agreement.” *Vaccine* 38.11 (2020): 2527–2541. Web.

Smith, Theobald. “ACTIVE IMMUNITY PRODUCED BY SO CALLED BALANCED OR NEUTRAL MIXTURES OF DIPHTHERIA TOXIN AND ANTITOXIN.” *The Journal of Experimental Medicine* 11.2 (1909): 241–256. Web.

Sonoda, Eiichiro et al. “B Cell Development under the Condition of Allelic Inclusion.” *Immunity* 6.3 (1997): 225–233. Web.

Stanfield, Robyn L., and Ian A. Wilson. “Antibody Structure.” *Antibodies for Infectious Diseases* (2019): 49–62. Web.

Subedi, Ganesh P., and Adam W. Barb. “The Structural Role of Antibody N-Glycosylation in Receptor Interactions.” *Structure* 23.9 (2015): 1573–1583. Web.

Sui, Jianhua et al. “Structural and Functional Bases for Broad-Spectrum Neutralization of Avian and Human Influenza A Viruses.” *Nature Structural & Molecular Biology* 16.3 (2009): 265–273. Web.

Suzuki, Kazuhiro et al. “Visualizing B Cell Capture of Cognate Antigen from Follicular Dendritic Cells.” *Journal of Experimental Medicine* 206.7 (2009): 1485–1493. Web.

Taki, Shinsuke, Myriam Meiering, and Klaus Rajewsky. “Targeted Insertion of a Variable Region Gene into the Immunoglobulin Heavy Chain Locus.” *Science* 262.5137 (1993): 1268–1271. Web.

Tas, Jeroen M. J. et al. “Visualizing Antibody Affinity Maturation in Germinal Centers.” *Science* 351.6277 (2016): 1048–1054. Web.

Tas, Jeroen M.J. et al. “Antibodies from Primary Humoral Responses Modulate the Recruitment of Naive B Cells during Secondary Responses.” *Immunity* 55.10 (2022): 1856-1871.e6. Web.

Tolar, Pavel, and Katelyn M. Spillane. “Chapter Three Force Generation in B-Cell Synapses Mechanisms Coupling B-Cell Receptor Binding to Antigen Internalization and Affinity Discrimination.” *Advances in Immunology* 123 (2014): 69–100. Web.

Vettermann, Christian, and Mark S. Schlissel. “Allelic Exclusion of Immunoglobulin Genes: Models and Mechanisms.” *Immunological Reviews* 237.1 (2010): 22–42. Web.

Victora, Gabriel D. et al. “Germinal Center Dynamics Revealed by Multiphoton Microscopy with a Photoactivatable Fluorescent Reporter.” *Cell* 143.4 (2010): 592–605. Web.

Victora, Gabriel D., and Michel C. Nussenzweig. “Germinal Centers.” *Annual Review of Immunology* 40.1 (2022): 1–30. Web.

Vieira, Paulo, and Klaus Rajewsky. “The Half-lives of Serum Immunoglobulins in Adult Mice.” *European Journal of Immunology* 18.2 (1988): 313–316. Web.

Vijay, Rahul et al. “Infection-Induced Plasmablasts Are a Nutrient Sink That Impairs Humoral Immunity to Malaria.” *Nature Immunology* 21.7 (2020): 790–801. Web.

Vono, Maria et al. “Maternal Antibodies Inhibit Neonatal and Infant Responses to Vaccination by Shaping the Early-Life B Cell Repertoire within Germinal Centers.” *Cell Reports* 28.7 (2019): 1773-1784.e5. Web.

Wang, Taia T., and Jeffrey V. Ravetch. “Functional Diversification of IgGs through Fc Glycosylation.” *Journal of Clinical Investigation* 129.9 (2019): 3492–3498. Web.

Wang, Taia T. et al. “Anti-HA Glycoforms Drive B Cell Affinity Selection and Determine Influenza Vaccine Efficacy.” *Cell* 162.1 (2015): 160–169. Web.

Wason, William M. “Regulation of the Immune Response with Antigen Specific IgM Antibody: A Dual Role.” *The Journal of Immunology* 110.5 (1973): 1245–1252. Web.

Willerford, Dennis M, Wojciech Swat, and Frederick W Alt. “Developmental Regulation of V(D)J Recombination and Lymphocyte Differentiation.” *Current Opinion in Genetics & Development* 6.5 (1996): 603–609. Web.

Wu, Nicholas C., and Ian A. Wilson. “Influenza Hemagglutinin Structures and Antibody Recognition.” *Cold Spring Harbor Perspectives in Medicine* 10.8 (2019): a038778. Web.

Yamaizumi, Masaru et al. “One Molecule of Diphtheria Toxin Fragment a Introduced into a Cell Can Kill the Cell.” *Cell* 15.1 (1978): 245–250. Web.

Zemlin, Michael et al. “Expressed Murine and Human CDR-H3 Intervals of Equal Length Exhibit Distinct Repertoires That Differ in Their Amino Acid Composition and Predicted Range of Structures.” *Journal of Molecular Biology* 334.4 (2003): 733–749. Web.

Zhang, Yang et al. “Germinal Center B Cells Govern Their Own Fate via Antibody Feedback.” *The Journal of Experimental Medicine* 210.3 (2013): 457–464. Web.